POLITECNICO
MILANO 1863

SCUOLA DI INGEGNERIA INDUSTRIALE
E DELL'INFORMAZIONE

Executive Summary of the Thesis

Modelling The Filling of Carbonated Soft Drinks

Laurea Magistrale in Food Engineering - Ingegneria Industriale e dell'Informazione

Authors: Claudia Madonia, Danièle Nanfack Logho

Advisor: Prof. Maurizio Masi

Co-advisor: Simone Gelosa

Academic year: 2020-2021

1. Introduction

Carbonated beverages, in the form of carbonated mineral water, are popular all over the world, with an impressive dominance in the global soft drink market. The olfactory sensations they release, marketing and branding, but most importantly the carbon dioxide present in them contribute to their success. In particular, the size and stability of the bubbles play an important role in determining, not only the level of pleasure for consumption, but also during the production process. Both properties are closely related to the life cycle of bubbles, including nucleation, growth, maturation, and bursting, all of which depend on the diffusive behavior of gases [Endan J., 2010]. The dynamics of bubbles forming in liquids, all the mechanisms of foam formation and the concept of foam stability over time are analysed and explained in depth. In addition, a laboratory analysis done with the aim of seeing if and how the different ingredients of a carbonated drink could influence the formation and stability of the foam that is formed during the bottling process. To do so, three mixtures comprising water, citric acid and a different type of sweetener were observed to have a higher foam formation and stability respectively.

2. Background and market

Carbonated Soft Drink is a solution in which, when carbon dioxide (CO_2) meets water (H_2O), these two react to form a dilute carbonic acid solution (H_2CO_3). The chemical reaction for this process is $H_2O + CO_2 \leftrightharpoons H_2CO_3$ [Gros L., 2006]. Industrial production of carbonated water began in 1972 when Swiss watchmaker Jacob Schweppe improved on the system devised by Priestley, increasing the volumes of carbon dioxide and thus achieving high levels of carbonation. In 1830 the addition of sweeteners in order to obtain non-

alcoholic beverages, as well as aromas and colorants, which instead gave them an attractive taste and color, caused the development of the consumption of carbonated beverages. The global market has been dominated for decades by two large groups, the American companies The Coca-Cola Company and PepsiCo. In fact, as can be seen from the chart in *Figure 1*, in 2015 the global leader is The Coca-Cola Company with a 30.2% market share, followed by PepsiCo with 21.6%. It is also followed by Nestlé S.A with 11.9% and Dr Pepper Snapple Group with 8.3%. However, the industry is full of many companies that have carved out their own role in the soft drink market, launching typical products of a certain territory or specific products with a worldwide share of 28.1% [Euromonitor International, 2015].

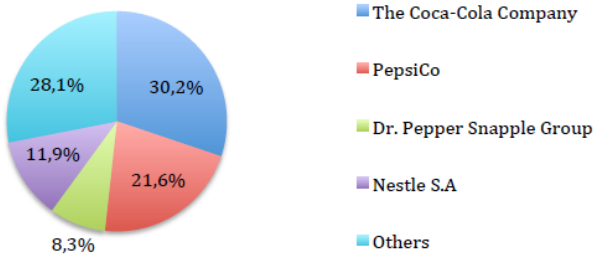

Figure 1: Percentages of world beverage market shares

The primary ingredients in carbonated beverages are water, sugars, and carbon dioxide. Carbonated beverages also contain other secondary ingredients, including acids, flavoring agents, colouring ingredients, emulsifiers, clouding agents, stabilizers and preservatives.

3. Core of the problem

The main issues related to the industrial bottling phase are foaming, time and temperature of the bottling phase and water use and wastewater generation. Generally, foams have two different structures that can manifest themselves in the form of spherical bubbles and polyhedral cells. At first, the foam that is created on the surface of the liquid is called "wet foam" and is characterised by the formation of spherical bubbles; subsequently, due to the effect of gravity, the bubbles drain and take on a polyhedral form, until the formation of "dry foam", as shown in *Figure 2*.

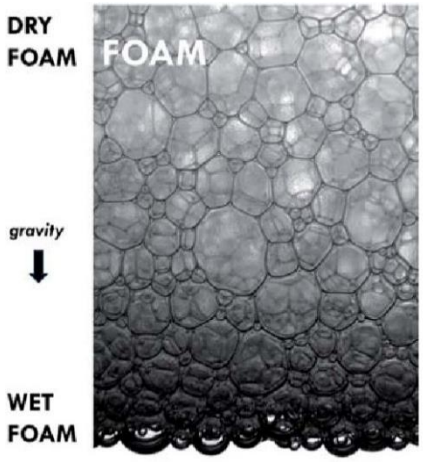

Figure 2: Wet and dry foams

Because it is lighter than wet foam, dry foam will always tend to be at the top of the total foam formed and, due to the opposite effect to gravity, will tend to rise very quickly and at high speeds. For this reason, when bottling carbonated drinks, there is a risk that too much foam will be formed and/or that the foam will rise at too high a rate to escape from the neck of the bottle [Drenckhan W., 2015]. As far as time is concerned, on the one hand it is necessary to try to bring the filling phase to a time high enough to avoid foam forming; on the

other hand, there is the need to bring this phase to a time as low as possible in order to increase hourly production. With respect to temperature, high temperatures lead to an expulsion of carbon dioxide from the liquid, causing more foam to form. On the contrary, low temperatures lead on the one hand to more dissolved carbon dioxide and less possibility of foam formation. In Figure 3 we can see the process of carbonated soft drinks production:

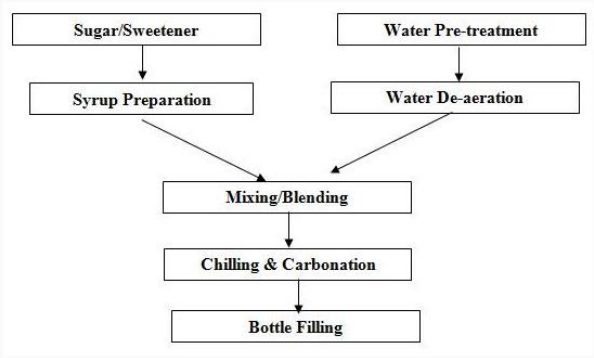

Figure 3: Process flow for the manufacture of carbonated soft drink

3.1. Mechanisms of foam production

3.1.1. Bubble formation

it's been discovered that the main source of bubble nucleation might be identified as supersaturation state in the system is achieved as a result of the decompression state which precedes the process of gas desorption from the solution; cavitation areas development in the fluid is due to the flow field that had been generated during the filling process; gas pockets are entrapped at surface discontinuities that are produced by the liquid flowing along the walls of the bottle; the impact of the filling jet causes the entertainment of bubbles under the liquid-free surface.

3.1.2. Bubble growth

Gas solubility is a concept that should be first introduce to understand how bubbles are nucleated by gas desorption. Gas solubility represents the amount of gas dissolved in a solution when it is in the equilibrium state. This property is a purpose of the temperature and pressure of the system. For dilute solutions that are sufficient, including carbonated beverages, Henry's law is applied in the form:

$$C_e = k_H\, p \qquad (1.1)$$

(C_e is the equilibrium concentration; k_H is Henry's constant function of the solvent nature and the temperature; p is the partial pressure).

Once the nucleation occurs, bubble growth until detachment. The speed of their growth depends on many factors, such as the surface tension, the viscosity and the speed of molecular diffusion rate at the bubble in the interface. This one is the leading phenomenon of the final growth. The reached bubble size depends on the level and on the nature of scrapings present on the solid surface and so it cannot be related to their cavitation speed [Hepworth N. J., 2004].

3.1.3. Detachment of bubbles

To prevent bubble detachment, the balance of forces, in *Equation 1.2,* must be taken into account:

$$F_D + F_S = F_I + F_P + F_B \qquad (1.2)$$

F_D is the friction with the surrounding liquid, due to bubble growth; F_S is the surface tension, F_I is the totality of inertial forces involved; F_P is the totality of pression forces that act in the system, and F_B is the comprehensive forces of buoyancy.

3.1.4. Foam stability

The factors playing a major role in the production of bubbles during bottling have already been revealed. The control of the foam might be possible when governing those factors by prevents or inhibiting its formation, at least. Every foam is thermodynamically unstable because their high interfacial free energy. Therefore, a column of foam will decay spontaneously over time, the rate of deterioration is dictated by the kinetics of four processes [Shokribousjein Z., 2011] that are disproportionation, gas diffusion, drainage and coalescence. Methods acting on foams that are prior to its complete formation are known as "antifoaming" methods, which are chemical additives (the use of chemical agents is not desirable since they alter the characteristic of the liquid product), ultrasonic vibrations and Electronic Pulse Volume Measurement [Min O., 2019].

4. Laboratory experiments about foaming

4.1. Input data and equipment

In this laboratory experiment, three different types of sugar mixtures and quantities listed in *Table 1* were studied:

Table 1: Three mixtures and quantities used in the experiment

MIXTURE 1	MIXTURE 2	MIXTURE 3
Water: 70 ml	Water: 70 ml	Water: 70 ml
Citric acid: 0,04 g	Citric acid: 0,04 g	Citric acid: 0,04 g
Granulated sugar: 7,89 g	Fructose: 7,89 g	Stevia: 7,89 g

The carbon dioxide used in this experiment was provided by a tank at an average pressure of about 6.5 bar. The amount of carbon dioxide emitted by the gas tank was measured using a rotameter attached to it. Each mixture was placed inside a cylindrical glass reactor at a pressure of 1 atm and at room temperature.

4.2. Description of the experiment

Each of the three mixtures, one at a time, was then poured into the cylindrical glass reactor from above. The gas cylinder is also connected to the rotameter, so that the flow rate of carbon dioxide entering the reactor can be regulated. Initially, the tap on the nozzle connecting the reactor to the gas cylinder is closed, Next, the nozzle inlet valve is opened and then gradually the gas cylinder valve is opened. At this point, the carbon dioxide starts to leave the cylinder valve and reach the reactor nozzle, through which it also meets the mixture, although the carbon dioxide comes into contact with the mixture, it can be seen that gas bubbles start to emerge from the nozzle and rise along the mixture to the free surface. When the number of bubbles begins to be sufficiently high, and therefore when the flow rate of carbon dioxide into the reactor reaches a certain range, the mixture begins to agitate until it forms foam on

the surface of the free surface. At a certain point both the nozzle tap and the cylinder valve are closed, instantly preventing carbon dioxide from leaving the gas cylinder and entering the reactor through the nozzle. From this moment, the foam that has formed begins its decay process until it is completely extinguished: the more stable the foam formed, the longer the decay and the longer it takes for the mixture to return to its initial conditions. The experiment was reproduced in exactly the same way for all three mixtures.

4.3. Data analysis

From the data collection, it can be seen that for all three mixtures, as the flow rate of carbon dioxide into the system increases, so does the height of the foam that forms on the free surface. However, it is evident how the growth of foam is different for all three cases. In fact, as can be seen from the graph in *Figure 4.*

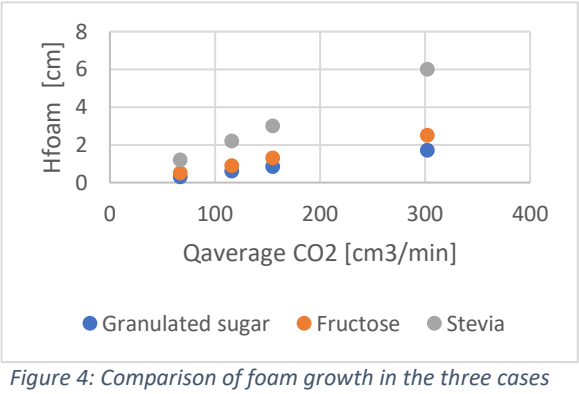

Figure 4: Comparison of foam growth in the three cases

At the end of the analysis, in *Equation 1.3*, the expression of the relaxation time τ is described:

$$\tau = \frac{3H_0\mu_{mix}}{2\,g\,\pi\,D\,\rho_{mix}\delta_0} \qquad (1.3)$$

and it is for mixture 1 about 2,1 seconds, for mixture 2 3,5 seconds and for mixture 3 8,4 seconds respectively. This means that the foam of mixture 3 is more stable than the other two. This phenomenon is explained by the fact that the surface energy of the liquid decreases when the height of the liquid rises and the fact that the gravitational potential energy of the liquid increases simultaneously. It is known that the surface tension of water, which is generally 0.072 N/m, increases with the addition of sugars [Hiemenz P. C., 1997].

4.4. Bottling model

Models for the calculation of the foam and liquid height during the filling and the defoaming phases are been developed, as it can be seen below:

$$H_{foam\ Filling\ N} = \frac{Q\,\tau\,S}{\Omega}\left(1 - e^{\left(\frac{-t\ step}{\tau}\right)}\right) + H_{foam\ Defoam\ N-1} \qquad (1.4)$$

$$H_{liquid\ Filling\ N} = \frac{Q\ t_{step}}{\Omega} + H_{liquid\ Defoam\ N-1} \qquad (1.5)$$

$$H_{foam\ Defoam\ N} = H_{foam\ Filling\ N}\, e^{\left(\frac{-t\ step}{\tau}\right)} \qquad (1.6)$$

$$H_{liquid\ Dedoam\ N} = H_{liquid\ Filling\ N} \qquad (1.7)$$

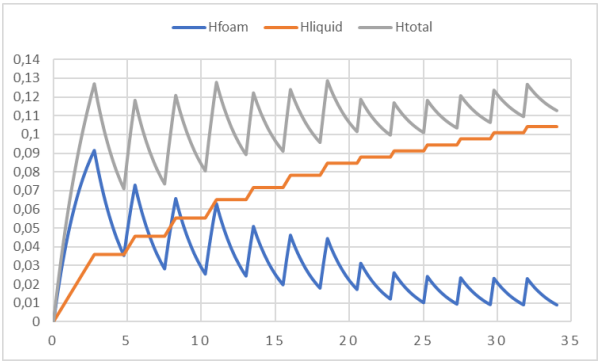

Figure 5: Height of foam, height of liquid and total height vs time of bottling

It was observed from mixture 1 in *Figure 5* that the height of the foam increases with each filling step but decreases with each degassing one, and for each step the foam formed is progressively smaller; the height of the liquid increases with each filling step in smaller quantities and remains constant in the degassing phases; the total height is given by the sum of the trends of the height ofthe foam and of the liquid and therefore increases both in the filling and in the degassing phases.

5. Discussion

The tests performed in the laboratory showed that the three mixtures analysed are characterised by different foam formations, under the same conditions of pressure, temperature and flow rate of carbon dioxide introduced into the system in which they were contained. In addition, the three mixtures, have been shown to foam with different stability.

6. Conclusions

In this thesis, after making a list of what can be the problems of a bottling company in the bottling phases of carbonated drinks, the dynamics and behaviour of gas bubbles inside a liquid, the mechanisms of foam formation and the concept of stability in time related to foam were described in detail. Subsequently, a bottling simulation was carried out through filling and degassing phases in a cylindrical reactor and the problem of foam formation was identified as one of the main problems. In particular, the main objective was to see how and if a different composition of the ingredients of a drink affected the process in question and therefore possibly how bottling companies should adjust accordingly, reprogramming machinery for the bottling process according to the drink in question. The desired objective was achieved by using a specially developed model able to measure the heights of foam and liquid at each step of both filling and degassing.

7. Reference

[Endan J., 2010]: Endan J., “A Survey on Rheological Properties of Fruit Jams”, *International Journal of Chemical Engineering and Applications,* 2010

[Gros L., 2006]: Gros L., “Chemistry changes everything”, *Chemistry and Industry for Teachers in European Schools,* 2006

[Euromonitor International, 2015]: https://www.euromonitor.com, 2015

[Drenckhan W., 2015]: W. Drenchan, “Structure and energy of liquid foams”, *Advances in Colloid and Interface Science,* 1-16, 2015

[Hepworth N. J., 2004]: Hepworth N. J., “Novel application of computer vision to determine bubble size distributions in beer”, Journal of Food Engineering, 2004

[Shokribousjein Z., 2011]: Shokribousjein Z., “Hydrophobins, Beer Foaming and Gushing.”, *Cerevisia*, 2011

[Min O., 2019]: Min O., “Development of High-Efficiency, High-Speed and High-Pressure Ambient Temperature Filling System Using Pulse Volume Measurement.” *Applied Sciences (Switzerland)* 9 (12), 2019

[Hiemenz P. C., 1997]: Hiemenz P. C., “Principles of colloid and surface chemistry”, Third edition, Marcel Dekker Inc., 1997

Politecnico di Milano

SCHOOL OF INDUSTRIAL AND INFORMATION ENGINEERING

Master of science – Food Engineering

Modelling the filling of Carbonated Soft Drinks

Supervisor

Ing. Maurizio Masi

Candidates

Claudia Madonia – 953235

Danièle Nanfack Logho – 928612

Academic Year 2020 – 2021

INDEX

ACKNOWLEDGEMENTS 1

ABSTRACT (in English) 2

ABSTRACT (in Italian) 3

1. INTRODUCTION 4

2. BACKGROUND 5

2.1. What are Carbonated Soft Drinks 5

2.2. History 5

2.2.1. Carbonated Soft Drinks growth and evolution 5

2.2.2. The evolution of the PET bottle 6

2.3. Carbonated Soft Drinks market 6

2.4. Ingredients of Carbonated Soft Drinks 8

2.4.1. Water 8

2.4.2. Sugars and intense sweeteners 9

2.4.3. Carbon dioxide 10

3. THE CORE OF THE PROBLEM 11

3.1. Problems related to bottling 11

3.1.1. Foaming 11

3.1.2. Time and temperature of the bottling phase 12

3.1.3. The choice of the bottle 12

3.1.4. Water use and wastewater generation 12

3.2. Carbonated Soft Drink production 13

3.2.1. Syrup preparation 14

3.2.2. Water treatments 15

3.2.3. Blending 15

3.2.4. Carbonation 15

3.2.5.Bottle filling 17

3.3. Mechanisms of foam production 19

3.3.1. Bubble formation 20
3.3.1.1. Desorption 20
3.3.1.1.1. Classical nucleation 22
3.3.1.1.2. Relevant parameters 25
3.3.1.2. Cavitation 26
3.3.1.3. Entrapment 28
3.3.1.4. Entrainment 29
3.3.2. Bubble growth 31
3.3.3. Detachment of bubble 31
3.4. Bubble dynamics 32
3.5. Foam stability 38
3.5.1. Disproportionation 39
3.5.2. Gas diffusion 39
3.5.3. Drainage 39
3.5.4. Coalescence 41
3.6. How to avoid foam 42
3.6.1. Chemical additives 42
3.6.2. Ultrasonic vibrations 43
3.6.3. Electronic Pulse Volume Measurement 44
4. LABORATORY EXPERIMENTS ABOUT FOAMING 47
4.1. Input data and equipment 47
4.2. Description of the experiment 50
4.3. Data collection 51
4.4. Data analysis 56
4.5. Bottling model 64
5. DISCUSSION 69
6. CONCLUSIONS 70
ANNEXES 71
ANNEX I: History of bottle 71

ANNEX II: Water treatments 72

ANNEX III: Ingredients 73

ANNEX IV: Bottle design 75

ANNEX V: Water Footprint, The Coca Cola Company case 79

ANNEX VI: Stretch-blow moulding 80

ANNEX VII: Rotameter 81

LIST OF FIGURES 90

LIST OF TABLES 92

7. REFERENCES 93

ACKNOWLEDGEMENTS

We would like to thank all the persons who have been by our side during our precious voyage. During our university path each person with whom we have the possibility to stay with left us something and has allowed us to grow every time by giving us good suggestions and training.

First of all, we wish to thank our families whom has given us the chance to study in the best Ateneo of Italy.

A harthfelt thank you to Professor Maurizio Masi for his competent and diligent guidance. Our esteem for him is due not only to his profound experience and knowledge of his subject matter, but also to his great humanity with which he has encouraged us.

So much gratitude to Simone Gelosa who supported us, advised and helped throughout our thesis, even involving us in the laboratory activities. We are deeply grateful to him because he allowed us to carry out this thesis by exposing ourself to an interesting laboratory experience.

We also want to tank our friends that have followed us and made us live nice and memorable moments. Each of them in their own way has been instrumental in our personal growth.

After years of hard work, we have finally reached the end of our study. We are sure that Politecnico di Milano has given to us the possibility to expand our capabilities and knowledge to be able to continue in our future life. Too much tank you to Politecnico di Milano too.

Claudia and Danièle

ABSTRACT (in English)

In this thesis, an analysis of the foam formation during the bottling phase of carbonated drinks has been carried out and in particular, it can be divided into three main sections. The first section introduces what carbonated drinks are, what ingredients they contain, the history of how they were born, how they came to be on the market and how they became so successful over the years. The second section not only describes the entire production process in detail, but also discusses the problems that companies face during the bottling process, focusing on one of the main problems which is foam formation. In this section, the dynamics of bubbles forming in liquids, all the mechanisms of foam formation and the concept of foam stability over time are analysed and explained in depth. In this section, a list of what are the ways and techniques to avoid or minimise foaming within a process is also present. Lastly, the third section includes a laboratory analysis done with the aim of seeing if and how the different ingredients of a carbonated drink could influence the formation and stability of the foam that is formed during the bottling process. To do so, three mixtures comprising water, citric acid and a different type of sweetener, the first containing granulated sugar, the second fructose and the third stevia, were observed to have a higher foam formation and stability respectively. This was explained by the fact that the surface tension of the water was increased by granulated sugar, fructose and stevia respectively. Lastly, a model was created to calculate the foam and liquid heights at each step of the bottling simulation, which was carried out by alternating filling and degassing phases in order to avoid any product leakage from the top of the bottle.

ABSTRACT (in Italian)

In questa tesi, è stata condotta un'analisi sulla formazione di schiuma durante la fase di imbottigliamento delle bevande gassate e in particolare, essa può essere divisa in tre sezioni principali. La prima sezione introduce cosa sono le bevande gassate, quali sono gli ingredienti che le compongono, la storia di come sono nate, approdate sul mercato e di come negli anni hanno acquisito un così grande successo tutt'ora ancora evidente. La seconda sezione, oltre a descriverne l'intero processo di produzione nel dettaglio, tratta di quali sono le problematiche che le aziende imbottigliatrici riscontrano durante il processo stesso, focalizzandosi su uno dei problemi principali, ovvero quello della formazione di schiuma. In questa sezione infatti, vengono analizzati e spiegati in maniera esaustiva le dinamiche delle bolle che si formano all'interno dei liquidi, tutti i meccanismi di formazione della schiuma e il concetto di stabilità nel tempo relativo ad essa. In questa sezione, è presente anche un elenco di quali sono le modalità e le tecniche per evitare o ridurre al minimo la formazione di schiuma all'interno di un processo. Infine, la terza sezione comprende un'analisi di laboratorio fatta con l'obiettivo di vedere se e come i diversi ingredienti di una bevanda gassata potessero influenzare la formazione e la stabilità della schiuma che si viene a formare durante il processo di imbottigliamento. Per fare ciò, tre miscele comprendenti acqua, acido citrico e un diverso tipo di dolcificante, la prima contenente zucchero granulato, la seconda fruttosio e la terza stevia, sono state osservate avere una formazione ed una stabilità di schiuma rispettivamente maggiore. Ciò è stato spiegato dal fatto che la tensione superficiale dell'acqua è stata aumentata in maniera crescente rispettivamente dallo zucchero granulato, dal fruttosio e dalla stevia. Infine è stato creato un modello per il calcolo delle altezze di schiuma e del liquido ad ogni singolo step della simulazione di imbottigliamento, avvenuta attraverso fasi di riempimento alternate a fasi di degasaggio, così da evitare eventuali fuoriuscite del prodotto dagli estremi superiori della bottiglia.

1. INTRODUCTION

Carbonated beverages, in the form of carbonated mineral water, are popular all over the world, with an impressive dominance in the global soft drink market. The olfactory sensations they release, marketing and branding, but most importantly the carbon dioxide present in them contribute to their success. The presence of carbon dioxide in carbonated beverages improves palatability by allowing the diluted carbonic acid formed through reaction with water to create a slight burning sensation on the consumer's tongue. In fact, many people like the feeling of bubbles bursting in their mouths when they drink them. In particular, the size and stability of the bubbles play an important role in determining the degree of creaminess and smoothness, and therefore the level of pleasure for consumption. Both properties are closely related to the life cycle of bubbles, including nucleation, growth, maturation, and bursting, all of which depend on the diffusive behavior of gases [Endan J., 2010]. The presence of carbon dioxide in carbonated beverages makes it possible to improve not only the palatability, but also the appearance of these products through the formation of a column of foam on the free surface of their surfaces. In industrial plants, however, foams appear as an undesirable product during the pressure filling phase and the subsequent decompression phase. To control, inhibit, or destroy a foam, one should know all the factors that govern its growth and stability. However, foams are very complex dynamic systems whose properties depend on a wide variety of chemical and physical parameters, such as product composition, surfactant adsorption kinetics, and the specific conditions underlying their development [Starov V., 2021]. As a result, although foams have been extensively studied in different areas and for many years, a comprehensive and general theory for foam formation is still lacking [Petkova B., 2020].

2. BACKGROUND

2.1. What are Carbonated Soft Drinks

Among the most known non-alcoholic beverages there are Carbonated Soft Drinks, in technical slang CSD. Non-alcoholic beverages are all those beverages which do not contain alcohol or, more precisely, in which the possible presence of alcohol is not higher than 1% by volume. This qualification is usually used with reference to cold beverages and, in the broadest sense of the term, includes the following categories: plain packaged waters, carbonated waters, carbonated sweet sparkling drinks (CSD), flat sweet drinks, fruit juices and nectars [Treccani, 2021]. So, the term "Carbonated Soft Drink" refers to those non-alcoholic beverages that are generally sweetened, flavored, colored, and acidified, sometimes containing added minerals and fruit juices or purees in almost negligible amounts, and artificially impregnated with carbon dioxide. In practical terms, it is a solution in which, when carbon dioxide (CO_2) meets water (H_2O), these two react to form a dilute carbonic acid solution (H_2CO_3). The chemical reaction for this process is $H_2O + CO_2 \leftrightharpoons H_2CO_3$ [Gros L., 2006].

2.2. History

2.2.1. Carbonated soft drinks growth and evolution

The birth of carbonated beverages dates back to 1693, when the Benedictine monk Dom Pierre Pérignon produced the first sparkling wine of history. According to the legend he, monk by profession and enologist by passion, by aromatizing wine with flowers and sugar, he would have noticed they produced a sort of foam when the bottles were opened [Long T., 2009]. In 1767, scientist Joseph Priestley created artificial sparkling water by suspending a bowl of water above a tank of beer in a brewery. Over the millennia, the consumption of beverages in their various features had the sole purpose of meeting the body's water needs. In particular, since Roman times, it was customary to believe that natural mineral waters had healing powers. Hoping to reproduce such healing qualities in the laboratory, pioneering inventors of soft drinks used chalk and acid to carbonate water. Industrial production of carbonated water began in 1972 when Swiss watchmaker Jacob Schweppe improved on the system devised by Priestley, increasing the volumes of carbon dioxide and thus achieving high levels of carbonation. In 1830 the addition of sweeteners in order to obtain non-alcoholic beverages, as well as aromas and colorants, which instead gave them an attractive taste and color, caused the development of the consumption of carbonated beverages. From here on, the carbonated beverage industry spread all over the world and each manufacturer filed a patent with its own recipe [Mahnazmezon, 2021]. Unfortunately, however, the negative impact of carbonated beverages on health conditions were recognized as early as 1942. Concerns grew when, through studies, links between their consumption and diseases such as tooth decay, obesity, and diabetes were confirmed. Many countries, as a result, decided to focus on

awareness campaigns to reduce consumption among the younger classes. Therefore, the consequences on the market have pushed the Food & Beverage sector towards the use of natural ingredients [Statista, 2019].

2.2.2. The evolution of the PET bottle

Until the 1970s, years when new materials such as polyethylene began to take hold, carbonated soft drink companies packaged their drinks in glass bottles. Before these years, the story of how the first bottle was born and its various innovations related to non-plastic materials can be found in *Annex I.* It was Nathaniel Convers Wyeth who discovered during a home experiment the properties of this new material. He filled an empty detergent bottle made of polypropylene with ginger ale, he put it in the refrigerator and during the night the bottle swelled up to the point of bursting: the sparkling bubbles of the beverage, effect of the addition of carbon dioxide, produced a pressure polypropylene could not stand. So, not convinced of the goodness of the material, he solved the problem by using instead of polypropylene, polypropylene terephthalate (PET), whose fibers were stretched and made more resistant to deformation induced by the gaseous content. This can be considered the initial phase of experimentation on PET that led towards the mid-1970s to the increasingly massive distribution in the market, a crucial step for the evolution of the beverage sector [Zugno S., 2017].

2.3. Carbonated Soft Drink market

The non-alcoholic beverage market is structured into retail sales for home consumption and retail sales or in food service establishments for consumption away from home. The home market, also called the off-trade market, covers all retail sales through a large-scale distribution (GDO) system of super and hypermarkets, convenience stores, or similar sales channels [GDO, 2021]. The out-of-home market, on the other hand, also called the on-trade market, away-from-home market, or HORECA (Hotellerie Restauran Café) market, covers all sales to hotels, restaurants, caterers, cafes, bars, and similar hospitality service establishments. Both the home and away-from-home markets are valued at retail prices, including all sales and consumption taxes [Horeca, 2020]. In the beverage world, the carbonated soft drink industry is the one where we see the most global competition and where we see the highest annual revenues. The global market has been dominated for decades by two large groups, the American companies The Coca-Cola Company and PepsiCo. In fact, as can be seen from the chart in *Figure 1*, in 2015 the global leader is The Coca-Cola Company with a 30.2% market share, followed by PepsiCo with 21.6%. It is also followed by Nestlé S.A with 11.9% and Dr Pepper Snapple Group with 8.3%. However, the industry is full of many companies that have carved out their own role in the soft drink market, launching typical products of a certain territory or specific products with a worldwide share of 28.1% [Euromonitor International, 2015].

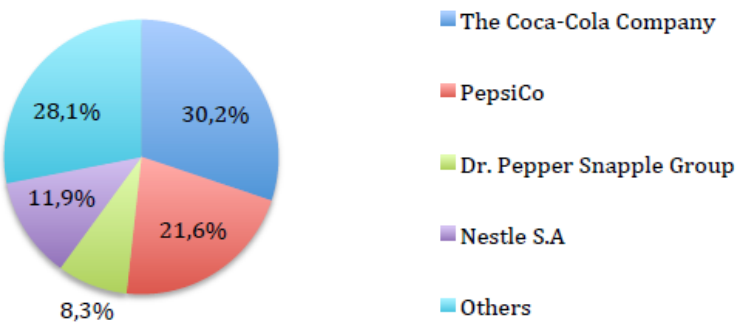

Figure 1: Percentages of world beverage market shares. [Euromonitor International, 2015]

The domain of Coca Cola, is much more impactful than PepsiCo, but analyzing one of the most interesting study parameters, namely differentiation and subdivision into smaller brands, the difference becomes much thinner, as shown in *Table 1* [Beverfood, 2019].

Table 1: Carbonated soft drink brands. [Beverfood, 2019]

Trademark	Company	2018 Rank
Coke	Coca-Cola	1
Pepsi	PepsiCo	2
Mountain Dew	PepsiCo	3
Dr Pepper	Keurig Dr Pepper	4
Gatorade**	PepsiCo	5
Nestlé Pure Life	NWNA	6
Sprite	Coca-Cola	7
Poland Spring	NWNA	8
Dasani	Coca-Cola	9
Aquafina	PepsiCo	10

In fact, the world of carbonated beverages is in a phase of strong evolution. Consumers demand products that reflect their habits, for example gender specific beverages, beverages that reflect particular popular cultures and those that respond to certain lifestyles are common. This is leading to a rapid and intense transformation of markets, making the offerings increasingly varied and rich. Nowadays, companies pay a lot of attention to the nutritional aspect and therefore need beverages that reflect this characteristic, such as light beverages

with low sugar content, as well as zero variants or those in which only sweeteners of natural origin are used. One of the main reasons linked to health campaigns is the fight against obesity, in fact in the USA a 40% reduction of sugar in drinks could prevent 2.48 million cardiovascular diseases and 750,000 cases of diabetes [Guzzonato C., 2021]. Also in Italy there has been a greater attention to health, especially by young people, in fact since 2009 there has been a 25% drop in beverage consumption and in 2020 an even greater drop of 30% [Assobibe, 2020]. Another of the reasons related to the campaigns in favor of reducing the sugar content within carbonated beverages is the famous "Sugar Tax", first introduced in France and Denmark in 2012, in the USA in 2018 and scheduled to be introduced in Italy in 2022 [Napolitano G., 2019]. The aspect of functionality in the non-alcoholic segment is now a parameter held in high regard by a large segment of consumers and large manufacturers, in fact, this will probably be the restart point in the coming years for the soft drink market. For example, The Coca-Cola Company, feeling threatened by a shift towards healthier consumption habits, has decided to invest in energy drinks by acquiring 17% of the shares of Monster Beverage and launching on the market the new "Coca Cola Energy", based on caffeine derived from natural guarana extract [Mente A., 2018].

2.4. Ingredients of Carbonated Soft Drinks

The primary ingredients in carbonated beverages are water, sugars, and carbon dioxide. Carbonated beverages also contain other secondary ingredients described in *Annex III*, including acids, flavoring agents, colouring ingredients, emulsifiers, clouding agents, stabilizers and preservatives.

2.4.1. Water

Water is the main ingredient in all beverages. It accounts for about 90% of the content of a regular carbonated soft drink and 98% of a low-calorie soft drink. Most of the water used in the production of soft drinks comes from mains water, which must undergo some additional treatment to remove microscopic and colloidal particles before being used for production. These treatments are discussed in *Annex II*. On the other hand, with regard to treatments for the removal of microorganisms, disinfection and chlorination remain the most widely used. The reason these types of waters need to be pretreated is that the water in a soft drink acts as a solvent for all the other ingredients, so its quality is primary. Each soft drink company has its own requirements for treated water that cover physical, chemical, microbiological and taste characteristics. However, it is possible to use spring water or natural mineral water, which is indicated on the product label [British Soft Drink Association, 2021]. In general, water used for the production of carbonated soft drinks must have the requirements shown in *Table 2:*

Table 2: Standards of water used in Carbonated soft drinks. [Dow, 2009]

Parameter	Unit	Raw Water Quality Range
Temperature	°C	10–18
Conductivity	µS/cm	5000–7000
pH		7.5–8.5
Total Hardness	meq/l	15
Turbidity	FNU	1–25
Bromide	mg/l	7.1–8.5
Silica (SiO_2)	mg/L	17.2

2.4.2. Sugars and intense sweeteners

Sweetener has three basic functions in carbonated beverages: imparting sweetness, providing substance and calories. The main sweetener used in carbonated beverages is crystalline sugar in the form of sugar syrup, which must be of very high purity. In particular, sugar, also known as sucrose, is the one extracted from beet or cane. It is a disaccharide which, in presence of acid as in drinks, hydrolyzes to form an equal mixture of glucose and fructose monosaccharides which make it up. Glucose, fructose and corn syrups can also be used to provide sweetness. The final concentration of sugar varies from 8 to 14% in the finished beverage. This is because all sugars have the same caloric content, about 4kcals/g, but have different levels of sweetness: for example, fructose is slightly sweeter than sucrose and glucose is less sweet than sucrose. In addition, there are intense sweeteners, which are non-sugar substances that can be added to food and beverages in place of sugar. Among the most common are acesulfame-k (E950), aspartame (E951), saccharin (E954), steviol glycosides (E960) and sucralose (E955). They are many times sweeter than sugar, meaning that much smaller amounts are needed to give a product the desired sweet taste. These types of sweeteners are primarily used in low-calorie carbonated beverages [British Soft Drink Association, 2021]. The development in the use of intensive sweeteners dates back to World War I when the supply of sugar was limited. Manufacturers found that blending different intense sweeteners, sometimes with sugar, can lead to better flavor profiles in the product. For this reason, many manufacturers use blends of sweeteners rather than a single intense sweetener in their beverages [International Sweeteners Association, 2021].

2.4.3. Carbon dioxide

Carbon dioxide (CO_2) imparts effervescence to carbonated beverages. It is an inert, non-toxic, nearly tasteless gas that is easy to produce, available at a relatively lower cost in liquid form, and impregnates in the liquid unlike other gases. In fact, it is soluble in liquids where its solubility increases when the temperature of the liquid is decreased and can exist as a gas, liquid or solid. CO_2 produces carbonic acid when dissolved in water which, in combination with other ingredients, produces an acidic, pungent flavor characteristic of carbonated beverages. The dissolved gas not only gives a characteristic taste to beverages, but also acts against bacteria and molds. It can be obtained from carbonates, calcareous, combustion of organic compounds and industrial fermentation processes. Following the production of carbon dioxide from any type of process, it must be purified to ensure it is free of impurities and suitable for human consumption. Purification of CO_2 is done by scrubbing with water to remove sulfur compounds and passing through activated carbon or charcoal tower to remove odorous compounds. Many beverage manufacturers produce CO_2 on their own directly at the packaging site [British Soft Drink Association, 2021].

3. THE CORE OF THE PROBLEM

3.1. Problems related to bottling

The main issues related to the industrial bottling phase are foaming, time and temperature of the bottling phase and water use and wastewater generation

3.1.1. Foaming

The main problem at the bottling stage is the formation of foam due to the incorporation of gas into the liquid matrix. Indeed, foams are colloidal systems consisting of a gas phase dispersed in a continuous liquid phase. Generally, foams have two different structures that can manifest themselves in the form of spherical bubbles and polyhedral cells. At first, the foam that is created on the surface of the liquid is called "wet foam" and is characterised by the formation of spherical bubbles; subsequently, due to the effect of gravity, the bubbles drain and take on a polyhedral form, until the formation of "dry foam", as shown in *Figure 2*.

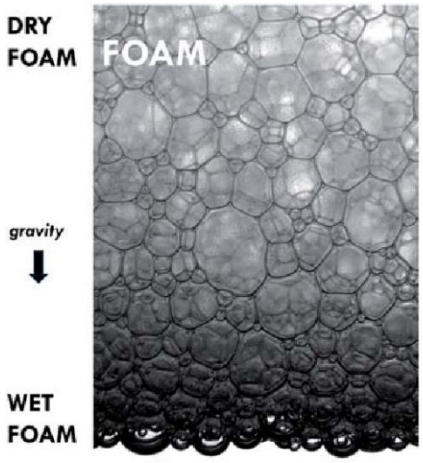

Figure 2: Wet and dry foams. [Drenckhan W., 2015]

Because it is lighter than wet foam, dry foam will always tend to be at the top of the total foam formed and, due to the opposite effect to gravity, will tend to rise very quickly and at high speeds. For this reason, when bottling carbonated drinks, there is a risk that too much foam will be formed and/or that the foam will rise at too high a rate to escape from the neck of the bottle [Drenckhan W., 2015]. This would not only lead to a waste of product, but also to a certain stickiness to the handle of the outer wall of the bottle due to the high

percentage of sugar present in the drink and difficult to remove from the bottle material. The mechanisms of foam formation will be explained in more detail in *Paragraph 3.3.*

3.1.2. Time and temperature of the bottling phase

In order to prevent the foam that has formed from escaping from the bottle, it is essential to control the parameters of time and temperature. As far as time is concerned, on the one hand it is necessary to try to bring the filling phase to a time high enough to avoid foam forming; on the other hand, there is the need to bring this phase to a time as low as possible in order to increase hourly production. A compromise between low and high filling times leads to an optimisation of the bottling time. For example, it is possible to estimate that the average filler speed ranges from 257-258 two-liter bottles/hour with a filling time of 14-15 seconds per bottle. A reduction to 10-12 seconds gives 360-300 bottles/hour, and so not only an improvement of 13%÷27% of bottles produced per hour, but also a reduction of the costs of production. That is why researches on the reduction of bottling phase are currently done. With respect to temperature, high temperatures lead to an expulsion of carbon dioxide from the liquid, causing more foam to form. On the contrary, low temperatures lead on the one hand to more dissolved carbon dioxide and less possibility of foam formation; on the other hand, they lead to high costs for energy consumption to reach these temperatures. In this case, a good compromise between high and low temperatures is to work at room temperature.

3.1.3. The choice of the bottle

Although carbonation gives overall rigidity to the corked bottle, making the handle firmer and excluding problems of bruising during transport, the pressure due to carbon dioxide acting on the bottle walls is a necessary problem to be overcome. For this reason, the choice of the right type of bottle to be used to contain a drink with a high carbon dioxide content must be one of the elements of great attention during the bottling phase. Once the bottle has been filled, the gas tends by its nature to deform some of its parts, making them take on a completely different shape from the one initially thought. The most critical points are the body, the neck, the shoulder, the handle, the bottom and the ribs, as can be seen in *Annex IV* [Zugno S., 2017].

3.1.4. Water use and wastewater generation

Freshwater is a key ingredient for the operations of many companies and effluents can pollute local hydrological ecosystems. Many companies have addressed these issues and formulated proactive

management strategies [Gerbens P. W., 2003]. A company can face four serious risks associated with not managing freshwater:

- Damage to corporate image;
- The threat of increased regulatory scrutiny;
- Financial risks caused by pollution;
- Insufficient availability of fresh water for operations.

One tool that helps companies extend their view of how they use water in their production processes is the Water Footprint. *Annex V* describes what is the Water Footprint and the Coca Cola Company case. In addition, there is also the issue of wastewater that occurs as a result of water treatment within the plant with the production of effluent and waste sludge from backwashing of filter units and removal of sedimented materials after chemical coagulation. The character and quantity of waste from water treatment depends on the quality of the local water supply and the type of treatment units used. For example, waste water from the bottle washing machine results from continuous discharge from the preliminary and final rinse, and from intermittent discharge from the cleaning solution compartments. The alkaline cleaning solution can be used for up to five or six weeks with the correct addition of chemicals at regular intervals to maintain the desired solution strength. The entire solution is then discarded. Some bottling plants re-use part of the final rinse as pre-rinse water, thus reducing the volume of waste water from bottle washing. Other wastes are those that occur intermittently as a result of cleaning the syrup mixing tank, the syrup storage tank and the syrup filters and spillage from the syrup and filling [Porges R., 1961].

3.2. Carbonated Soft Drinks production

The step previous to the manufacturing of carbonated soft drinks is the production of the PET bottles that are to be filled, through a technique of stretch-blow moulding of the preforms described in *Annex VI.* Water purification is the opening procedure of the drink production process. Water undergoes a series of purification stages marked by the preparation of a mixture of sugar syrup with concentrate and purified water in a particular unit to a strict formula. The result sees pure water and flavoured syrup transferred to the bottling unit in which they appear mixed in strict proportions in a special vessel called “the agitator” and the drink is carbonized. The consequent bottling process is performed by an automatic machine called “filler” which is put

into practise to fill each bottle with a strictly specified volume according to the drink. After the filling part, each bottle is closed with a cap screwed on the top under pressure tight conditions. Then each bottle must pass through a coder, employed to stamp on the surface information about date, time, factory and line code and expiry date of the drink. Afterwards, the bottle is covered by a label containing information addressed to the customer, such as manufacturer's address, content of the drink and an available hotline number. In *Figure 3* [Jana A., 2021] steps to prepared carbonated soft drinks are outlined.

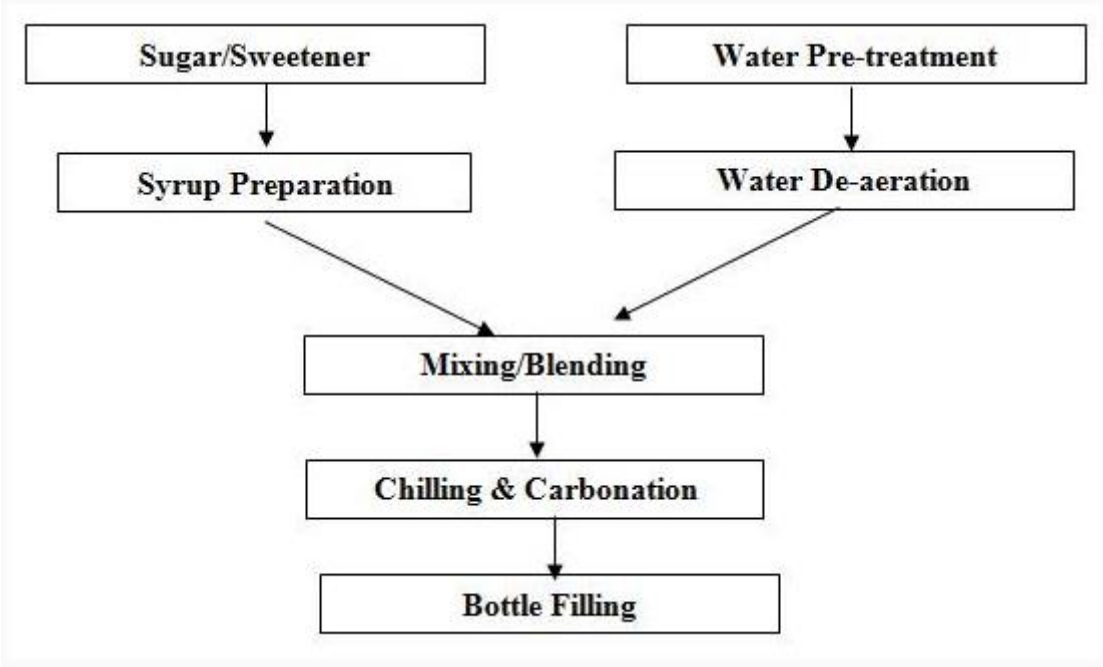

Figure 3: Process flow diagram for the manufacture of carbonated soft drink [Jana A., 2021]

3.2.1. Syrup preparation

Syrup production is carried out in batch mode. If two syrup tanks are used, the syrup can be prepared continuously. The syrup is kept perfectly mixed. Liquid sugar usually contains a lot of oxygen, depending on the dissolution process. With the addition of CO_2 in the circulation line, the oxygen is expelled from the syrup. What remains is a desired pre-carbonation of the syrup [Inter Upgrade, 2021]. In contrast, granulated sugar, used for syrup production, is generally supplied in sachet form and is then dissolved in treated water to produce a 'simple syrup' or liquid sugar solution. Generally, syrups are delivered by tanker vehicles and pumped into storage tanks at the production plant. The storage area or tanks must be cooled to keep the syrup below 0°C. The syrup concentrate can be pumped directly from the storage tanks to the mixing for

dilution with water, or for mixing with other concentrates before dilution. This simple syrup is then pumped to the mixing zone [Pollution Research Group, 2015].

3.2.2. Water treatments

The treatment of beverage water plays a major role in the hygienic production process, as well as for the right taste of the product. The necessary treatment technology always depends on the different composition of the raw water available on site and the requirements of the beverage produced. Each beverage requires a tailor-made water treatment which places great demands on having different water treatment technologies listed in *Annex III* [EUWA, 2021]. An important step in this phase is the deaeration of the water prior to the blending process, in which the water is pumped into a deaeration tank under vacuum which takes care of removing the air from the water. This is done because excess air can have an impact on the carbonation process and can cause foaming. In fact, the lower the air content of the drink before carbonation, the more effective the carbonation process.

3.2.3. Blending

Blending is the process of combining liquids and this can take place in a continuous or batch operation. In batch processes, concentrated syrup and deaerated water are mixed in a tank in a given volume, and then transferred to the next process step before another batch can be mixed. Samples are taken at the end of each batch produced to ensure quality. Continuous or in-line mixing involves the continuous mixing of liquids on their way to the next process step through a buffer tank. The resulting product is sampled continuously and the flow rate of concentrate and water is adjusted to ensure the correct quality is achieved. Flavourings, colourings, acids, preservatives and other additives are added to the simple syrup at this stage to form the final syrup mixture to be mixed with treated water prior to carbonation [Pollution Research Group, 2015].

3.2.4. Carbonation

In the carbonation process, carbon dioxide is injected into the drink in a closed carbonation tank, which is pressurised with gas. The equilibrium between the gas in the liquid and the corresponding pressure in the tank will be achieved after a certain time. At this point the carbon dioxide will be absorbed into the drink and remain in a dissolved state while the drink is kept under pressure. The content of carbon dioxide that can be solubilised in water by the drink, as can be seen from the graph in *Figure 4*, depends on the pressure in the carbonation tank and the temperature of the drink. The higher the required carbon dioxide content, the higher

the required saturation pressure at a given temperature. Conversely, the lower the temperature for a given content, the lower the required saturation pressure. The basic system for carbonating water is shown in *Figure 5*. In particular, the water is pumped into a carbonation tank which is pressurised with carbon dioxide. A CO_2 injector is placed between the pump and the tank, which is more efficient and faster to promote absorption than simply exposing the beverage to a CO_2 atmosphere. The CO_2 content of the beverage has the main effect on filling performance and the cost efficiency of the filling process, while the oxygen content of the beverage has a great influence on preserving the quality of the beverage. Although the mixing and carbonation processes are continuous, a sufficient volume of the beverage is retained in the carbonation tank for decantation before filling. [Steen D. P., 2006].

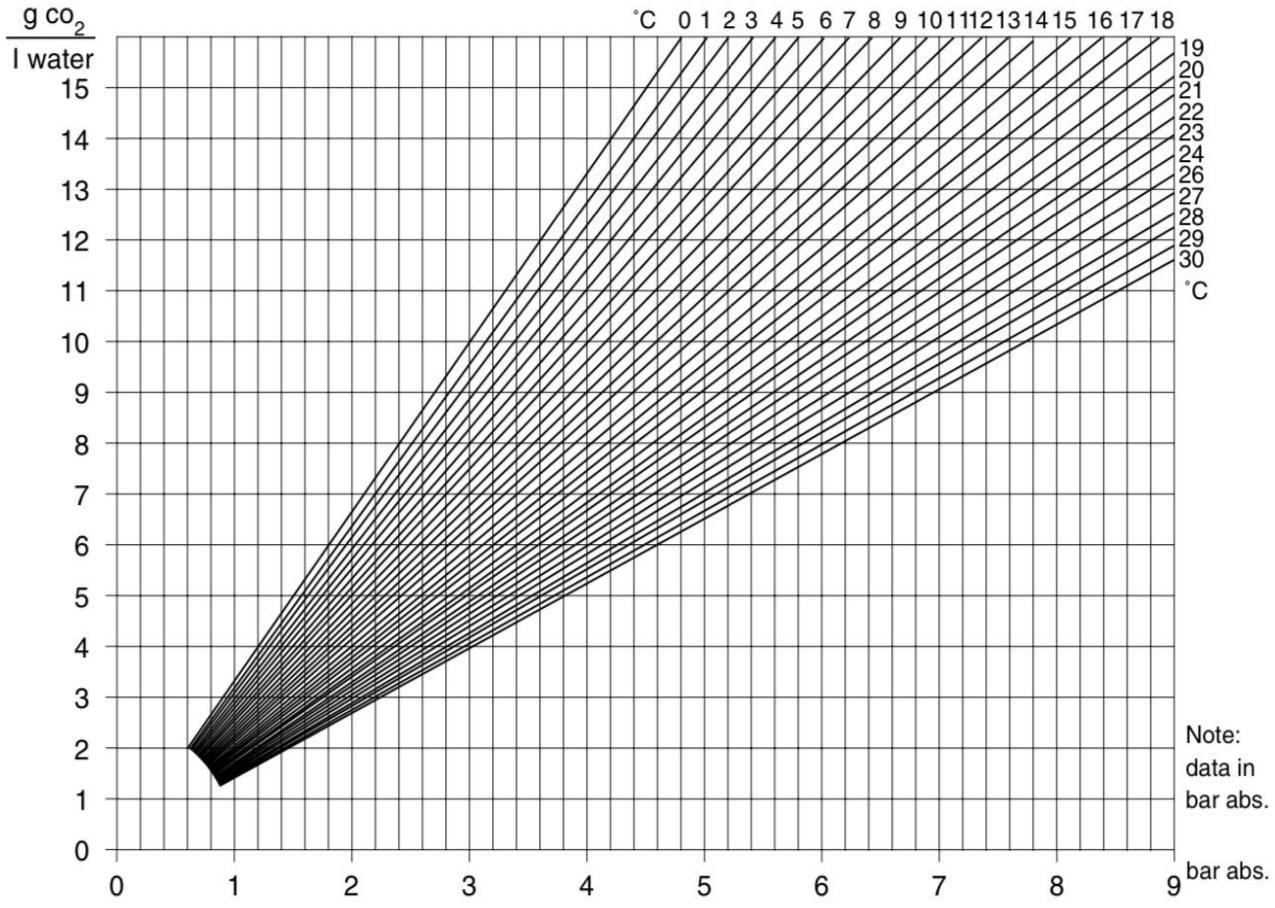

Figure 4: Carbon Dioxide solubility in water [Steen D. P., 2006]

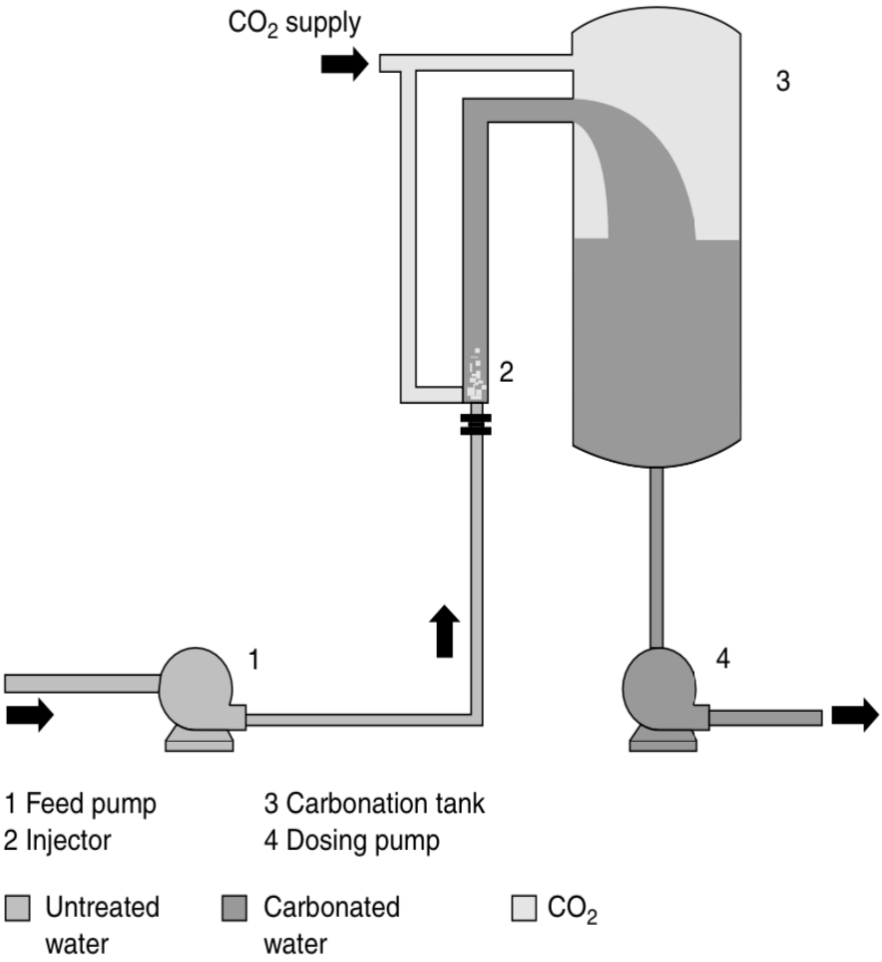

Figure 5: Basic carbonation system [Steen D. P., 2006]

3.2.5. Bottle filling

Bottle filling is carried out on a counterpressure filling machine and the complete process can be divided into the following stages:

1. First evacuation: following an electronic impulse, the vacuum valve opens and produces a connection to the vacuum channel. The bottle is vacuumed and the air content in the bottle is reduced to about 10% of the atmosphere.
2. Flushing phase: a pneumatically controlled gas needle opens the connection to the ring bowl and, as a result, almost pure CO2 flows from the ring bowl into the bottle, equalising the pressure between the bottle and the ring bowl.

3. Second evacuation: the pneumatically controlled vacuum valve opens again and produces a second vacuum in the bottle. The vacuum thus generated in the process reduces the percentage of air in the bottle to around 1%.

4. Pressuring: A pneumatically controlled cylinder opens the gas needle, allowing the gas mixture to enter the bottle through the return air tube. This causes the filling pressure to accumulate in the bottle. As a result, the pressure in the bottle and in the ring cup is the same.

5. Filling: When the pressure is equal, the liquid stem opens under the control of the spring and the filling process begins. The product flows into the bottle along the return air tube and the small spreader, mounted on the return air tube, deviates the liquid towards the inside wall of the bottle to ensure a gentle flow of product. The pressurisation gas is forced out of the bottle during the filling process and flows into the ring bowl through the return air pipe.

6. Completed filling cycle: as soon as the liquid reaches the lower edge of the return air pipe, the return gas flow is interrupted, ending the filling process automatically. Here the bottle is deliberately overfilled. The double-lift pneumatic cylinder closes the product piston rod and the gas needle remains open.

7. Correction phase: Following an electronic impulse, the correction valve opens and pure CO2 flows into the bottle with a slight overpressure of about 0.2 bar, the excess liquid is forced back into the ring bowl via the return air pipe.

8. Completed correction phase: Due to the overpressure of pure CO2, the liquid is completely removed from the return air pipe. As the amount of CO2 used is precisely defined, a precise filling level can be achieved.

9. Snifting: The snift valve opens the connection to the snift channel. As a result, the pressure in the bottle neck can escape until atmospheric pressure is reached again. The lifting cylinder moves downwards, and the bottle is lowered and transferred to the discharge star.

The representation of a counter-pressure filler is shown in *Figure 6.*

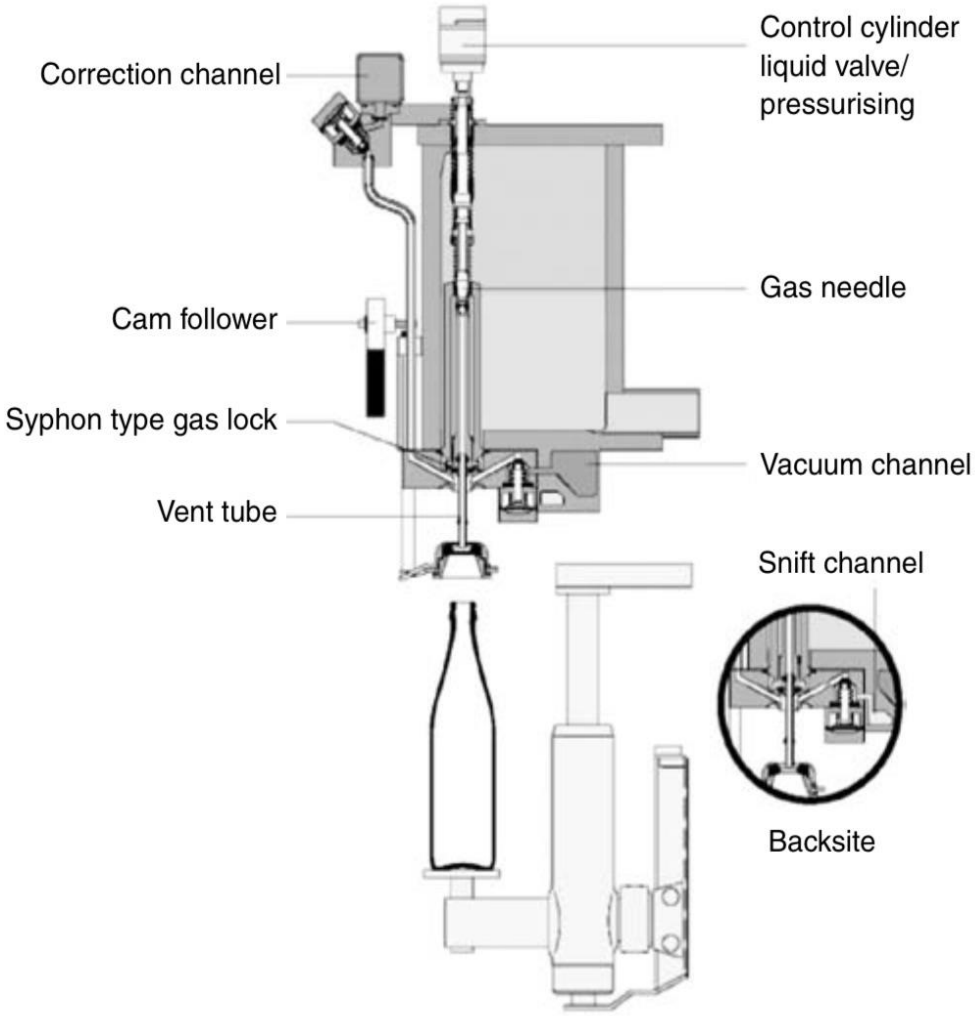

Figure 6: Counter-pressure filler system [Steen D. P., 2006]

3.3. Mechanisms of foam production

Foam is an emulsion of a gas, constituting the dispersed phase, in a continuous liquid phase generally containing a soluble surfactant molecule. The formation of foam is a consequence of the formation of gas within the continuous liquid phase. In turn, the gas is generated in the liquid, generally by heterogeneous nucleation, according to the three phases:

1. Bubble formation
2. Bubble growth
3. Detachment of bubbles

3.3.1. Bubble formation

After a deep examination of the operational sequence, it's been discovered that the main source of bubble nucleation might be identified as follows:

1. Supersaturation state in the system is achieved as a result of the decompression state which precedes the process of gas desorption from the solution;

2. Cavitation areas development in the fluid is due to the flow field that had been generated during the filling process;

3. Gas pockets are entrapped at surface discontinuities that are produced by the liquid flowing along the walls of the bottle

4. The impact of the filling jet causes the entertainment of bubbles under the liquid-free surface.

The following sections will concern these mechanisms and all the factors involved on their occurrence.

3.3.1.1. Desorption

According to chemistry, carbonated beverages are liquid solutions made up of dissolved gases mostly composed of carbon dioxide (CO_2). Therefore, gas solubility is a concept that should be first introduce to understand how bubbles are nucleated by gas desorption. Gas solubility represents the amount of gas dissolved in a solution when it is in the equilibrium state. This property is a purpose of the temperature and pressure of the system. For dilute solutions that are sufficient, including carbonated beverages, Henry's law is applied in the form:

$$C_e = k_H\, p \qquad (1.1)$$

Henry's law is adopted to relate the solubility or equilibrium concentration (in the formula: C_e) of the dissolved gas to the partial pressure (in the formula: p) of the gas over the liquid. k_H in the formula is henry's law constant that depends on three features: the solute, the solvent nature and the temperature. Both k_H and C_e decrease

with increasing the temperature (T). The solution is defined as saturated when gas concentration (C) is equal to gas solubility (C_e). Under this condition, the system is said to be at equilibrium due to the deficiency of a net gas molecules transfer inside or outside the solution. Contrary to this system, if C is higher or lower than V, the solution is defined as undersaturated or supersaturated. Consequently, the liquid has a tendency to absorb gas molecules from the atmosphere or to desorb part of the dissolved gas until it reached equilibrium. The state of saturation is marked by the temperature of the system rising to a fixed pressure [Cyr D. R., 2001]. The same result is given by the gas pressure above the liquid decreasing to a fixed temperature. The bottling process of carbonated beverages is dictated by this second case: the fluid, containing a concentration C_e^{in} of dissolved gas, is initially in an equilibrium state at pressure pin. Then the beverage, whose pressure is lowered to a value p_{fin}, is poured into the container. As a result, Henry's law is no longer satisfied. After the pressure is released, the system is in a supersaturated state in which desorption carbon dioxide takes place in order to reach a new equilibrium state, marked by the new equilibrium concentration C_e^{fin}. Based on these introductory considerations, supersaturation level can be defined as:

$$S = \frac{C_e^{in} - C_e^{fin}}{C_e^{fin}} \qquad (1.2)$$

In case Henry's law is incorporated to *Equation 1.2*, S can also represent the function of the gas partial pressure above the liquid.

$$S = \frac{\rho_{in} - \rho_{fin}}{\rho_{fin}} \qquad (1.3)$$

The excess of gas molecules can be expelled out of the supersaturated solution through the liquid-free surface or, as in the case of interest, can give rise to the generation of bubbles [Lubetkin S. D., 1989].

3.3.1.1.1. Classical Nucleation

Classical nucleation theory is a simple thermodynamic tool that is able to describe the phenomenon of nucleation and to predict kinetic aspects through bubble nucleation speed. Four types of mechanisms of bubble nucleation have been identified:

1. Classical homogeneous nucleation: bubbles grow spontaneously in the bulk of the liquid through a mechanism that must be high-energized in order to provide the formation of a new gas-liquid interface, a high oversaturation value and, therefore, the need to have a large number of nearby gas molecules between them;

2. Classical heterogeneous nucleation: the creation of a new interface take place in small cavities due to the presence of impurities. The oversaturation values are comparable to those in case 1 but the overall process is considered more favoured than the homogeneous one owing to the lower value of energy barrier that the gas nuclei must pass to form bubbles.

3. Pseudo-classical nucleation: it takes place in the pre-existing gas cavities that are on the surface of the container, in the suspended particles and in the micro-bubble appearing in the bulk of the solution, through bot homogeneous and heterogeneous nucleation. Non-classical nucleation can occur as well.

4. Non-classical nucleation: any energetic nucleation barrier is not necessary to be overcome; this nucleation occurs in the pre-existing gas cavities in the surface of the container or in a point of the bulk [Karthika S., 2016].

According to the Classical Nucleation Theory (CNT), a supersaturated liquid solution provides bubble formation thermodynamically. Under suitable conditions, transferring dissolved gas molecules to a gas phase implicates a lowering of the bulk free energy of the system. However, this theory attributes a value of zero to the size of the bubble, so that gas cavities are not present in the system before it is made supersaturated. In the first step the overcome of liquid surface tension is involved, as well as the production of significant interfacial energy. Consequently, the two competing effects head to a global reduction of the system free energy exclusively if the creation of bubble occurs with a certain minimum size. A demonstration of this assumption might start from Laplace's equation, used to describe the steady-state equilibrium of a spherical bubble in a liquid:

$$p_b = p_{liq} + \frac{2\gamma}{R} \qquad (1.4)$$

From *Equation 1.4* it can be deduced that bubbles are able to survive in the liquid as long as its internal pressure (p_b) is higher than the liquid pressure (p_l) of the quantity 2γ/R, where γ represents the liquid surface tension at the liquid gas-gas interface and R is the bubble radius. In case this condition is not satisfied, surface tension acts to contract the bubble. It has been shown that the bubble assumes a thermodynamic equilibrium with the solution only if the concentration of gas that is inside the bubble (C_b) is equal to the residual concentration of gas present in the liquid (C_l). When Henry's law and Laplace's equation are combined, it's been discovered that both conditions are fulfilled only when the radius satisfies the following reaction:

$$R^* = \frac{2\,\gamma}{S\,p_{liq}} \qquad (1.5)$$

Thereupon, if the contribution given by the hydrostatic pressure is registered as neglected and the bubble appears from a pressure release at a fixed temperature, the identity $p_l = p_{fin}$ is obtained. It is important to introduce Δg_v for the estimate of the nucleation process in energetic terms and this index represents the change in the bulk free energy per unit volume associated with the gas molecules transfer from the liquid to the gaseous phase. The variation of this energy is found to be equivalent to the work required in the formation of bubbles in the bulk solutions. Taking the partial derivative of Δg_v with respect of the, it is possible to demonstrate that free energy change has a minimum when R = R*. [Cyr D.R., 2001] is a source for a complete derivation of these expressions. The maximum of free energy change is specified in *Equation 1.6*:

$$\Delta G_v^{max} = \frac{-2\,\gamma}{R^*} \qquad (1.6)$$

Δg_v^{max} represents the energy barrier that must be exceeded in order to have a spontaneous nucleation of bubbles when it is in a supersaturated liquid solution. As proven in *Equation 1.5,* bubble need to be larger than R* to overcome this barrier, so that R* stands for the critical nucleation radius. If the bubble radius appears as lower that R*, gas concentration in the solution is lower than the gas concentration present in the bubble ($C_l < C_b$). Under these conditions, the solution itself tends to re-absorb gas molecules. Consequently, bubbles will shrink until disappearing, unless local energy fluctuations are high enough to sustain the nucleus. On the contrary, bubble that are R > R* ($C_l > C_b$) will continue their growth spontaneously. Classical Nucleation Theory

is useful in offering conceptual basis to understand the phenomenon of nucleation and in allowing a prediction of the kinetic aspects of bubble nucleation through the thermodynamic analysis. In fact, the index of thermodynamic potential, Δg_v^{max}, is the activation of parameters in the expression of J, that is known as the number of "critical" nuclei that had been formed per unit time and per unit volume [Jones S.F., 1999]:

$$J = A \exp\left(\frac{-\Delta G_v^{max}}{k_B T}\right) \qquad (1.7)$$

J represents the nucleation rate and in the *Equation 1.7*, k_B is the Boltzmann constant and Δg_v^{max} represents the energetic barrier multiplied by the volume. The index A is the pre-exponential factor, related to the transfer rate of gas molecules to the nucleus. However, CNT is containing some questionable aspects. Firstly, a thermodynamic approach is used in the description of systems that are not at equilibrium. Secondly, thermodynamic parameters, such as surface tension, are supposedly unchanged at the molecular scale. Thirdly, the theory provides a plausible interpretation of the nucleation phenomenon as long as high supersaturation levels are taken into account. This statement can be clearer if the process in which gas molecules participate in the bubble formation is considered. To get an embryo with a certain critical size, it is necessary to cluster a number of gas molecules. When collateral phenomena, such as turbulent flows, are not present, vibrations or diffusion towards has already dealt with the formation of cavities, gas molecules have organized through random thermal motions. As a consequence, there is a higher probability to have a number of molecules gathered around some point increases with S. In addition, the critical radius R* and the number of molecules required decreases when the saturation level increases, as established in *Equation 1.5.* Many theorical and practical studies as well, have demonstrate that S-values thar are higher than 100 are in the need of obtaining bubble nucleation. This is accurate in case nucleation occurs in the liquid bulk of a homogeneous solution in the lack of pre-formed gaseous cavities. This situation is associated to the Classical Homogeneous Nucleation [Jones S.F., 1999]. When bubbles are nucleated on the surface of the container or on the particles suspended in the bulk (as in Classical Heterogeneous Nucleation) comparably higher values of saturation are required. When it comes to the presence of a surface that is solid, the interface free energy of the bubble is lowered due to an amount that depends on the geometry and wettability of that surface, and the liquid surface tension [Pugh R.J., 1996]. However, thanks to a series of experiments performed on different solutions in gas capillary tubes, a supersaturation levels equal or greater than 100 are obtained to get to bubble formation on the smooth walls of the container, after the complete removal of pre-existing gaseous nuclei [Gerth W.A., 2014]. Bubble nucleation might be preferred at a hydrophobic smooth surface or in small crevices present on the surface than at a hydrophilic smooth surface. In such cases, bubble shape appears to be more similar to a

spherical cap or spherical sector and, the number of gas molecules composing the embryo is reduced, despite the critical radius remains unchanged [Cyr D.R., 2001].

3.3.1.1.2. Relevant parameters

A deep analysis of the literature has distinguished four factors involved in affecting bubble production in supersaturated liquid solutions:

1. The modality of decompression
2. The properties of the solid surfaces immersed in the solution
3. The fluid chemical composition
4. The flow field of the liquid phase

Studying the effects of depressurization in living being, it has been noticed a higher number of produced bubble if the decompressions step ($p_{in} - p_{fin}$) is increased with no changing the decompression rate ($\partial p/\partial t$) and the final pressure when a faster decompression is applied. Results don't show any sign of dependence on the decompression step ($p_{in} - p_{fin}$) and on the saturation pressure (p_{in}) [Skogland S., 2002]. Some experiments on polymeric foams have reported similar trends: the increase of the nucleation rate, the growth rate and the number of bubbles per unit volume when pressure release rate increases [Taki T., 2008]. By considering supersaturating non-Newtonian fluids under different pressure of CO_2, it has been shown that bigger bubbles are nucleated under atmospheric conditions as higher degrees of initial supersaturation are applied [Frank X., 2021]. Studies conducted on soda bottles pointed out that those bubbles are preferentially formed with defects on the surface. Properties of the surface such as roughness and wettability, can enhance or suppress bubble formation. For a given solution, bubble size controls the size of the nucleation sites at detachment. Chemical compounds contained in the solution, that is the type, the concentration and the solubility, also play an active role in bubble nucleation kinetics. A large variety of ingredients, besides carbon dioxide, is present in carbonated beverages: sugars, sweeteners, acids, flavourings, colours, preservatives, alcohol, caffein, salts and proteins. The majority of those substances makes the distinction of the various ingredients effect impracticable. In many cases, it is not possible to know the exact composition of beverages because off the protection of copyright. Nevertheless, literature has been found to possess useful indications of their influence: bubble nucleation rates increase with the concentration of dissolved CO_2 [Belair G., 2006], [Bamforth C. W., 2004]. Bubble growth is governed by diffusion by the concentration gradient VC between the liquid bulk and the bubble interface. This is what is stated in the first Fick law:

$$\Phi = D\ \Delta C \qquad (1.8)$$

The index ϕ represents the flux of gas molecules across bubble interface, meanwhile D is known as the diffusion coefficient. By Pouring champagne wines having different CO_2 content, it's been noted that the larger is the concentration of carbon dioxide, the higher is the column of foam and the faster is its growth [Cilindre C. 2010]. Potassium benzoate and aspartame are example of ingredients that have been identifies as the major responsible for surface tension reduction in carbonated beverages, and they play a role in the explosive behaviour of foam observed in other processes [Coffey T.S., 2008]. Others such as salt, acids and organic compounds are found to be modifiers of the solubility of carbon dioxide since they are able to affect the attractive forces between liquid and gas molecules. Henry's constant k H contains a different values of action results. A decrease in gas solubility has a different way of reflection on bubble formation. On one hand, Henry's law depicted in *Equation 1.1* affirms that a lower gas content can be dissolved in the solution, at parity of pressure and temperature. The pressure of the system must therefore be increased in order to obtain a greater equilibrium. The result might appear in a higher number of bubbles when the pressure is released to the same final pressure, seeing that the decompression step is higher [Balaban M.O., 2021]. On the other hand, when gas solubility is lower, the production of bubbles assumes a reduces speed: according to Graham's law, the rate of diffusion of gas molecules through a liquid phase is directly proportional to its solubility. When bubble nucleation takes place in a moving liquid, the final size of the bubble is smaller [Lockwood G., 2002], [Lee W. T., 2011]. What must be included in the balance quotation for bubble detachment is the shear stress. The liquid role is to remove the bubble from a solid substrate and cause an earlier detachment of the bubble, which remains smaller [Bisperink C. G. J., 1994]. Analysing the formation of bubbles during the pouring of a pre-saturated beer, it's been observed that the mean bubble diameter decreases when increasing the flow rate, while more bubbles are produced per unit time, which helps in indicating the inclusion of shear stress is not sufficient to explain the effect of the flow fields upon nucleation properly. The resulting contribution of the transformation of mechanical shear energy into the surface free energy must be taken into account. This transformation energy appears in a lower energetic barrier (Δg_v^{max}) that needs to be overcome in order to obtain bubble nucleation. As a consequence, a production of s higher bubble nucleation rate is found, as established in Equation 1.7 [Zhou Z. A., 1998].

3.3.1.2. Cavitation

It's been discovered that bubbles can form in a liquid solution by mechanical agitation, independently on the saturation state. This process occurs, for example, when a liquid is stirred. The appearance of bubbles can be

perceived in the flow generated by marine propellers and in Venturi tubes, in the turbulent region downwards the constriction. it is possible to achieve similar effects when exposing the system to ultrasonic field under specific conditions [Wu J., 2008], [Leong T., 2011]. Cavitation is a mechanism underlying all of those situations. Conventionally, cavitation occurs in a flowing liquid system when hydrodynamics effects results in regions of the flow where the pressure falls below the vapour pressure p_{vap}. The result sees a vapour bubble to be nucleated and attracting other gas molecules dissolved in the liquid due to local fluctuations of concentration. The cavitation number σ is introduced, to characterize the dynamical phenomenon of this
fluid. The following expressions defines this non- dimensional parameter:

$$\sigma = \frac{p_{\infty} - p_{vap}}{\frac{1}{2}(\rho_l U_{\infty}^2)} \qquad (1.9)$$

p_{∞} and U_{∞} represent the pressure and the reference velocity of the flow respectively, while ρ_l is the index of liquid density. Through calculation of its value, it is possible to predict if cavitation might occur, once the threshold required to initiate cavitation is known. The cavitation threshold refers to the incipient cavitation number and it is represented by σ_i. Its evaluation might be immediate for a steady flow under the hypothesis according to which the vapour bubble appears instantaneously as soon as the minimum pressure in liquid (p_{min}) reaches p_{vap}. In this case, it is possible to equate the incipient cavitation number to the minimum pressure coefficient Cp_{min}:

$$\sigma_i = -Cp_{min} \qquad (1.10)$$

The minimum pressure coefficient is defined as:

$$Cp_{min} = \frac{\rho_{min} - \rho_{\infty}}{\frac{1}{2}(\rho_l U_{\infty}^2)} \qquad (1.11)$$

Therefore, the value of the incipient cavitation number might be assessed from experimental measurements or from simple theories of calculation of the single-phase flow. Then, for $\sigma > \sigma_I$ (i.e. $\sigma > - Cp_{min}$ and $p_{min} > p_{vap}$) cavitation does not occur. On the contrary, for $\sigma < \sigma_I$ a cavitating flow is obtained. In a real situation, the process is not immediate as it has been assumed and supposedly the cavitation begins as soon as the liquid pressure equates the vapour pressure leads, in general, in order to inadequate conjectures [Brennen C. E., 2013]. One of the main factors causing σ_I to be different from Cp_{min} is the surface tension. Cohesive forces between the liquid molecules give the liquid the possibility to withstand much lower pressure than the equilibrium vapour pressure without the occurrence of cavitation. Many experimental evidenced have supported this thesis and have showed that a pure liquid does not cavitate unless a pressure, high and negative, are reached, up to more than 200 bars [Hu H., 1998].

3.3.1.3. Entrapment

Paragraph 3.3.1.2. highlighted that, gaseous cavities trapped in solid surface, defects ensure useful sites for bubble formation. The filling procedure used in bottling plants for carbonated beverages is an example of how nuclei can be rapidly generated: when the solution flows along the bottle walls, small gas pockets of the pre-existing gaseous ambient remain trapped on the surface. This is a case in which a liquid front advances on a solid surface that contains scratches and conical pits that had been examined: if a sheet of liquid is considered which advances with unidirectional motion and over a conical groove of half angle β, it is possible to obtain two configurations as in *Figure 7*. When the contrast angle θ appears to be lower than 2β, the liquid wets the groove entirely, as the pre-existing gas phase is expelled. On the contrary, when $\theta > 2\beta$, the liquid fronts flow over the groove without reaching its bottoms. Gas cavity in which the entrapment of gas cavity is set. The thickness of the liquid sheet, the half angle β, the size of the groove and the static and dynamic contract angles determine the radius of curvature of the formed meniscus [Enqvist K., 1992].

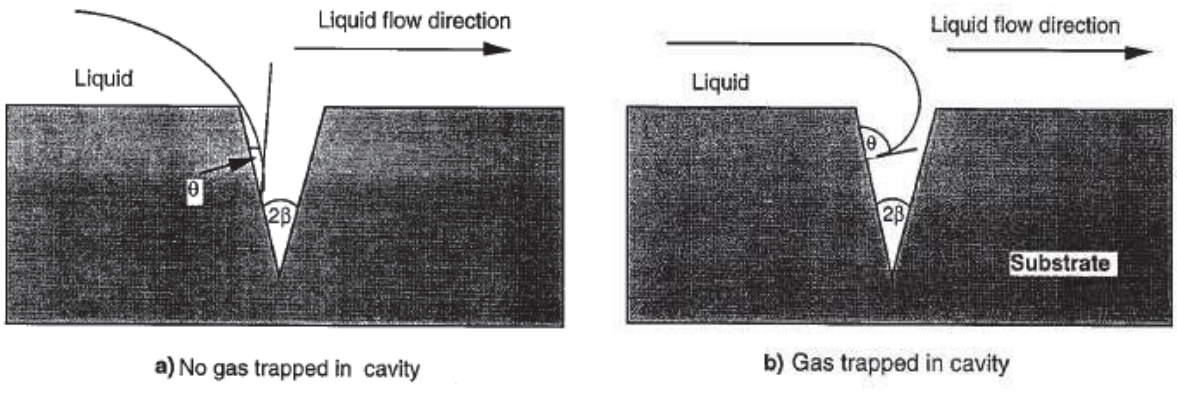

Figure 7: Criterion for gas entrapment when a semi-infinite sheet of liquid advances over a conical groove with half-angle

3.3.1.4. Entrainment

When a liquid jet impinges on a liquid free surface, gas entrainment may happen. This process represents a further mechanism under which and external gas may be integrated inside the liquid in the filling process. In low-viscosity liquids, just like carbonated beverages, gas entrainment only depends on disturbances along the surface of the filling jet [Khezzar L., 2011]. This has been confirmed after the observation of the gas entrainment that didn't occur in the case of a smooth, uniform jet, event with a high Reynolds number (about 14000). Contrary to this, when jet instabilities an involved, gas entrainment becomes readily visible as the jet disturbances reach the liquid free surface. *Figure 8* depicts how the process is leading to bubble formation under the liquid free surface under the action of an impinging cylindrical jet.

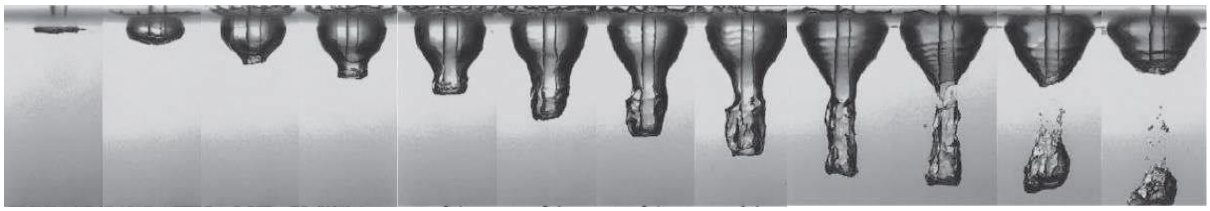

Figure 8: Development of an air crater under the liquid free surface of a deep water pool caused by the impact of a jet disturbance

The sequence of images shows a crater that forms under the liquid surface, when a jet disturbance impinges on the liquid pool. The crater expands thanks to the transformation of the jet kinetic energy into potential energy. After the impact, the jets penetrates further and the crater assumes a deformed condition. When a certain depth is reached, the local hydrostatic pressure counterbalances the outward velocity that was initially imparted to the crater walls. The result registrates a necked form in the crater and the collapse finally starts. The bottom potion of the crater detaches causing a large toroidal bubble and the entrained air continues its movement downwards until it breaks into several smaller bubbles. The upper portion of the crater, instead, retracts towards the free surface. Once the impact process began, the impact of following disturbance produces the entrainment of new bubbles, but then the impact crater is no longer visible [Prosperetti A., 2000]. A continuous entrainment regime is established, as depicted in *Figure 9*, in which the existence of four distinct regimes of gas entrainment have been highlighted by experiments on the impact of continuous liquid jets [Qu X., 2013]. Both the conditions for their occurrence and their characteristics features, on the level of penetrations depth pf the bubble plume, bubble size distribution and void fraction are controlled by several properties, for example liquid viscosity and surface tension, jet impact velocity, transient liquid motion that is induced at impact, and jet turbulence level on which the quality of the jet surface depends. The jet falling

length is known for having a great influence on the impact process. First of all, it happens because L_j affects the impact velocity V_j that can be approximated by the following relation, valid for a vertical falling jet:

$$V_i = \left(V_0^2 + 2\, g\, L_j\right)^{\frac{1}{2}} \qquad (1.12)$$

V_0 and g represents the jet speed at the nozzle outlet and the gravitational acceleration respectively. Second, L_j controls the evolution of jet surface instabilities between the nozzle and the pool surface. This has subsequent development of the impact crater.

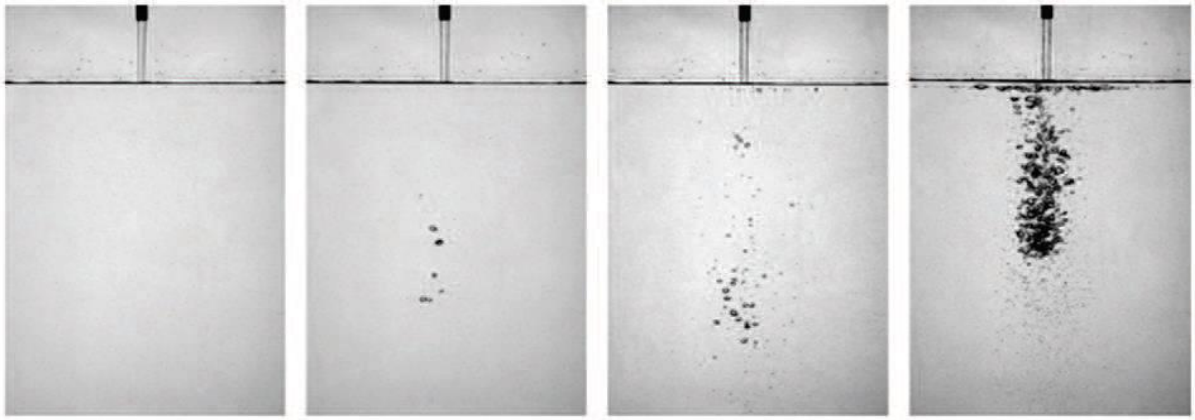

Figure 9: Entrainment regimes produced by a cylindrical liquid jet impinging on a deep pool of the same liquid

For a given system, falling length and impact determine the boundaries between the different entrainment regimes. As L_j and V_j are gradually increased, the system is, therefore, moving from a "no entrainment regime" to a "incipient entrainment regime"; so that, under these conditions, some sporadic and isolated bubbles become visible. When L_j and V_j have higher values, bubble clusters appear intermittently because of the irregular ruptures of the jet before the impact. Finally, for very high values of L_j and V_j, bubble clusters are entrained without interruptions, producing a "continuous entrainment regime". Once fully formed, bubble move deeper inside the pool until the buoyancy force dominates. Bubbles can reach a maximum depth when increasing the jet speed at the nozzle outlet, and they decrease when L_j becomes larger [Khezzar L., 2011]. This kind of behaviour has not been clarified yet however, it is likely to be related to specific features of the jet

stabilities at the moment of the impact. Smaller bubbles are able to go deeper, where they are retained for longer times. Later on, they begin to rise towards the free surface with helical trajectories. However, the conclusion reached after experimental studies on entrainment, are not immediately suitable for the bottling process. First of all, jet turbulence, that is responsible of instabilities attributed to the jet, is strictly connected to the specific conformation of the nozzle. Therefore, the conditions determining the entrainment regime are said to dependent on the particular system. Furthermore, while most of the published studies have to do with a cylindrical jet that is impinging on a deep pool of liquid filled at a constant level, in real bottling applications the beverage is injected with an axial symmetric distribution along walls of the bottle. The conformation of the container affects the evolution of the entrainment mechanism, since the expansion of the impact crater is limited by the proximity of the solid walls. It must not be excluded that the configurations comparable to what is reported in literature can be obtained during filling. Indeed, the flow is prevented by the specific bottle conformation in order to remain confined along the bottle walls throughout the descent. It is more likely that the filling jet detaches from the bottle side: the falling direction of the filling jet should also be considered. It has been shown that impact craters produced by a tilted jet are not symmetric. In fact, crater pinch-off occurs before on the upstream side of the jet, like in its side closer to the free surface. The subsequent crater collapse produces a cloud made of bubbles that is driven to the downstream side of the jet: a turbulent biphasic flow is produced. Finally, the free surface of the beverage should be observed as not fixed in the course of filling. Its rising reflects on the jet falling length L_j which reduces more and more. Therefore, there are different typologies of entrainment that might occur during the process. Moreover, if the jet is tilted, the ascent of the free surface can be seen as a translation of the jet, according to a reference system fixed to the free surface. Based on the direction of translation of the jet relative to its inclination angle, the asymmetry of the crater will either be enhanced or reduced [Duncan J. H., 2011].

3.3.2. Bubble growth

Once the nucleation occurs, bubble growth until detachment. The speed of their growth depends on many factors, such as the surface tension, the viscosity and the speed of molecular diffusion rate at the bubble in the interface. This one is the leading phenomenon of the final growth. The reached bubble size depends on the level and on the nature of scrapings present on the solid surface and so it cannot be related to their cavitation speed [Hepworth N. J., 2004].

3.3.3. Detachment of bubble

To prevent bubble detachment, the balance of forces, in *Equation 1.13,* must be taken into account:

$$F_D + F_S = F_I + F_P + F_B \quad (1.13)$$

F_D is the friction with the surrounding liquid, due to bubble growth; F_S is the surface tension, F_I is the totality of inertial forces involved; F_P is the totality of pression forces that act in the system, and F_B is the comprehensive forces of buoyancy. The first one is responsible for maintaining the bubble in the substratum, while the second one is responsible for removing the bubble from the same substratum. When the first one prevails on the second one, foams are formed.

3.4. Bubble dynamics

The bubble dynamics of three commercial bottled carbonated waters was analysed and the results reported in *Table 3* deal with the concentration of carbon dioxide and of the mixture oxygen/nitrogen of each of them, as well as their dynamic viscosity. What was clearly demonstrated is the significant differences regarding bubble behaviour and their kinetics of dissolved CO_2 escaping the water bulk, under standard tasting conditions. *Table 3* represents the physicochemical pertinent properties of the three carbonated waters investigated, particularly, dissolved CO_2, and non-CO_2 gases (O_2 and N_2) initially held in the closed PET bottled waters, as well as their dynamic viscosity [Belair G., 2015].

Table 3: Physicochemical pertinent properties of the three carbonated waters investigated

Water sample	$[CO_2]$ c_i ($g\,L^{-1}$)	Non-CO_2 gases (O_2/N_2) ($mg\,L^{-1}$)	Viscosity η ($\times 10^{-3}$ Pa s)
LCW	3.25 ± 0.08	17	0.98 ± 0.01
MCW	4.53 ± 0.15	8.5	0.99 ± 0.01
HCW	6.87 ± 0.28	9.5	0.99 ± 0.01

1. A low carbonated water (labeled LCW);
2. A medium carbonated water (labeled MCW); and
3. A highly carbonated water (labeled HCW).

It was certainly demonstrated that, the higher the concentration of dissolved CO_2 initially found in the water bulk:

(1) The lower the lifetime of the cloud of bubbles, as it can be seen in *Figure 10.*

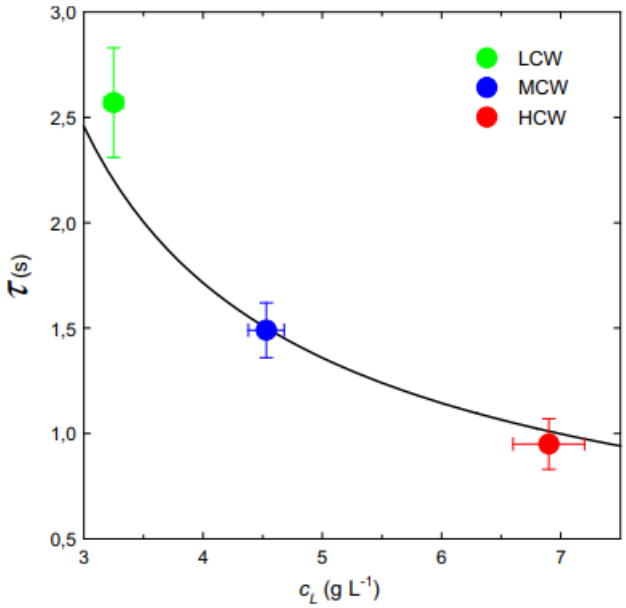

Figure 10: Lifetime of the cloud of bubbles as a function of the initial dissolved CO_2 concentration for the three different cases of carbonated water

(2) The higher the kinetics of dissolved CO_2 discharging from the water bulk (as well as corresponding volume fluxes of gaseous CO_2 outgassing from the goblet) and,

(3) The more rapidly bubbles increase when they are stuck on the plastic goblet.

A series of snapshots show the progressive growth of bubble that is stuck on the bottom of a plastic goblet poured with HCW, in a 30 seconds period, as displayed in *Figure 11*. This image shows a close examination of the sequences about several coalescence events between bubbles growing close to each other. Coalescence events can also increase artificially the growth rate of bubble, and therefore the average of bubble size distribution on the bottom of the goblet.

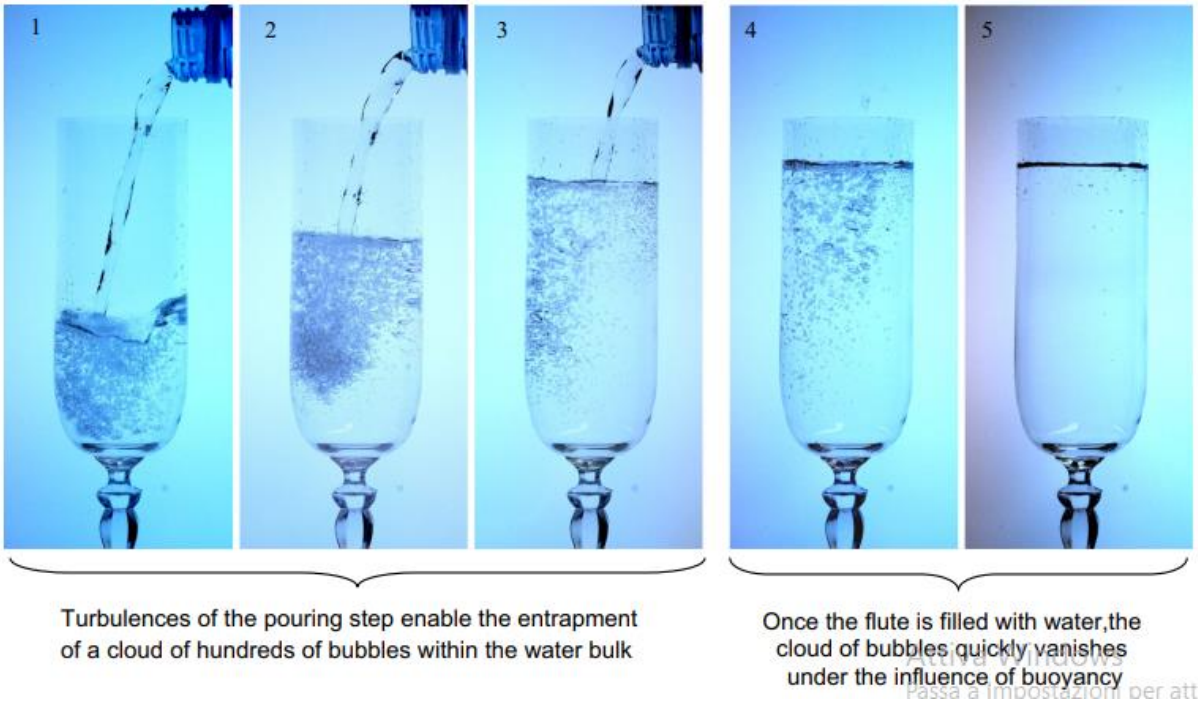

Figure 11: Series of snapshots during the pouring process

Moreover, it is important to point out that bubbles grow very closely to each other but, without coalescing, and they show growth rates that are much smaller than single bubbles that growth far from their neighbours, as in *Figure 12*. In these cases, bubble compete with each other for dissolved CO_2, since they literally bubbles "feed" with dissolved CO_2 that comes from the same environment, which contributes to decrease their respective growth rates. Growing bubble represented in *Figure 13* confirm that in the same period of time, the single bubble (S) grows faster than the three bubbles growing close to each other [Belair G., 2015].

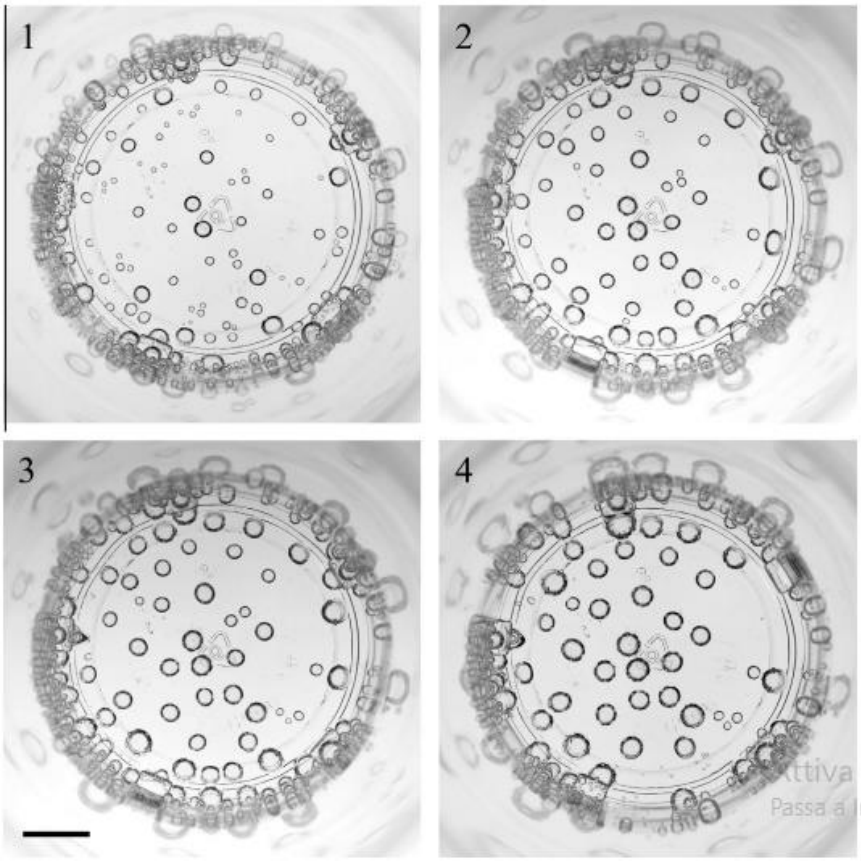

Figure 12: Time sequence showing bubbles growing stuck on the bottom of the plastic goblet poured with the carbonated water sample

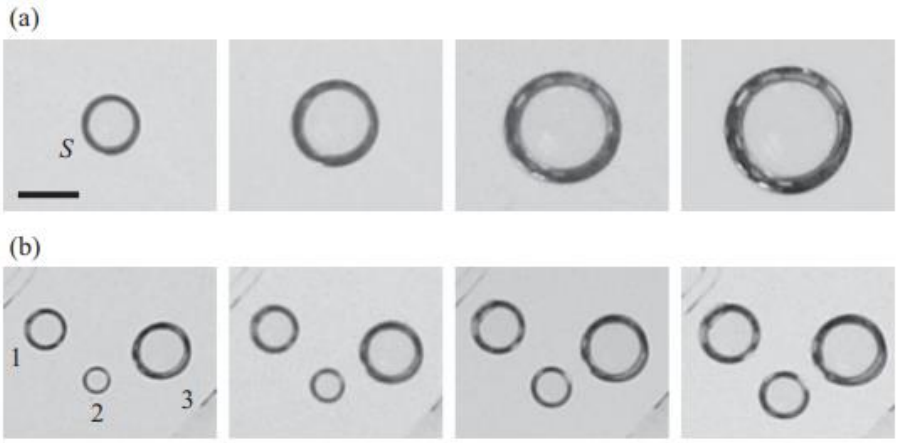

Figure 13: The diameter of the single bubble far from neighbouring bubbles (a), grows faster than the diameters of the three bubbles growing close to each other's (b)

This observation is self-consistent with a recent study in an aqueous solution slightly supersaturated with carbon dioxide. The study observed that the growth rate of a pair of bubbles that grow close to each other is actually slower than the single bubble case, and this suggests that each bubble, when paired, influences the growth rate of the other one [Enriquez O. R., 2013]. To get to compare the respective bubble growth rate of other bubbles growth rate with each other in many water samples, the progressive increase of many bubble diameters was systematic followed with time, that is for a single bubble that grows as far as possible from the neighbours, to prevent both coalescence and competition with regard to diffusion of dissolved CO_2. *Figure 14* collects three various kinetics of bubble diameter increasing with time, in a 30 seconds period of time and 5 minutes after pouring, in the three various carbonated water samples. The general trend of data series demonstrate that bubble diameters increase linearly with time in an ambiguous way, therefore it confirms the likely growth of CO_2 bubbles under convention conditions, as *Equation (1.14)*

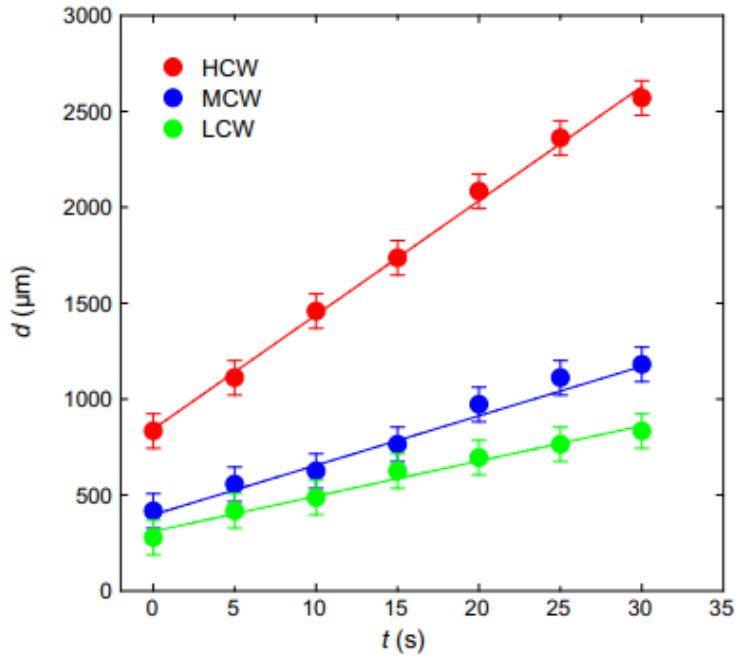

Figure 14: Bubble diameter vs. time, for single bubbles for the three various carbonated water samples

$$r\,(t) \propto \frac{R\,T\,D}{P}\,\frac{\Delta C}{\lambda}\,t \qquad (1.14)$$

Here P is the pressure inside the bubble, $\Delta c = c_L - c_0$ is the dissolved CO_2 molar contraction between the water bulk and the bubble interface in Henry's equilibrium with gas phase CO_2 in the bubble, as in *Figure 15*, and λ is the thickness of the diffuse boundary layer in which the gradient of dissolved CO_2 contraction is in existence. In particular, *Figure 15* shows that the concentration of dissolved CO_2, where is close to the bubble interface, is in equilibrium with the gas phase CO_2 into the bubble and that it is equal to c_0; when it is, instead, far from the bubble interface, the concentration of dissolved CO_2 is equal to the liquid bulk c_L; a gradient of dissolved CO_2, which is the leading mechanism behind diffusion of dissolved CO_2 and bubble growth, exists within the diffusion boundary layer.

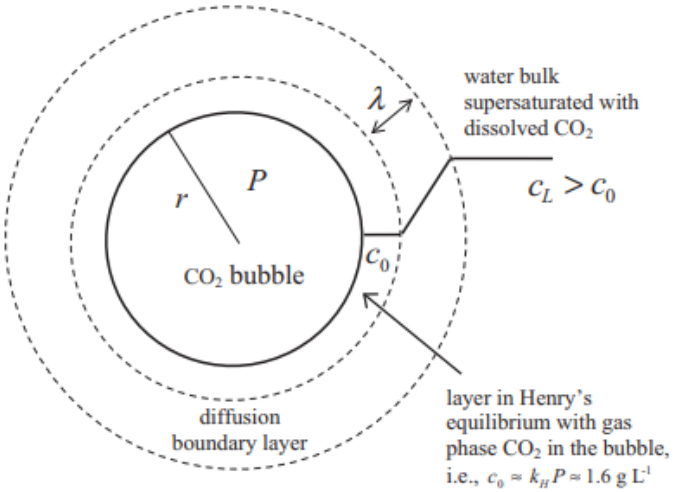

Figure 15: Diffusion boundary layer and bubble interface

As mentioned before, *Figure 14* shows how the diameter of bubbles has a function in time and in the bubble growth rate, which can be derived by linearly fitting bubbles diameter increase with time. The slop of each data represented in that same figure, corresponds to the experimental growth rate k of a given bubble growing in each water sample. Then, *Equation 1.14* shows how the slope of the diameter vs time data series corresponds to the theoretical prefactor, in which represents the only unknows parameter. Indirectly, it can be found by equalling this theoretical perfactor with the corresponding experimental bubble growth rate k, as appears in *Equation 1.15:*

$$\lambda = \frac{R\,T\,D}{P}\,\frac{\Delta C}{K} \qquad (1.15)$$

Table 4, reports the thickness of the diffusion boundary layer and the bubble growth rate k, related with the difference in dissolved CO_2 between water bulk and bubble surface in Henry's equilibrium with gas phase CO_2 within the bubble [Belair G., 2015].

Table 4: Experimental bubble growth rates, and corresponding thickness of the diffusion boundary layer around the growing bubble, in relation with the difference in dissolved CO_2

Water sample	$\Delta c = c_L - c_0$ (5 min after pouring, g L^{-1})	Bubble growth rate, k (µm s^{-1})	Diffusion boundary layer thickness, λ (µm)
LCW	1.46 ± 0.09	9 ± 2	166 ± 47
MCW	2.55 ± 0.18	13 ± 2	201 ± 45
HCW	3.98 ± 0.42	28 ± 6	146 ± 47

3.5. Foam stability

The factors playing a major role in the production of bubbles during bottling have already been revealed. The control of the foam might be possible when governing those factors by prevents or inhibiting its formation, at least. Methods acting on foams that are prior to its complete formation are known as "antifoaming" methods. It's been identified an alternative approach to the reduction of foam I about the acceleration its collapse once it is developed. Methods acting on existing foams are known as "defoaming" methods. To have a better understanding of how foam destruction can occur, the mechanism occurring in the column of foam after its formation must be examined. Every foam is thermodynamically unstable because their high interfacial free energy. Therefore, a column of foam will decay spontaneously over time, the rate of deterioration is dictated by the kinetics of four processes [Shokribousjein Z., 2011] that are:

- Disproportionation
- Gas diffusion
- Drainage
- Coalescence

3.5.1. Disproportionation

Disproportionation, also named Ostwald ripening, involves the diffusion of gas molecules between adjacent bubbles with different sizes. From Laplace's equation, that is *Equation 1.4*, it can be claimed that smaller bubbles possess larger internal pressures compared to bigger bubbles. Therefore, a concentration gradient is created and it causes the diffusion of gas molecules across bubble interfaces. Larger bubbles are able to grow further at expense compared to smaller ones. As a result, the skin of larger bubble becomes weaker and weaker, meanwhile smaller bubble collapse. The process of disproportionation is more active when dealing with soluble gases, so that, for example, in the case of carbon dioxide in carbonated beverages. Thanks to this, the diffusion rate is faster. Moreover, the gas transfer is favoured when the bubble interface is settled by simple surfactant monolayers rather than by thick elastic layers that are made of proteins or polymeric films. Indeed, the properties of the surfactant layers, can affect gas permeability [Salerno E., 2014].

3.5.2. Gas diffusion

Similar to the case of disproportionation, gas molecules can be moved to the ambient atmosphere from those bubble that are located at the top of the foam column. Here, the process is dictated of pressure gradients too, but the difference is that pressure arises between the interior of the bubbles and the external environment. Once the gas is expelled, bubble radius decrease and the pressure difference become larger, so accelerating the diffusion process. In addition, gas transfer is favoured when the bubble interface is settled by simple surfactant monolayers rather than by thick elastic layers that are made of proteins or polymeric films. Indeed, the properties of the surfactant layers, can alter gas permeability [Salerno E., 2014].

3.5.3. Drainage

Foams can be seen as the aggregation of bubble separated by liquid film. The liquid drains downwards in the foam column through the network of channels around the bubble, all due to gravity. So that, bubble film gets thinner and thinner, until the bubble collapses. Bubble rupture is usually happening from the top of the foam column, since films are thinner and more liable to external disturbances [Starov V., 2021]. As a second effect of gravity-induced drainage, structural changes are clear in the foam column and spherical evolve more and more into polyhedral cells with almost flat sides. The junction channels between the cell interfaces carries the name of Plateau borders, as in *Figure 16*. Differences in curvature lead to pressure differences between adjoining thin films: the pressure is low, and the film thicker, at Plateau borders compared to the space between two bubbles. As a consequence, the liquid might be sucked by capillarity in the Plateau borders, producing a second form of drainage and resulting in a further thinning of the liquid films.

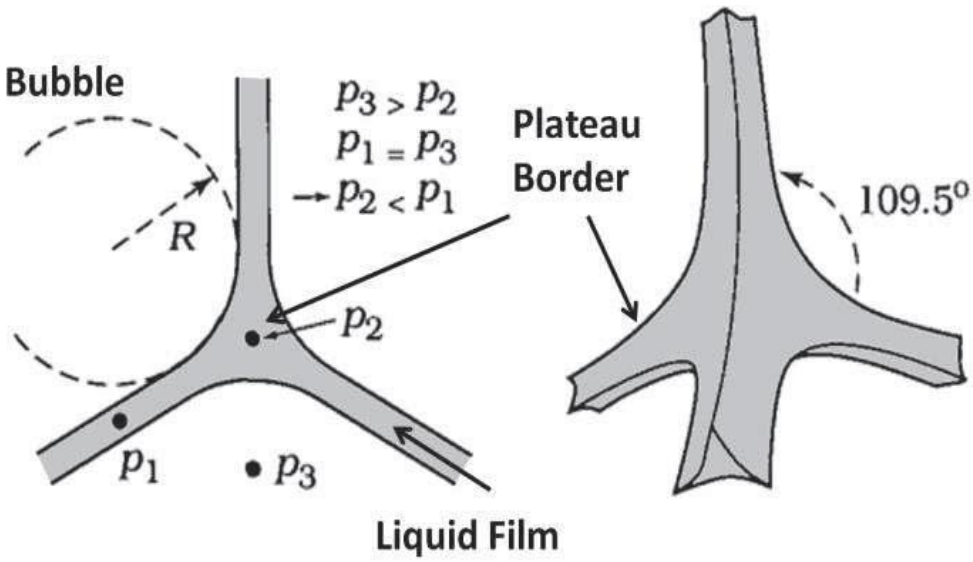

Figure 16: Plateau borders

The drainage rate is lower for those liquids that have a higher bulk viscosity. High surfactant on the bubble interfaces participates in decreasing the kinetic of foam drainage, since their production of a higher surface viscosity through adhesive or cohesive bounding. However, bulk and surface viscosity improve the resistance to thinning and rupture but don't take part directly to foam stabilization. As *Figure 17* shows, liquid drainage stimulates a dilatation of the bubble interfaces, which result in a lower density of the absorbed molecules. Therefore, surface tension (γ) increases locally and this is in contrast to further surface deformation by virtue of surface elasticity (Gibbs effect). Under dynamic conditions, surface tension increases causing the diffusion of surfactant molecules from the region at lower γ to the depleted zones (Marangoni effect). This kind of displacement of surfactant molecules is able to carry a considerable amount of underlying liquid by viscous drag, so that the initial film thickness is restored. Via restoring mechanism, foams can remain up to some tens of seconds after their formation. The magnitude of the restoring force provided by the Gibbs-Marangoni effect is governed by the concentration and the diffusivity of surfactants at the interfaces and in the liquid film. If the solution appears to be too dilute, the differential surface tension is insufficient to neutralise liquid drainage. When surfactant concentrations are high, surfactant molecules in the liquid film spread instantaneously to the interfaces filling the depleted sites. Afterwards, the differential tension relaxed in a way too fast and Gibbs-Marangoni effect provides an opposite result, accelerating the thinning of the liquid, instead of neutralise.

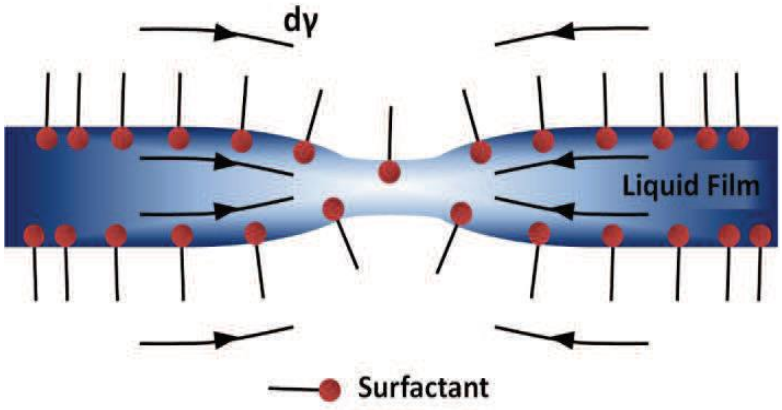

Figure 17: Thinning of the liquid film between two adjacent bubbles due to drainage

Different effects are included in foams containing stronger surfactant molecules, such as detergents and suspended particles, proteins and long-chain fatty acids in high concentration, that are near or above the critical micellar concentration. The thinning of the liquid film that follows drainage provides interfacial forces between the bubble interfaces and those forces cover van der Waals interactions, electrostatic double layer repulsion and structural repulsion that are caused by steric hindrance. Their combined action appears in a positive pressure, referred to a disjoining pressure, that compensates the capillary pressure and neutralise further drainage. This is encountered when the liquid films are so much thin that their thickness is in order of magnitude of intermolecular forces. However, if external disturbances don not intervene, such as vibrations, temperature gradients, evaporation and diffusion processes, then the thin liquid films remain stable almost in an indefinite way, and foams having a lifestyle ranging from a few minutes to several hours are obtained. In carbonated beverages, interfacial forces play an important role in the case of beers, since the protein content is fairly high in those systems. As for soft carbonated beverages, the transient behaviour of the foams formed from these solutions supposes that only the Gibbs-Marangoni effect is contributing to foam stabilization [Petkova B., 2020].

3.5.4. Coalescence

The last process taking part in foam decay is coalescence. Coalescence happens when the interfaces of two adjacent bubbles merge by producing a single and bigger bubble. The new bubble appears as unstable, due to the increased size. Coalescence can be mediated by hydrophobic particles dispersed in the liquid film that bridge the bubble interfaces. As represented in *Figure 18*, contact angles involved in such a configuration produce an increase in the pressure of the liquid film adjacent to the particle. This makes the liquid to flow

away from the particle leading to enhanced drainage and the formation of a hole. This mechanism of collapse is known as “bridging-dewetting” [Ronteltap A. D., 1989].

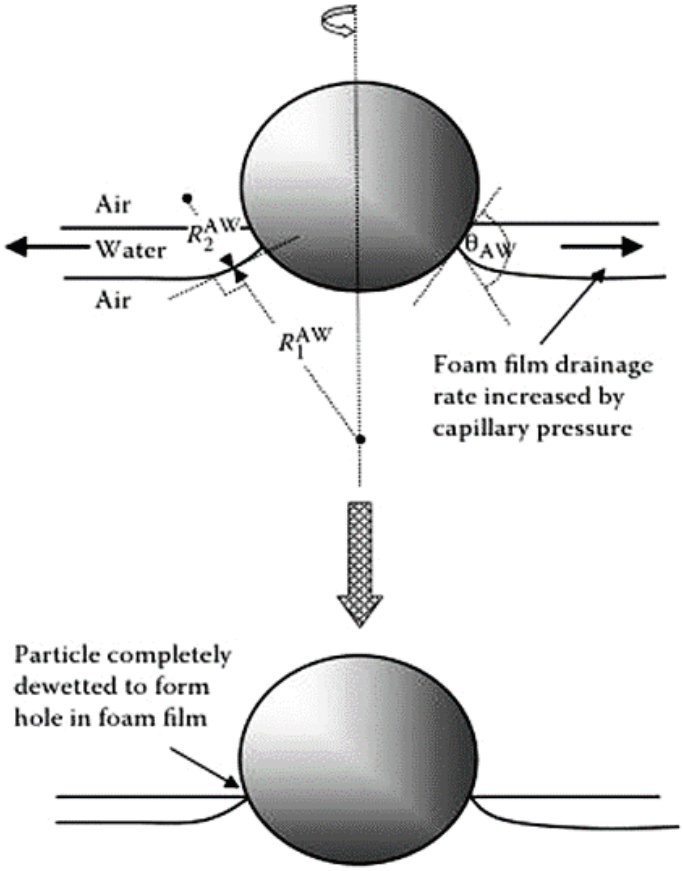

Figure 18: Coalescence mediated by a spherical hydrophobic particle bridging two bubbles

3.6. How to avoid foam

3.6.1. Chemical additives

Despite the complexity of the entire process, it is easy to deduce that using chemical additives is the most immediate method to suppress foam. Indeed, the production of antifoaming chemical agents and their research methods of investigation have been largely grown in the latest decades. Their application against mechanical methods have been favoured by reduced costs associated to chemical methods. Depending on the principle of their operation, four groups of chemical additives have been identified [Karakashev S., 2012]:

- Substances that reduce bulk viscosity and so enhance drainage;

- Substances that reduce surface viscosity and elasticity by counteracting or replacing absorbed molecules;
- Substances that nullify the electrostatic repulsion between bubble interfaces and,
- Substances that promote coalescence and interface rupture

3.6.2. Ultrasonic vibrations

However, in some applications, it's not acceptable the use of chemical agents since they might alter the characteristics of the liquid product, as in the case of carbonated beverages. A reliable alternative to chemical additives is the application of ultrasonic waves that produce thickness fluctuations in foam films and lead to accelerated drainage and film rupture. The notion of stabilizing foams by ultrasonic vibrations was developed several years ago [Anjali C., 2004], [Winterburn J., 2007]. However, the arrangement of ultrasonic defoaming systems for commercial use has been restricted for a long time by the scarcity reliable quantitative outcomes. In many studies, it has been demonstrated that ultrasound can produce foam destruction, however, they are also able to increase its formation and stability. Results illustrated in [Leong T.,2011], [Kentish S., 2014], [Hung S., 2011] embodied this contradictory behaviour. In [Winterburn J., 2007] was underlined the effect produced by vibrations on the foam system which is depending on the frequency and amplitude of the waves that are emitted. Another affecting parameter is the positions as well as the dimension of the vibrating unit. In particular, it has been proved by those authors that the application of vibrations of 20 kHz in frequency are favourable in promoting foam destruction. It is attributed to the excitation of squeezing mode surface waves present in the liquid film between bubble, with drainage acceleration as a consequence. Ultrasonic vibrations increase effectively, when using a broader vibrating tip at a small distance from the top of the foam column. Under these conditions, faster destabilization and energy consumptions that occur are reduced. ([Morey M., 1999] monitored that the use of ultrasound in foam destruction can also happen under dynamic conditions, that is the course of bubbles production. From the balance between the generation and rupture process, an equilibrium foam height can be measured from experiments: the collapse is faster and the equilibrium height decreases as the amplitude of the ultrasonic waves increases. The faster rate of foam collapse in an applied ultrasound field is not an exclusive consequence of the enhanced drainage. As the work of [Anjali C., 2004] revealed the rupture of the liquid film in the presence of ultrasonic vibrations might occur at a larger critical film thickness. Moreover, an increase in the emitter diameter results appears in a larger exposed area of the column. Therefore, foam collapse across the column cross-section is more uniform and its diameter is a relevant parameter in the determination of the rate of collapse, since it is affecting both the migrations and the drainage of the liquid towards the walls of the container. Instead of continuous vibrations, periodic

ultrasound vibrations cab also be applied in foam destabilization. This method, might be a reliable option for a fully development of foams. In this case, the rate of deterioration is slower, so a drastic reduction in the energetic costs, that is related to the power consumption, is obtained. More detailed work is required in order to find the optimal conditions for the application of this technique, as for duration and periodicity of the pulses, stage of foam development and type of solution.

3.6.3. Electronic Pulse Volume Measurement

A flow rate filling valve was designed and built by [Min O., 2019] in order to understand the. filling features of a high-speed carbonated soft drink fill system, as it is shown in *Figure 19*; an electronic flow meter was used in order to conduct tests to understand the characteristics of the flow supply and filling. The authors achieved the high flow rate filling by using a pulse output type flow meter. The system was built by adding a dualizing control system so that it could charge at high speeds.

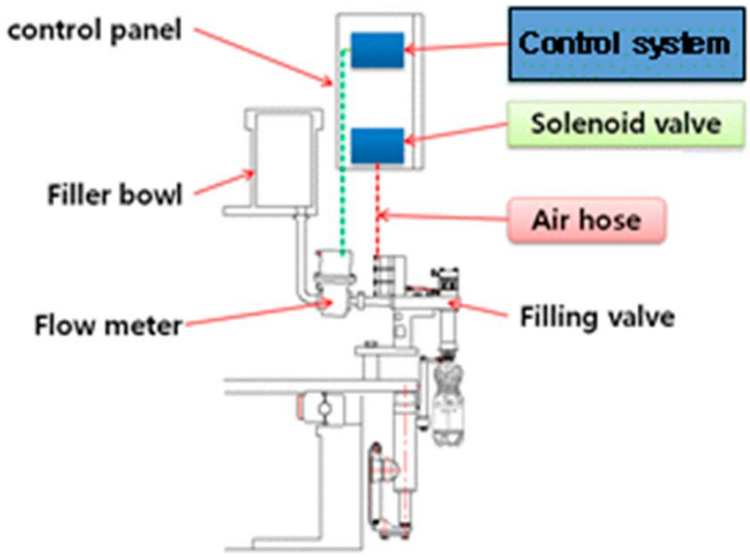

Figure 19: Components of a high-speed carbonated soft drink flow rate filling system

The filling process algorithm of a filler that is using the pulse flow rate method is shown in the flow chart in *Figure 20*. According to this demonstration, the filling valve counter pressure is a process in which the pressure of the filler bowl and the bottle are balanced. The filling valve and the liquid valve is the process in which the main valve filling up the bottle, is opened and the filling valve slow-fast fill valve is the process in which the filling speed moves from the initial high speed to a lower speed when the bottle is almost full; 80% full when

the target volume is 500 gr, at 400 gr, the snifting valve is a process in which the residual pressure inside the bottle is displaced after the filling is over. When filling the bottle, the main element is the control of the level of the bottle and its pressure. In case both level and pressure should be controlled as in carbonate filling, a small amount of change in the pressure can cause significant modification on the filling precision.

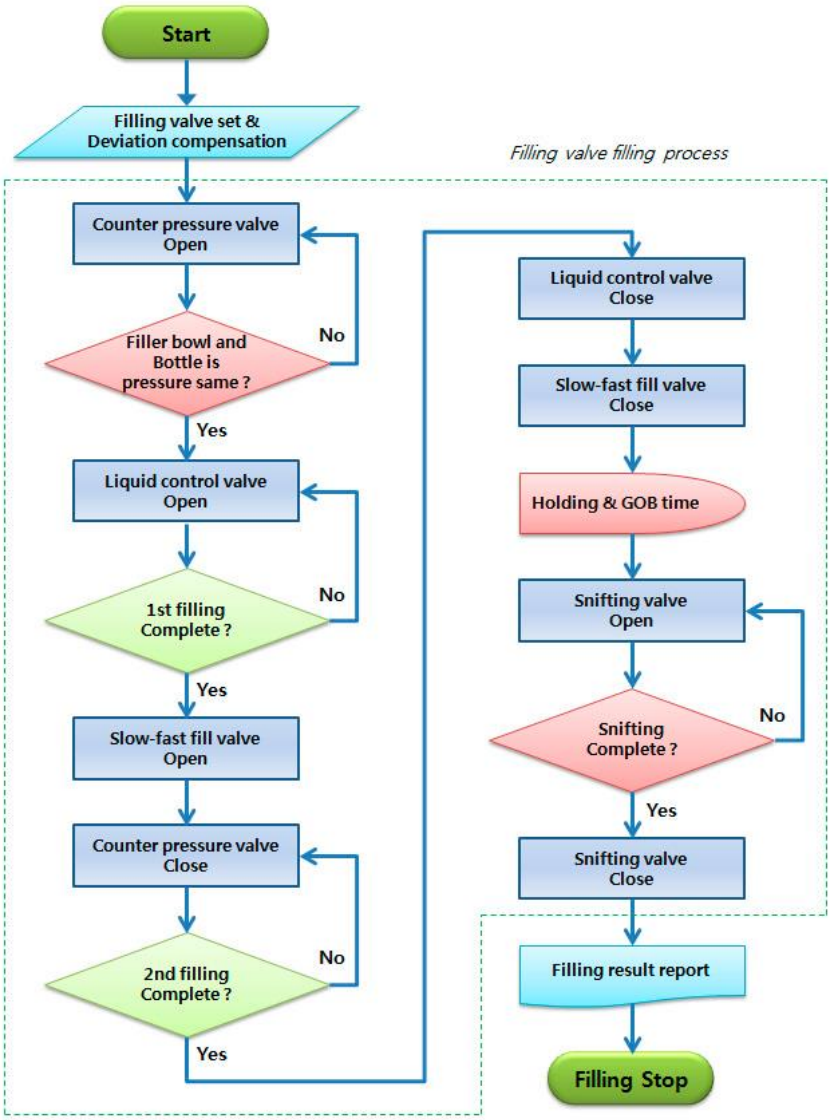

Figure 20: Filling process algorithm

What is represented in *Figure 21* is the interface that shows and configure the PID (a piping and instrumentation diagram) of the level and the pressure of the filling bottle. Then, for the controller, the automatic tuning configuration and programs were applied to optimise the pressure of the filling bottle and the level; pressure and level are in charge of controlling PID value. Therefore, the optimised PID value can be

found with a single touch. The pressure control is implemented as represented above. Thus, the system is competent of controlling the pressure up to ± 0.1 kg/cm 2 and the level ± 3 mm.

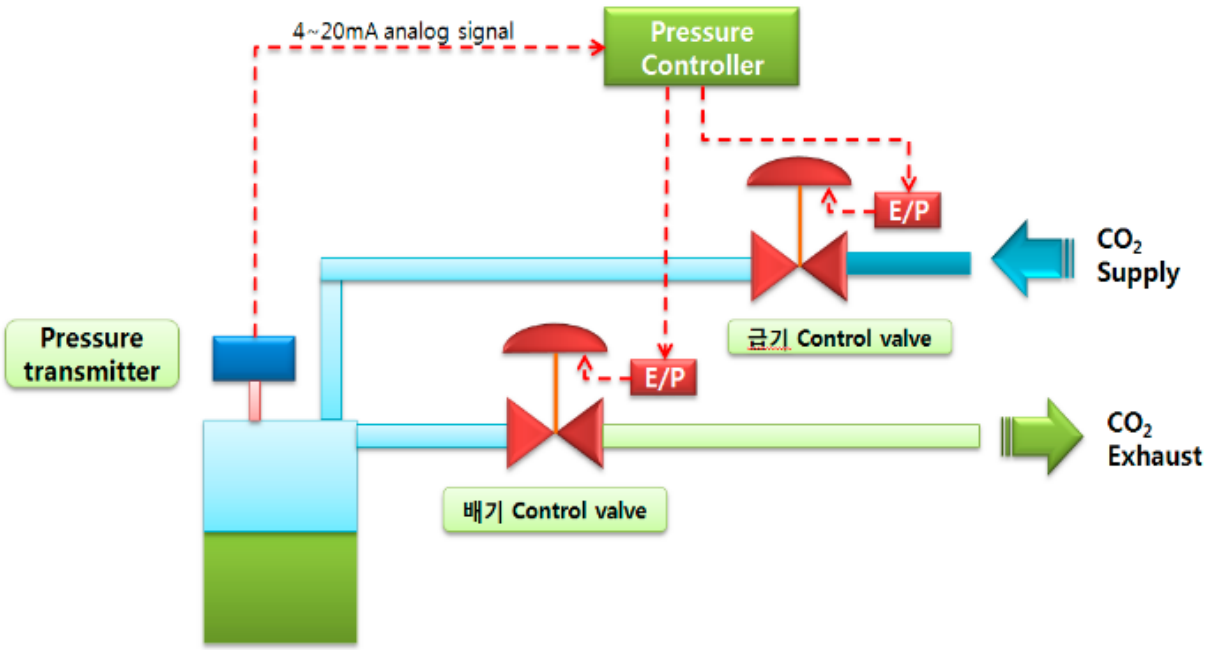

Figure 21: Filler bowl pressure control structure

According to this, filling can be controlled by the flow rate control when solving the inconstancy in filling pressure by adjusting the back pressure during filling. However, in mechanical filling, various filling conditions cannot be controlled since they are variable, such as pressure, time, temperature etc., individually, but a switched to the pulse flowmeter type electronic filling valve, removed every ambiguity of the inconstancy in the electronic flow rate pressure through compensation, so that optimisation might be implemented. When filling with pressurized fluid occurs, there are valves that match the filling pressure to the pressure of the filler bowl and the pressure of the filling bottle, and the filling valve separately, so we are capable of matching the same pressure, decreasing faulty filling and increasing filling efficiency. This leads to an increase in the filling time since back pressure is applied if there is differential pressure. So now, pressure can be monitored in the case of filling valves, faulty filling decreases and filling efficiency increases by gas volume when filling carbonate by the control of the differential pressure and the calibration of the pressure deviation by adjusting the differential process. Therefore, it is possible to complete the filler with high versatility and good efficiency.

4. LABORATORY EXPERIMENTS ABOUT FOAMING

Foam stability, as explained in *Paragraph 3.5.,* is a factor that plays one of the most important roles in the bottling process of carbonated drinks. The objective of bottling companies is to maximise the flexibility and efficiency of their bottling processes, minimising not only the impact they can have on the environment, but also the waste of the final product. With regard to process flexibility and efficiency, both in terms of costs and quantity of final product, time plays a fundamental role: the shorter the bottling time, the more drinks will be bottled in a given amount of time and the lower the production costs related to the same amount of time. With regard to the waste of the end product, the formation of foam and its relative stability must be considered in order to minimise this waste. Obviously, this argument cannot be unique to all types of beverages, because for each one of them, different times, foam formation and stability must be considered, and therefore different management of the process in question. To this end, three different mixtures were observed to see if it is indeed the different types of ingredients that lead to different foam growth and stability.

4.1. Input data and equipment

In this laboratory experiment, three different types of sugar mixtures listed in *Table 5* were studied:

Table 5: Three mixtures used in the experiment

MIXTURE 1	MIXTURE 2	MIXTURE 3
Water	Water	Water
Citric acid	Citric acid	Citric acid
Granulated sugar	Fructose	Stevia

The three mixtures consist of only three simple ingredients: water, citric acid and sugar. As can be seen from *Table 5*, they differ only in the sugar component they contain. In fact, the three mixtures contain equal amounts of granulated sugar, fructose and stevia, mixed in an identical amount of water and citric acid, as can be seen in *Tables 6, 7* and *8*:

Table 6: Ingredients of mixture 1

MIXTURE 1	**Quantity**
Water	70 ml
Citric acid	0,04 g
Granulated sugar	7,89 g

Table 7: Ingredients of mixture 2

MIXTURE 2	**Quantity**
Water	70 ml
Citric acid	0,04 g
Fructose	7,89 g

Table 8: Ingredients of mixture 3

MIXTURE 3	**Quantity**
Water	70 ml
Citric acid	0,04 g
Stevia	7,89 g

Carbon dioxide is a fourth key ingredient common to all three mixtures and is only added to them later than the other ingredients. Furthermore, while the other ingredients such as water, citric acid and sugar were added in clearly defined quantities, carbon dioxide was added later to the mixtures in variable but comparable quantities for each of them. The carbon dioxide used in this experiment was provided by a tank shown in *Figure 22* at an average pressure of about 6.5 atm.

Figure 22: Tank containing carbon dioxide

The amount of carbon dioxide emitted by the gas tank was measured using a rotameter attached to it. The rotameter, which is an instantaneous meter for small flow rates, is described in *Annex VII.* After being formed, each mixture was placed inside a cylindrical glass reactor at a pressure of 1 atm and at room temperature, as shown in *Figure 23.*

Figure 23: Cylindrical glass reactor

It is within this device that, through a nozzle, carbon dioxide has been inserted into each of the three mixtures. The nozzle is the end part of the pipe that joins the cylindrical reactor to the gas cylinder. The size of its diameter determines the average size of the diameter of the bubbles created inside the mixtures after the carbon dioxide has been added: the smaller the diameter of the nozzle, the smaller the diameter of the bubbles formed. Since the desired bubbles in this case must be as small as possible, the size of the diameter of this nozzle has been reduced by inserting a very fine wire mesh into the nozzle duct. The characteristic dimensions of the cylindrical reactor, the nozzle and the wire mesh are listed in *Table 9:*

Table 9: Characteristic dimensions of the cylindrical reactor, nozzle and wire mesh

Reactor height	13 cm
Reactore volume	102 cm^3
Reactor diameter	3,16 cm
Reactor section	7,84 cm^2
Nozzle diameter	3 mm
Wire mesh size	0,18 mm

4.2. Description of the experiment

First of all, the three mixtures were created separately by combining water, citric acid and granulated sugar for mixture 1; water, citric acid and fructose for mixture 2 and water, citric acid and stevia for mixture 3. Each of the three mixtures, one at a time, was then poured into the cylindrical glass reactor from above. It is important to specify that, when switching from one mixture to another, the cylindrical glass reactor was thoroughly washed and dried to avoid any contamination. The system consists of a graduated cylindrical reactor. It is connected from below to the gas cylinder through a nozzle which has an adjustable tap. In turn, the gas cylinder is connected to the nozzle through a valve which, when open, allows carbon dioxide to escape. In addition, the gas cylinder is also connected to the rotameter, so that the flow rate of carbon dioxide entering the reactor can be regulated. Initially, the tap on the nozzle connecting the reactor to the gas cylinder is closed, as is the valve that allows carbon dioxide to flow out of the cylinder. At this moment of no flow, the rotameter also marks zero and therefore the mobile float is positioned at the bottom of the tube. Next, the nozzle inlet valve is opened and then gradually the gas cylinder valve is opened. At this point, the carbon dioxide starts to leave the cylinder valve and reach the reactor nozzle, through which it also meets the mixture. The precise

moment when the carbon dioxide comes into contact with the mixture can be seen when gas bubbles start to emerge from the nozzle and rise along the mixture to the free surface. As the flow rate of carbon dioxide into the mixture increases, so does the number of bubbles create. As the flow rate increases, the float inside the rotameter rises to indicate the increased flow from the gas cylinder. When the number of bubbles begins to be sufficiently high, and therefore when the flow rate of carbon dioxide into the reactor reaches a certain range, the mixture begins to agitate until it forms foam on the surface of the free surface. By observing the graduated lines on the reactor, from the moment when the foam starts to form, a rise in the mixture and thus also in the free surface in contact with the atmosphere above can be seen. A further increase in the amount of carbon dioxide entering the reactor corresponds to an increasing amount of foam forming on the free surface. At a certain point both the nozzle tap and the cylinder valve are closed, instantly preventing carbon dioxide from leaving the gas cylinder and entering the reactor through the nozzle. From this moment, the foam that has formed begins its decay process until it is completely extinguished: the more stable the foam formed, the longer the decay and the longer it takes for the mixture to return to its initial conditions. The experiment was reproduced in exactly the same way for all three mixtures and it was noted that not only the amount of foam formed on the free hair, but also the time it took to return to its initial conditions, were different in each of the three cases. Therefore, since the only ingredient to change is the sugar component, the behaviour of the foam depends on the type of sugar used in the experiment and in particular its chemical and physical properties.

4.3. Data collection

Once the rotameter had been calibrated, as it can be seen in *Annex VII,* the experiments for the three mixtures were started one at a time. Each mixture was placed in the cylindrical reactor under quiet conditions: the nozzle tap and cylinder valve are now closed. Subsequently, carbon dioxide was also added in quantities equal to the range of values previously measured by means of the rotameter, and at four different times, corresponding to the four equilibrium positions of the float, the variation in the height of the foam formed on the free surface of the mixture was measured. It is important to specify that the free surface of the mixture is at an initial value of 9.5 cm in height. In *Table 10*, the variations in the height of the foam corresponding to the quantities of carbon dioxide introduced into the system of mixture 1 are shown, as well as the variation of the free surface of the liquid:

Table 10: Variation of foam as CO_2 flow rate changes (mixture 1)

Q CO_2 [cm^3/min]	$Q_{average}$ CO_2 [cm^3/min]	Rotameter value	H_{liquid} [cm]	H_{foam} [cm]
from 65 to 69	67	4	9,8	0,3
from 113 to 119	116	8	10	0,6
from 148 to 162	155	10	10,2	0,85
from 288 to 316	302	20	10,7	1,7

Figure 24 shows the development of foam as the average flow rate of carbon dioxide delivered changes:

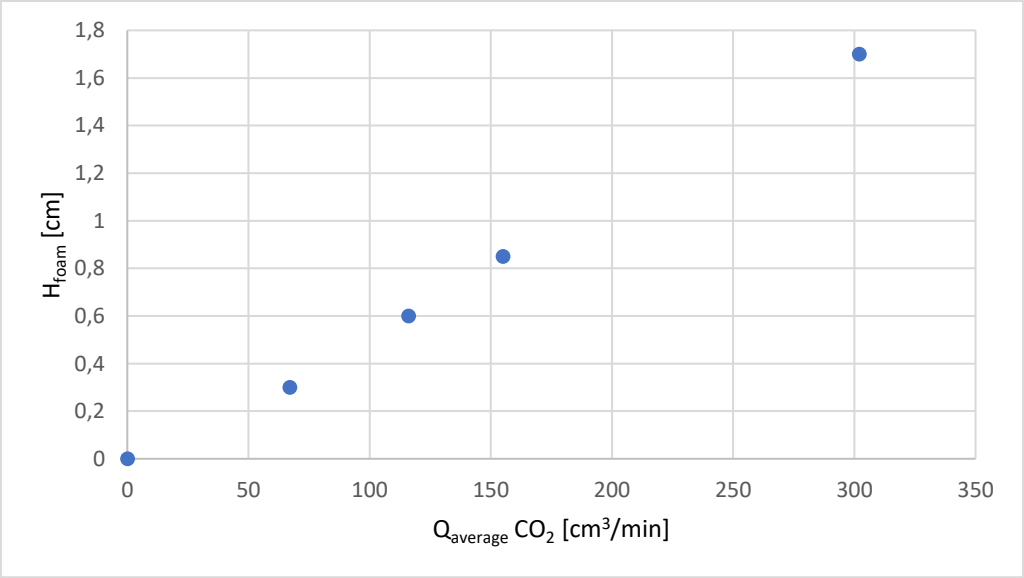

Figure 24: Trend of foam at CO_2 variation (mixture 1)

The graph in *Figure 24* shows that as the amount of carbon dioxide injected into the system increases, so does the height of the foam. In *Figure 25* a screenshot of the variation of the foam formed on the free surface of the mixture 1 is shown.

Figure 25: Screenshot of the variation of foam on the free surface of mixture 1

In *Table 11*, the variations of the height of the foam corresponding to the quantities of carbon dioxide injected into the system of mixture 2 are shown, as well as the variation of the free surface of the liquid:

Table 11: Variation of foam as CO_2 flow rate changes (mixture 2)

Q CO_2 [cm^3/min]	**$Q_{average}$ CO_2 [cm^3/min]**	**Rotameter value**	**H_{liquid} [cm]**	**H_{foam} [cm]**
from 65 to 69	67	4	10	0,5
from 113 to 119	116	8	10,2	0,9
from 148 to 162	155	10	10,5	1,3
from 288 to 316	302	20	11	2,5

Figure 26 shows the development of foam as the average flow rate of carbon dioxide delivered changes:

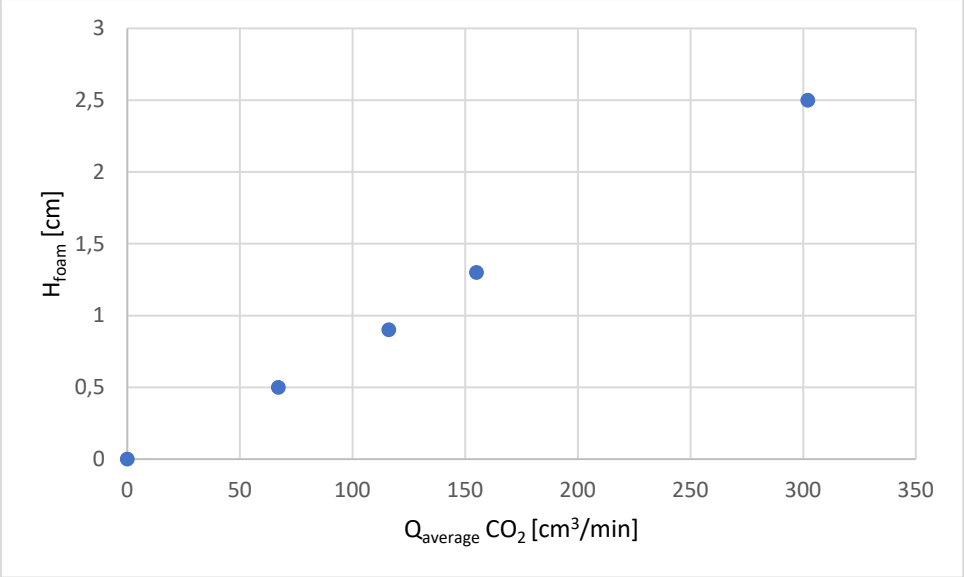

Figure 26: Trend of foam at CO_2 variation (mixture 2)

The graph in *Figure 26* shows that as the amount of carbon dioxide injected into the system increases, so does the height of the foam. In *Figure 27* a screenshot of the variation of the foam formed on the free surface of the mixture 2 is shown.

Figure 27: Screenshot of the variation of the foam formed on the free surface of the mixture 2

In *Table 12*, the variations of the height of the foam corresponding to the quantities of carbon dioxide injected into the system of mixture 3 are shown, as well as the variation of the free surface of the liquid:

Table 12: Variation of foam as CO_2 flow rate changes (mixture 3)

Q CO_2 [cm^3/min]	**$Q_{average}$ CO_2 [cm^3/min]**	**Rotameter value**	**H_{liquid} [cm]**	**H_{foam} [cm]**
from 65 to 69	67	4	10,5	1,2
from 113 to 119	116	8	11	2,2
from 148 to 162	155	10	11,9	3
from 288 to 316	302	20	12,8	6

Figure 28 shows the development of foam as the average flow rate of carbon dioxide delivered changes:

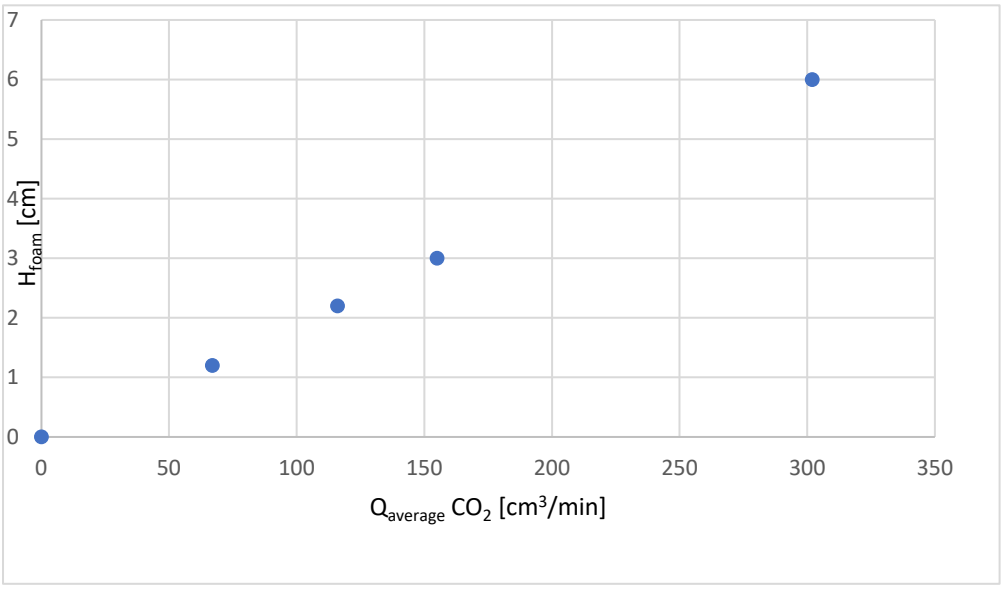

Figure 28: Trend of foam at CO_2 variation (mixture 3)

The graph in *Figure 28* shows that as the amount of carbon dioxide injected into the system increases, so does the height of the foam. In *Figure 29* a screenshot of the variation of the foam formed on the free surface of the mixture 3 is shown.

Figure 29: Screenshot of the variation of foam formed on the free surface of the mixture 3

4.4. Data analysis

Observing *Tables 13, 14* and *15*, it can be seen that for all three mixtures, as the flow rate of carbon dioxide into the system increases, so does the height of the foam that forms on the free surface. However, it is evident how the growth of foam is different for all three cases. In fact, as can be seen from the graph in *Figure 30*, the foam growth in the case of stevia (mixture 3) is greater than that in the case of fructose (mixture 2), which in turn is greater than that in the case of granulated sugar (mixture 1). In particular, the foam growth in mixture 3 is much higher than in the other two cases.

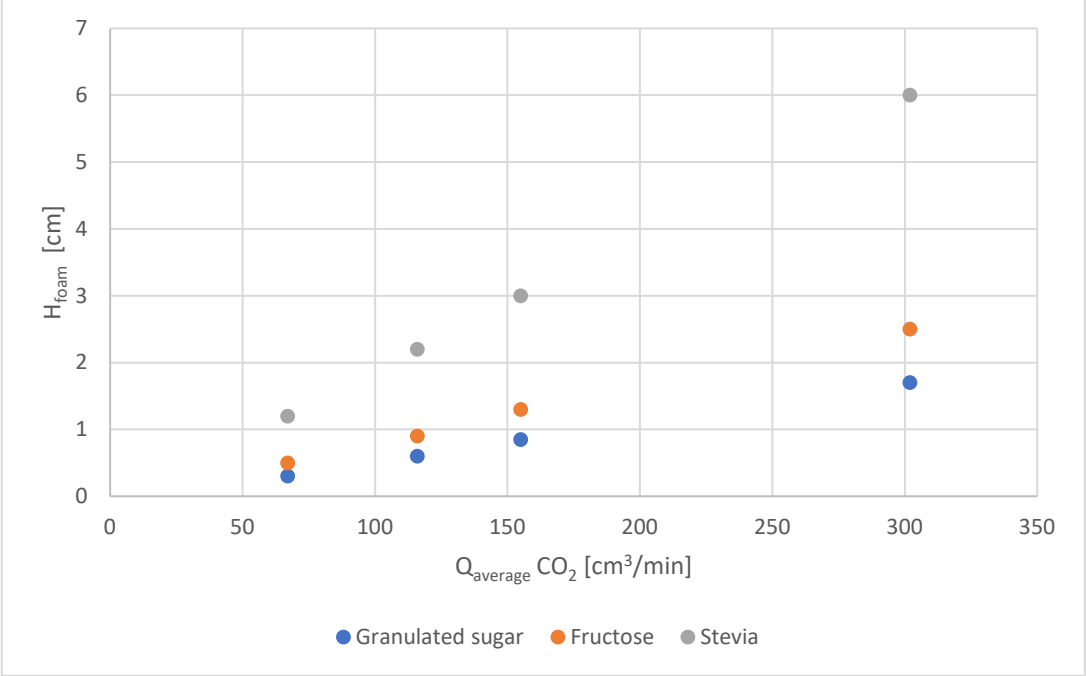

Figure 30: Comparison of foam growth in the three cases

In order to understand why the behaviour of the three foams was so different, it was essential to also compare their decay time under quiet conditions in which there was no carbon dioxide supplied. In particular, under these quiet conditions, the time it takes for the foam to completely disappear until the mixture returns to its initial conditions is called the relaxation time τ. Since it was not possible to obtain this time with the naked eye, it was obtained from well-known equations in the literature. Starting with the total mass m_{tot} of each mixture being 77.93 g, the massive fractions w_{ij} of water, sugar and citric acid are 0.898, 0.101 and 0.001 respectively. The molecular weight of mixture 1 PM_{mix1} is 19.92 g/mol and was derived from *Equation 2.1*, knowing that the molecular weights PM_i of water, granulated sugar and citric acid are 18 g/mol; 342.29 g/mol and 192.12 g/mol respectively [Perry R. H., 2007]:

$$PM_{mix} = \frac{1}{\sum \frac{w_{ij}}{PM_i}} \qquad (2.1)$$

Knowing the total mass and molecular weight of the mixture 1, it is possible to derive the number of total moles n_{tot} through their ratio, obtaining a value of 3.91 mol. The same procedure was followed to derive the number of moles n_i of each species, from the ratio of the mass of each species mi to the molecular weight of

each of them PM_i and values were obtained for water, granulated sugar and citric acid of 3.89 mol; 0.02 mol and 0.002 mol respectively. At this point, dividing each number of moles of each individual species n_i by the number of total moles n_{tot}, the molar fractions xi of water, granulated sugar and citric acid were obtained as 0.99, 0.0051 and 0.0049 respectively. Of relevance was also the calculation of the mixture density ρmix1 of 994.06 kg/m^3 through *Equation 2.2*, knowing that the densities ρ_i of water, granulated sugar and citric acid are 1000 kg/m^3; 1.59 kg/m^3 and 1.66 kg/m^3 respectively [Perry R. H., 2007]:

$$\rho_{mix} = \sum x_i \, \rho_i \qquad (2.2)$$

Table 13 summarises the data for mixture 1.

Table 13: Properties of mixture 1

	mi [g]	wi [-]	PMi [g/mol]	ni [-]	xi [-]	ρi [kg/m^3]
Water	70	0,898	18	3,89	0,99	1000
Granulated sugar	7,89	0,101	342,29	0,02	0,0051	1,59
Citric acid	0,004	0,001	192,12	0,002	0,0049	1,66
Mixture 1	77,93	1	19,92	3,91	1	994,06

The same procedure was done for mixtures 2 and 3 (*Tables 14* and *15):*

Table 14: Properties of mixture 2

	mi [g]	wi [-]	PMi [g/mol]	ni [-]	xi [-]	ρi [kg/m^3]
Water	70	0,898	18	3,89	0,99	1000
Fructose	7,89	0,101	180,16	0,04	0,0092	1,69
Citric acid	0,004	0,001	192,12	0,002	0,0008	1,66
Mixture 2	77,93	1	19,81	3,93	1	988,83

Table 15: Properties of mixture 3

	mi [g]	wi [-]	PMi [g/mol]	ni [-]	xi [-]	ρi [kg/m^3]
Water	70	0,898	18	3,89	0,99	1000
Stevia	7,89	0,101	804,87	0,01	0,0093	1,5
Citric acid	0,004	0,001	192,12	0,002	0,0007	1,66
Mixture 3	77,93	1	19,99	3,90	1	997,44

Furthermore, the values of the μ viscosities at room temperature of mixture 1 and mixture 2, which are 1.26 mPa s and 1.18 mPa s, respectively, are known from the literature [Gabas A. L., 2007]. The value of the viscosity of mixture 3 was derived from the values of the μ_i viscosities of water and stevia, which are 1000 mPa s and 27770 mPa s, respectively, through *Equation 2.3* [Alipour B., 2012]:

$$\mu_{mix} = \sum \left(x_i \, (\mu_i)^{\frac{1}{3}} \right)^3 \qquad (2.3)$$

Given all this information about the mixtures, it is possible to determine the gas supply Q_0 under steady-state conditions via *Equation 2.4*:

$$Q_0 = \Omega \, u_D = \frac{\pi \, D^2 \, g \, 2 \, \pi \, D \, \delta \, \rho_{mix}}{12 \, \mu_{mix}} \qquad (2.4)$$

where Ω represents the section of the cylindrical reactor which is equal to 7.84 cm^2 and u_D represents the exit velocity of the gas. Turning *Equation 2.5*, it is possible to calculate the only unknown variable, namely the thickness δ of the liquid layer that traps the bubbles under the conditions of flux of carbon dioxide present, obtaining *Equation 2.5:*

$$\delta = \frac{6\,\mu_{mix}\,Q_0}{g\,\pi^2\,D^3\,\rho_{mix}} \qquad (2.5)$$

where Q_0 is the flow rate of carbon dioxide entering the system, D is the diameter of the cylindrical reactor which in this case is 0.0316 m and g is the gravity constant of 9.81 m^2/s. Knowing that the ratio between δ under conditions of carbon dioxide flow and the height of the foam H_{foam} that is formed is proportional to the ratio between δ_0 under conditions of no flow and the height of the mixture H_0 under the initial conditions of no foam, it is possible to calculate δ_0 from *Equation 2.6:*

$$\delta_0 = \frac{\delta\,H_0}{H_{foam}} \qquad (2.6)$$

the gas input is zero, $Q_0 = 0$, the gas outlet velocity becomes negative and the variation of foam over time can be expressed by *Equation 2.7:*

$$\frac{\partial H_{foam}}{\partial t} = -u_D = \frac{-2\,g\,D\,\pi\,\delta\,\rho_{mix}}{3\,\mu_{mix}} = \frac{H_{foam}}{\tau} \qquad (2.7)$$

And so from *Equation 2.7* the expression of the relaxation time τ, shown in *Equation 2.8*, can be derived:

$$\tau = \frac{3\,H_0\,\mu_{mix}}{2\,g\,\pi\,D\,\rho_{mix}\,\delta_0} \qquad (2.8)$$

Therefore, for each average value of the delivered carbon dioxide flow rate, the relaxation time was calculated. In *Table 16* are the relaxation times for mixture 1, in *Table 17* those for mixture 2 and in *Table 18* those for mixture 3:

Table 16: Release times of mixture 1

Rotameter value	**Q CO_2 [cm^3/min]**	**H_{foam} [m]**	**δ [nm]**	**$δ_0$ [nm]**	**τ [s]**
4	67	0,003	2, 799	88,63	2,10
8	116	0,006	4,824	76,38	2,43
10	155	0,0085	6,449	72,08	2,58
20	302	0,017	12,57	70,24	2,65

Table 17: Release times of mixture 2

Rotameter value	**Q CO_2 [cm^3/min]**	**H_{foam} [m]**	**δ [nm]**	**$δ_0$ [nm]**	**τ [s]**
4	67	0,005	2, 621	49,79	3,50
8	116	0,009	4,517	47,68	3,66
10	155	0,013	6,039	44,13	3,95
20	302	0,026	11,77	43,00	4,06

Table 18: Release times of mixture 3

Rotameter value	**Q CO_2 [cm^3/min]**	**H_{foam} [m]**	**δ [nm]**	**$δ_0$ [nm]**	**τ [s]**
4	67	0,012	2, 355	18,64	8,40
8	116	0,022	4,058	17,52	8,94
10	155	0,030	5,425	17,17	9,12
20	302	0,060	10,58	16,75	9,35

It is evident that the relaxation times of mixture 1 are shorter than those of mixture 2, which in turn are shorter than those of mixture 3. This means that the foam of mixture 3 is more stable than the foam of mixture 2, which in turn is more stable than the foam of mixture 1. This phenomenon is explained by the fact that the surface energy of the liquid decreases when the height of the liquid rises, according to *Equation 2.9:*

$$dE_{sup} = 2\,\pi\,r\,\gamma\,dh \qquad (2.9)$$

and the fact that the gravitational potential energy of the liquid increases simultaneously, according to *Equation 2.10:*

$$dU = \rho_{mix}\,\pi\,r^2\,h\,g\,dh \qquad (2.10)$$

Under conditions of equilibrium, and therefore at the moment when the flow of carbon dioxide is no longer allowed to enter the cylindrical reactor, *Equation 2.9* and *Equation 2.10* are equal. In this way, the surface tension ϒ, which is the only unknown of the system, can be obtained through *Equation 2.11:*

$$\gamma = \frac{\rho_{mix}\,r\,g\,h}{2} \qquad (2.11)$$

where ρ_{mix} is the mixture density, r is the radius of the cylindrical reactor, h is the foam height and g is the gravitational acceleration of 9.81 m^2/s. *Tables 19, 20* and *21* below show how the surface tension varies as the foam height of mixture 1, mixture 2 and mixture 3, respectively, varies:

Table 19: Surface tension values of mixture 1

H_{foam} [m]	ϒ [N/m]
0,003	0,231116937
0,006	0,462233874
0,0085	0,654831321
0,017	1,309662642

Table 20: Surface tension values of mixture 2

H_{foam} [m]	ϒ [N/m]
0,005	0,383167
0,009	0,6897
0,013	0,996234
0,026	1,992468

Table 21: Surface tension values of mixture 3

H_{foam} [m]	ϒ [N/m]
0,012	0,927604
0,022	1,700607
0,030	2,319009
0,060	4,638018

It is known that the surface tension of water, which is generally 0.072 N/m, increases with the addition of sugars [Hiemenz P. C., 1997]. In particular, the *Tables 19, 20* and *21* show that a greater increase in surface tension occurs in the case of mixture 3, followed by mixture 2 and mixture 1. It is also known that the higher the surface tension, the more foam is formed, with mixture 3 foaming more than mixture 2 and mixture 2 foaming more than mixture 1. This means that, as confirmed by the experimental data, stevia has a greater ability to increase the surface tension of water and therefore to form more foam, followed by fructose and granulated sugar.

4.5. Bottling model

With all this information in mind, a filling model of the cylindrical reactor, which can be compared to a filling model of a bottle, was simulated. In particular, filling phases, taking care not to allow the mixtures to escape from the reactor, were alternated with degassing phases until the reactor was full of liquid and as free of foam as possible. Starting with mixture 1, thirteen filling phases were alternated with thirteen degassing phases. Given a relaxation time τ of approximately 2 seconds, as calculated in *Paragraph 4.4,* the duration of the degassing phases was always assumed to be 2 seconds, in order to allow the foam to disappear from the system as much as possible. The duration of the filling phases, on the other hand, was decreased as the liquid level in the reactor increased, in order to avoid possible liquid leakage from above due to high foam formation. For the calculation of the H_{foam} height, the H_{liquid} height and the total height at each step, the following data in *Table 22* were used:

Table 22: Experimental data useful for the filling model

C_0 [g/L]	C* [g/L]	ρ_{gas} [kg/m^3]	S	τ [s]	Q [m^3/s]	Ω [m^2]
9,766	1,502	1,801	4,589	2,1	1,02*10^{-5}	0,000784

Where C_0 is the concentration of carbon dioxide in the initial conditions at a pressure of 6.5 atm, C* is the final carbon dioxide concentration at a pressure of 1 atm, S is the solubilisation parameter of CO_2 in the mixture and is obtained through *Equation 2.12,* τ is the relaxation time of the foam, Q is the flow rate of the mixture into the system and Ω is the section of the cylindrical reactor.

$$S = \frac{C_0 - C^*}{\rho_{gas}} \qquad (2.12)$$

Equation 2.13 allows the calculation of the foam height at the first filling step F1 and *Equation 2.14* allows the calculation of the liquid height at the first filling step F1.

$$H_{foam\ F1} = \frac{Q\ \tau\ S}{\Omega}\left(1 - \exp\left(\frac{-\ t_{step}}{\tau}\right)\right) \quad (2.13)$$

$$H_{liquid\ F1} = \frac{Q\ t_{step}}{\Omega} \quad (2.14)$$

Concerning the first degassing step D1, the foam height can be calculated from *Equation 2.15*, and the liquid height from *Equation 2.16:*

$$H_{foam\ D1} = H_{foam\ F1}\ exp\left(\frac{-\ t_{step}}{\tau}\right) \quad (2.15)$$

$$H_{liquid\ D1} = H_{liquid\ F1} \quad (2.16)$$

From step 2 onwards, the foam height at filling step FN is described by *Equation 2.17,* while the liquid height at filling step FN is described by *Equation 2.18:*

$$H_{foam\ FN} = \frac{Q\ \tau\ S}{\Omega}\left(1 - exp\left(\frac{-\ t_{step}}{\tau}\right)\right) + H_{foam\ D\ N-1} \quad (2.17)$$

$$H_{liquid\ FN} = \frac{Q\ t_{step}}{\Omega} + H_{liquid\ D\ N-1} \quad (2.18)$$

As regards the degassing phase, from the second step onwards, the foam and liquid heights are calculated using the same procedure as in step 1. In general, considering a DN degassing step, the height of the foam and the height of the liquid can be obtained from *Equations 2.19* and *2.20* respectively:

$$H_{foam\,DN} = H_{foam\,FN}\, exp\left(\frac{-t_{step}}{\tau}\right) \qquad (2.19)$$

$$H_{liquid\,DN} = H_{liquid\,FN} \qquad (2.20)$$

The total height of each step, both filling and degassing, is given by the sum of the foam height and the liquid height at each reference step. In *Table 23*, the foam height, the liquid height, the total height and the length of each step are summarised schematically.

Table 23: The foam height, the liquid height, the total height and the length of esch step

STEP	Step Lenght [s]	H_{foam} [m]	H_{liquid} [m]	H_{total} [m]
F1	2,75	0,091463	0,03575	0,127213
D1	2	0,035288	0,03575	0,071038
F2	0,75	0,072914	0,0455	0,118414
D2	2	0,028132	0,0455	0,073632
F3	0,75	0,065758	0,05525	0,121008
D3	2	0,025371	0,05525	0,080621
F4	0,75	0,062997	0,065	0,127997
D4	2	0,024305	0,065	0,089305
F5	0,5	0,050849	0,0715	0,122349
D5	2	0,019619	0,0715	0,091119
F6	0,5	0,046163	0,078	0,124163
D6	2	0,017811	0,078	0,095811

F7	0,5	0,044355	0,0845	0,128855
D7	2	0,017113	0,0848	0,101613
F8	0,25	0,031174	0,08775	0,118924
D8	2	0,012028	0,08775	0,099778
F9	0,25	0,026089	0,091	0,117089
D9	2	0,010066	0,091	0,101066
F10	0,25	0,024127	0,09425	0,118377
D10	2	0,009309	0,09425	0,103559
F11	0,25	0,02337	0,0975	0,12087
D11	2	0,009016	0,0975	0,106516
F12	0,25	0,023078	0,10075	0,123828
D12	2	0,008904	0,10075	0,109654
F13	0,25	0,022965	0,104	0,126965
D13	2	0,00886	0,104	0,11286

In total, the time taken to fill the cylindrical reactor is 34 seconds. In the graph in *Figure 31*, the trend of foam height, liquid height and total height is represented as a function of the time of the reactor filling process.

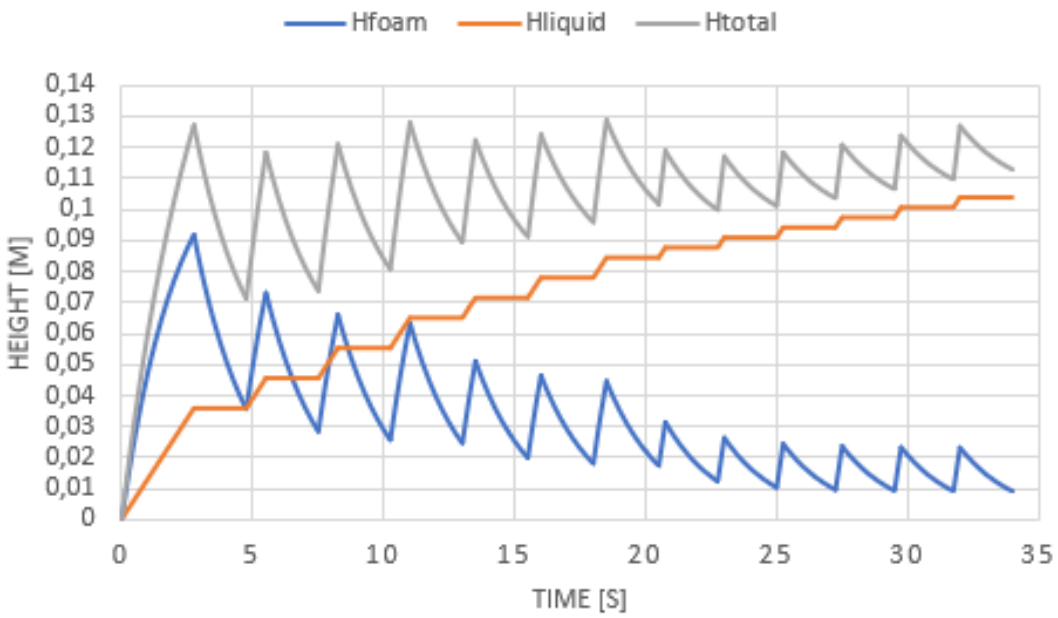

Figure 31: Height of foam, height of liquid and total height vs time of bottling (mixture 1)

As can be seen from *Figure 31*, the height of the foam increases with each filling step but decreases with each degassing one, and for each step the foam formed is progressively smaller; the height of the liquid increases with each filling step in smaller quantities and remains constant in the degassing phases; the total height is given by the sum of the trends of the height of the foam and of the liquid and therefore increases both in the filling and in the degassing phases.

5. DISCUSSION

The tests performed in the laboratory showed that the three mixtures analysed are characterised by different foam formations, under the same conditions of pressure, temperature and flow rate of carbon dioxide introduced into the system in which they were contained. In particular, the first mixture, consisting of water, citric acid and granulated sugar, shows a lower foam formation than mixture two, consisting of water, citric acid and fructose, which in turn shows an even lower foam formation than mixture three, consisting of water, citric acid and stevia. In addition, the three mixtures, consisting of equal amounts of water, citric acid and type of sweetener, have been shown to foam with different stability. This means that the foam formed on the free surface of mixture 1 takes less time to disappear completely than that formed in mixture 2, and that the foam formed on the free surface of mixture 2 takes less time to disappear completely than that formed in mixture 3. The bottling simulation, carried out under the same conditions and by alternating filling and degassing phases inside the cylindrical reactor to avoid product leakage from the top, also showed the same characteristics as the previous laboratory tests.

6. CONCLUSIONS

In this thesis, after having made a list of what can be the problems of a bottling company in the bottling phases of carbonated drinks, where the core of the problem is to increase the bottling time, the dynamics and behaviour of gas bubbles inside a liquid, the mechanisms of foam formation and the concept of stability in time related to foam methods for the abatement of the foam, in the field of beverages have been described in detail. Subsequently, a bottling simulation was carried out through filling and degassing phases in a cylindrical reactor and the problem of foam formation was identified as one of the main problems. In particular, the main objective was to see how and if a different composition of the ingredients of a drink affected the process in question and therefore possibly how bottling companies should adjust accordingly, reprogramming machinery for the bottling process according to the drink in question. Specifically, this simulation was carried out for three types of mixtures, which consist of water, citric acid and sweetener and differ only in the sugar component used: in the first case it is granulated sugar, in the second case fructose and in the third case stevia. A careful observation of all three mixtures shows that the total filling times are longer in mixture 3, followed by mixture 2 and 1. The reasons for these results are the amount of foam formed and the stability associated with it. In fact, mixture 3 presented a very high foam column and a very high stability compared to the other two mixtures; mixture 2 presented an intermediate foam formation and relative stability and finally mixture 1 presented much lower values of foam height and stability. These data, analysed with the development of a suitable model, through which the foam and liquid heights were calculated at each step of both filling and degassing, showed that it is the type of ingredients that make the difference in a bottling process. A scientific explanation for this is related to the fact that the surface energy of the liquid decreases as the height of the foam rises, at the same time as its gravitational potential energy increases. In other words, varying surface tension of the ingredient within the mixtures: the higher its surface tension, the more foam is formed in a mixture, as is its stability and therefore also the timing of its disappearance. In fact, the surface tension of water alone at room temperature, which is 0.072 N/m, increases with the addition of sweeteners: with granulated sugar it becomes 0,231 N/m, with fructose it becomes 0,383 N/m and with stevia it becomes 0,927 N/m. This explains why granulated sugar, fructose and stevia form a greater and more stable amount of foam respectively.

ANNEXES

ANNEX I: History of bottle

Over the centuries, humans have used all kinds of objects as containers for liquids, but the Egyptians were the first to create the first glass bottle: they were primitive vessels, made by shaping a mould of earth or clay around a wooden cylinder, then coating the mould with pulverised glass mixed with adhesive substances and then immersing it in a furnace filled with molten glass. Blown glass vessels, however, did not appear until 200 BC. A curious detail was that the first bottles did not have a stopper and could therefore only be used for serving drinks on the table, but not for long-term storage [Focus, 2002]. The appearance of the first corks, and in particular those made of cork, can be attributed to the Benedictine monk Dom Pierre Pérignon for imprisoning sparkling wine and the gas contained in the liquid. However, with the use of the cork, drinks still had a limited commercial life, far removed from that of the industrial era [Long T., 2009]. In 1872 the British Hiram Codd, the owner of a bottling company in a small town in London, designed and patented a bottle specifically for carbonated drinks, using the principle of the ball valve and made by means of a double restriction on the neck, at the base and at the mouth, so as to contain a glass bead and a rubber gasket near the mouth (*Figure A1*).

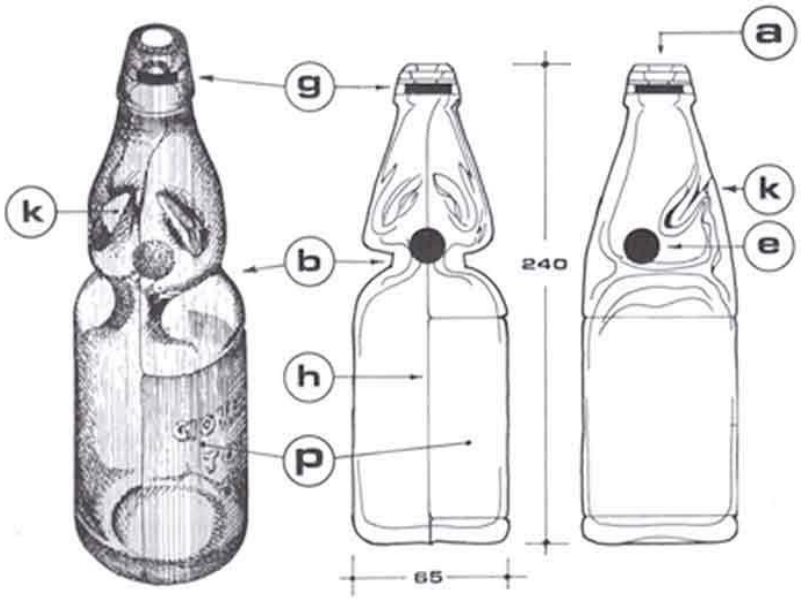

Figure A1: Codd's bottle

After being filled with the drink, the bottle was turned upside down and carbon dioxide was injected at high pressure (usually 6 atmospheres). When the bottle returned to its position, the pressure of the gas pushed the ball up towards the gasket at the mouth, sealing the bottle. In order to open the bottle, it was necessary to press the pellet with the fingers to release the gas and eliminate the pressure: at this point the pellet descended, although it remained in the neck thanks to the restriction that prevented it from reaching the bottom [Bruno D., 2015]. The breakthrough came when in 1892, William Painter found a better way to seal glass bottles through the so-called "Crown Cork" depicted in *Figure A2*: made of metal, with a corrugated end in the shape of an inverted crown, spill-proof, it was lined on the inside with a thin disc of cork in turn covered with a special film that sealed the contents of the bottle, preventing it from coming into direct contact with the metal [Giornale della Birra, 2014].

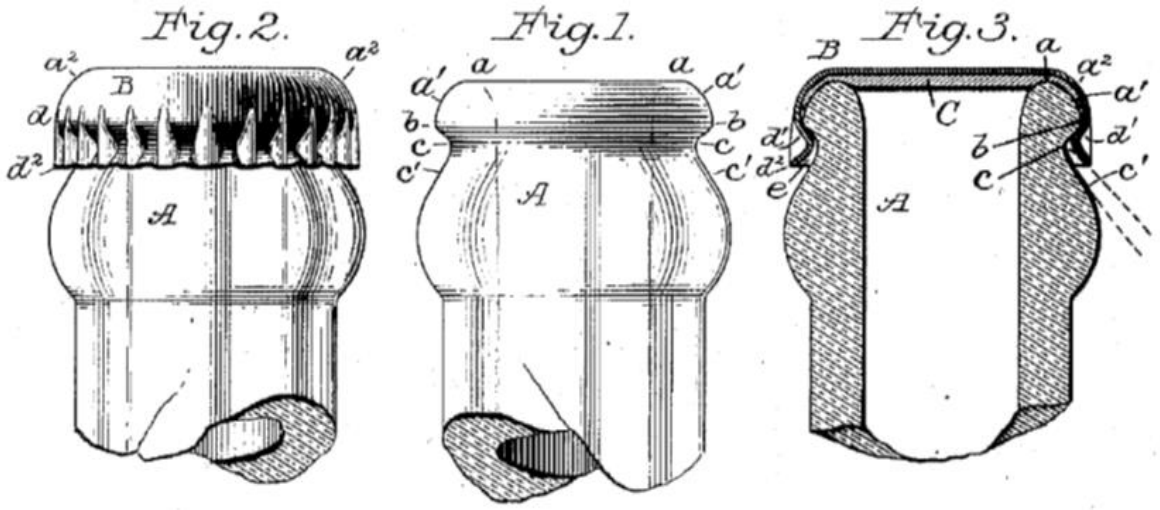

Figure A2: The Crown Cork by William Painter

ANNEX II: Water treatments

Each beverage requires a tailor-made water treatment which places great demands on having different water treatment technologies listed below [EUWA, 2021]:

- Adsorption: Water filtration through special adsorbent materials removes unwanted substances such as arsenic, uranium, iron, manganese, but also hydrogen sulphide from the water to be treated;

- Ultrafiltration: The ultra-small pores of the high-efficiency membranes retain even the smallest particles in the water. With a pore size of around 0.02 µm, bacteria and even viruses are retained. This beverage water treatment technology thus creates an effective barrier against germs. Ultrafiltration is also an ideal pre-treatment for subsequent reverse osmosis to reduce the potential for fouling caused by organic deposits;

- Activated carbon filtration: Beverage water treatment with activated carbon filtration is used for dichlorination and elimination of foreign taste, odours and water discolouration;

- Reverse osmosis: Reverse osmosis is a very efficient method to reduce the concentration of solutes in the drinking water to be treated. The natural osmosis process on a semi-permeable membrane is reversed by applying pressure on the concentrate side. Water can pass through the membrane while its constituents are almost completely retained. Reverse osmosis plants for beverage water treatment can be operated very economically and with a high efficiency of up to 95%;

- Disinfection: For the disinfection of beverage water, depending on the particular application, different treatment methods are used. A very effective and efficient method is disinfection by means of chlorine dioxide. However, the use of a somewhat more expensive ozonation can be useful, for example, when it comes to protecting the treated drinking water until it is bottled and sealed. Another method of disinfection is irradiation with UV light, but this has no deposition effect on the water;

- UV treatment: In addition to the field of application of disinfection, UV irradiation can also be used for the photochemical dechlorination of the beverage water to be treated. For UV treatment, however, pre-treatment is required to remove turbidity from the incoming water to ensure highly efficient transmission of UV radiation into the water.

ANNEX III: Ingredients

The secondary ingredients of carbonated drinks are listed below:

- Acids: the application of acids improves the flavour and also contributes to the preservation of the drink. A wide variety of acids are available for the production of carbonated drinks, but citric, malic, fumaric, tartaric and phosphoric acids are the most widely used. For example, phosphoric acid is mainly used in cola-type drinks and citric acid in orange soda and Sprite [British Soft Drink Association, 2021].

- Flavouring agents: Flavouring agents are present in almost every soft drink. They can be obtained from natural or artificial sources and are used to meet the growing consumer demand for a wide range of different flavoured foods and drinks. Natural flavourings are derived from a wide range of fruits, vegetables, nuts, barks, leaves, herbs, spices and oils. Artificial flavourings, on the other hand, are produced synthetically but are not preferred due to uncertain safety [British Soft Drink Association, 2021]. Fruit flavouring can be added in the form of juice, as chopped up, in the case of citrus fruits, or as an essence. Juice is normally used as a concentrate, citrus fruits; especially oranges are more widely applied. Citrus juice is finely chopped to avoid flavour defects. Natural citrus essences are largely composed of essential oils from the skin of the fruit. Hydrocarbons, especially limonene, make up more than 90% of the oil, but contribute little or nothing to the flavour, acting mainly as a vector. Fruit flavourings are most commonly used, except in colas. Colas are flavoured by a cola root extract together with about 10% caffeine and a blend of essences. As far as the flavouring component of sugar syrup is concerned, it has a great influence on the taste of the final product, even when used in very small amounts, i.e. 0.01 to 0.02% [Food Standards Agency, 2021].

- Colouring agents: colouring agents are used in soft drinks to make the product more aesthetically appealing and to help preserve the identity or character by which the drinks are recognised. There are three basic categories of colouring agents: natural colouring agents, artificial colouring agents and caramels [British Soft Drink Association, 2021]. Natural colourants can be extracted from plants, fruits and vegetables and can also be produced synthetically. There are two main categories: carotenoids, which include a range of colours from yellow to orange, and anthocyanins, which include a range of colours from bright red to purple. Even when natural fruit extracts or juices are used, their colours are generally supplemented with synthetic ones because the latter have greater colouring and stabilising power. Artificial colours include a full range of colours, blue, green, red, yellow, etc. All permitted artificial colours used in soft drinks have been thoroughly tested and approved as safe. However, due to the growing consumer preference for natural colourants, the trend in the UK market in recent years has been for manufacturers and retailers to reduce the use of artificial colourants in products. Finally, caramels are one of the oldest, most widely used, non-synthetic colours made from heated or burnt sugar. They are used in cola and ginger ale drinks and can also be used in beer and shandies [Natural Food Colours Association, 2021].

- Emulsifiers, clouding agents and stabilisers: emulsifiers can be used to impart cloudiness in the form of neutral emulsions and/or as a flavouring agent as flavoured emulsions. An oil-in-water (O/W) emulsion is formed using a two-stage homogeniser to produce droplets of 1-2 mm in diameter for optimum stability and turbidity. The oil phase typically consists of a citrus essential oil containing an oil-soluble clouding agent, while the aqueous phase consists of a gum arabic solution, or a suitable

hydrocolloid with similar properties. A clouding agent must contribute to opacity without affecting stability by producing creams, rings or separation, and must also not affect colour, taste or odour. Brominated vegetable oil (BVO) has been used as a clouding agent for many years, but has now been banned due to potential toxicity. Many alternatives have been tried, including sucrose esters, rosin esters, protein clouds, benzoate esters of glycerol and propylene glycol, waxes and rubber exudates. However, none of them proved satisfactory, only a soy protein-based cloudifying agent was found effective. Stabilisers are used both to stabilise emulsions and to keep fruit components in dispersion. They also improve the mouthfeel and viscosity of drinks. The most commonly used ones include guar gum, gum arabic, pectin, CMC and alginates [Food Standards Agency, 2021].

- Preservatives: preservatives allow products to have a longer shelf life by slowing or stopping the growth of microorganisms such as yeasts, moulds and bacteria. Not all soft drinks contain preservatives; the need for a preservative depends on the type of product and the process used. Soft drinks containing fruit juice and sugar typically need preservatives to prevent microbiological spoilage. The most commonly used preservatives are benzoates (E210-E213), sorbates (E200-E203), sulphites (E220-228) and dimethyldicarbonates (E242) [Food Additives and Ingredients Association, 2021].

ANNEX IV: Bottle design

The most critical points are the body, the neck, the shoulder, the handle, the bottom and the ribs [Zugno S., 2017]. The first criticality to be addressed is that of the body of the bottle and in particular the section it must have. There are many types of section for bottles: circular, rectangular, square, octagonal, triangular; but the only one suitable for carbon dioxide content is the circular one because the others would not be able to support the internal pressure on the walls. In addition to the type of section, the type of bottle profile must also have certain characteristics. Among the profiles for bottles containing carbonated beverages are the "contour" profile for small to medium formal formats, the "straight" profile for medium to large formats and finally the "convex" profile for small to medium premium formats (*Figure A3*).

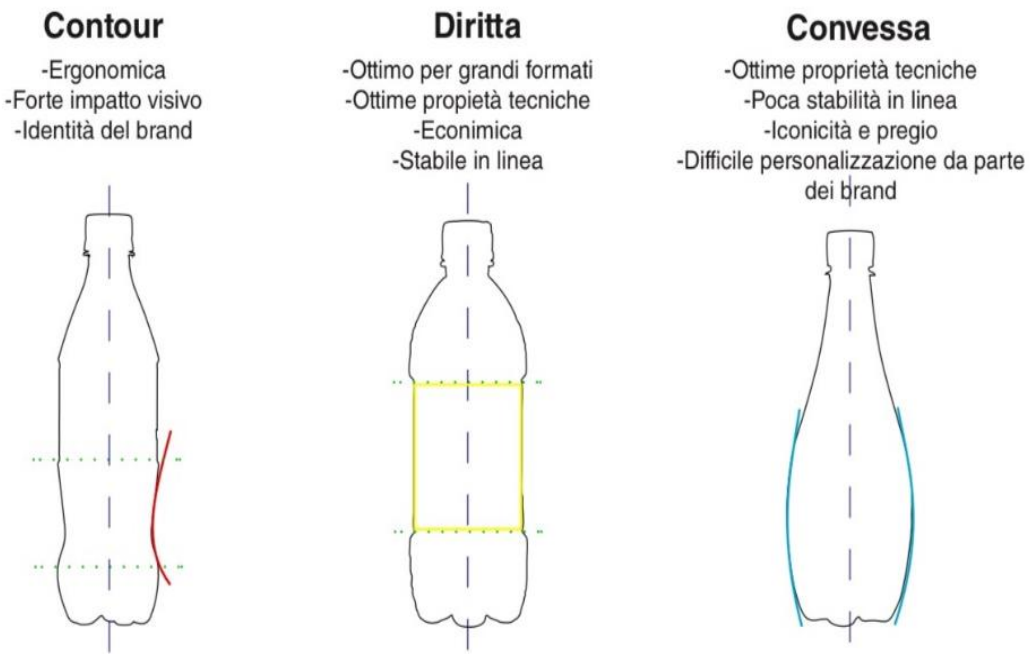

Figure A3: Type of profiles of bottles for carbonated soft drinks.

In the corking phase, in order to be able to screw the cork, a force is required that compresses the neck of the bottle. A problem that can occur is that the neck collapses into the shoulder due to the high weight acting on the area concerned. It is therefore important that a suitable geometry is adopted to resist this type of inconvenience. In *Figure A4*, some of these examples are shown.

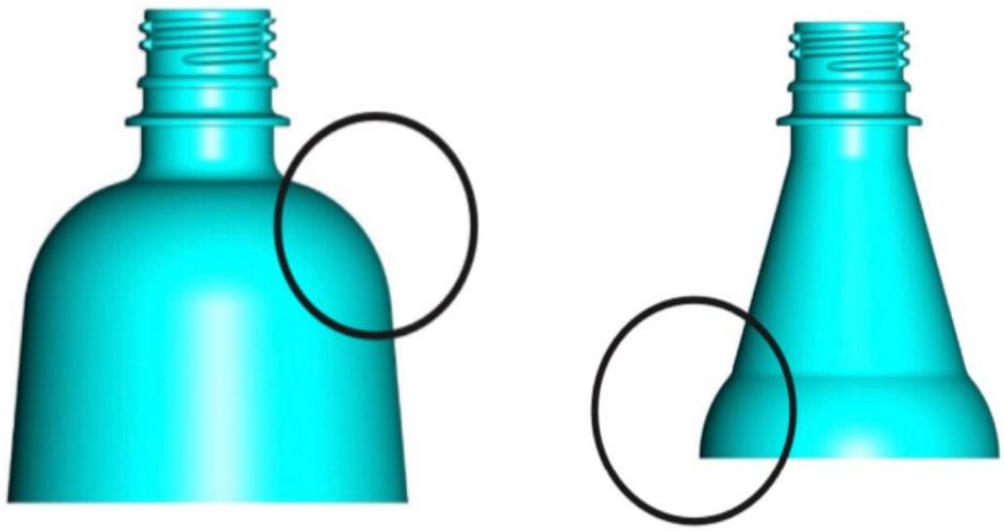

Figure A4: The shoulder and the neck of bottles for carbonated soft drinks

Generally, a bottle with a petaloid bottom is used in carbonated drinks. The petals are structured in such a way as to resist the internal pressure, without changing, and are designed according to strict parameters concerning height, profile and angle. The number of petals is usually five or six, but a five-petalled bottom is more efficient because the reaction forces, which are created by the gases contained in the bottle, are always interrupted since the petals are not symmetrical with respect to each other, unlike the six-petalled conformation (*Figure A5*).

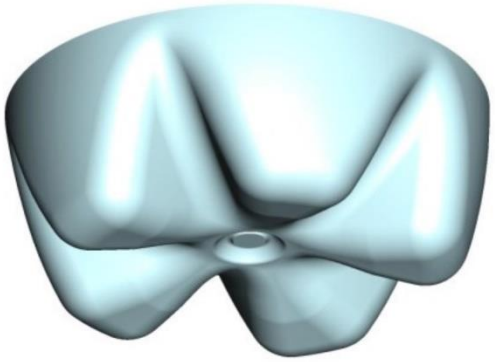

Figure A5: Petaloid bottom of bottles for carbonated soft drinks

Even a Champagne-type bottom (*Figure A6*) can be used for a bottle that is to contain carbonated drinks, as long as it has a bottom with sufficient material both in the side and in the lower dome to withstand high concentrations of carbon dioxide: in fact, thicknesses of approximately 0.8 mm on the side and 2.5/3 mm on the dome are possible. For bottles of the same geometry, bottles with a petaloid bottom have a preform of about 36 grams, while those with a Champagne bottom have a preform of about 49 grams.

Figure A6: Champagne bottom of bottles for carbonated soft drinks

The bottle must be designed in such a way as to resist the gas pressure exerted on the internal walls when it is full, but it is equally important that it does not lose its resistance when the volume of the product inside it drops. In particular, its handle will tend to widen, approaching its maximum diameter and causing the bottle to rise. It is therefore necessary to have a narrow handle and a difference between the maximum and minimum diameters that is as high as possible, as shown in *Figure A7*.

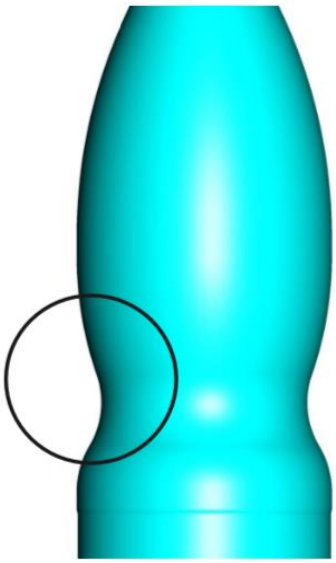

Figure A7: The handle of bottles for carbonated soft drinks.

Since they are inside the bottle, they are subject to gas pressure and consequently tend to flatten their structure and raise the surface of the bottle by the same amount as the stretching of the ribs. This increase in height, however, must not exceed a limit value. For example, *Figure A8* shows how the handles almost disappear, leaving an almost cylindrical handle and raising the bottle by approximately 6/8 mm.

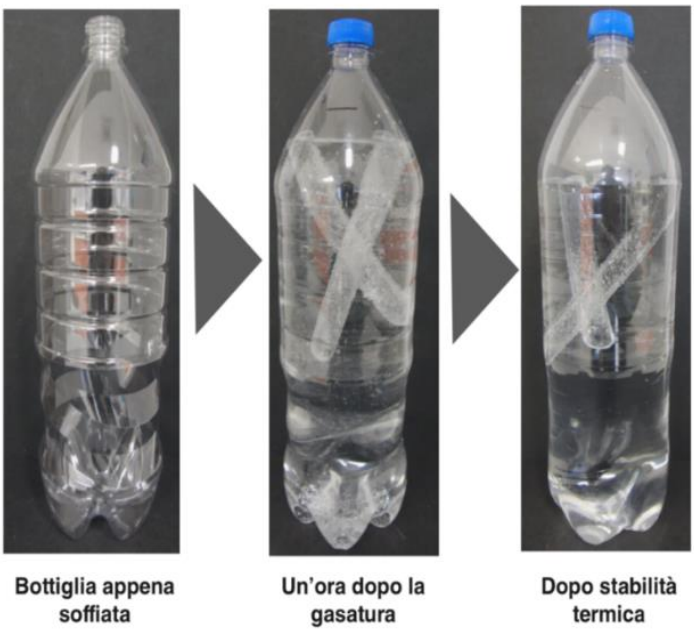

Figure A8: The ribs of bottles for carbonated soft drinks.

ANNEX V: Water Footprint, The Coca Cola Company case

The Water Footprint is a tool that helps companies extend their view of how they use water in their production processes. This is an indicator that is defined as the total volume of fresh water that is used to produce a company's product. Compared to other water accounting systems, the Water Footprint considers both direct and indirect water use and water use is measured in terms of volumes of water consumed and polluted per unit of time [Aldaya M. M., 2010]. It can be said, therefore, that the Water Footprint is the key factor in improving water efficiency by reducing or eliminating water use in production processes. For example, The Coca Cola Company, over the years, has made significant investments in new technologies and operating procedures that replace or reduce water use in their manufacturing operations. The company embarked on a path in 2004 where it used 2.7 litres of water to produce 1 litre of product. This means that 1 litre of water was in the product and another 1.7 litres was used in the production process, mainly to keep the equipment clean. In 2017 it managed to achieve a result of 1.92 litres of water to make 1 litre of product, with a gradual improvement year on year, as shown in *Figure A9*.

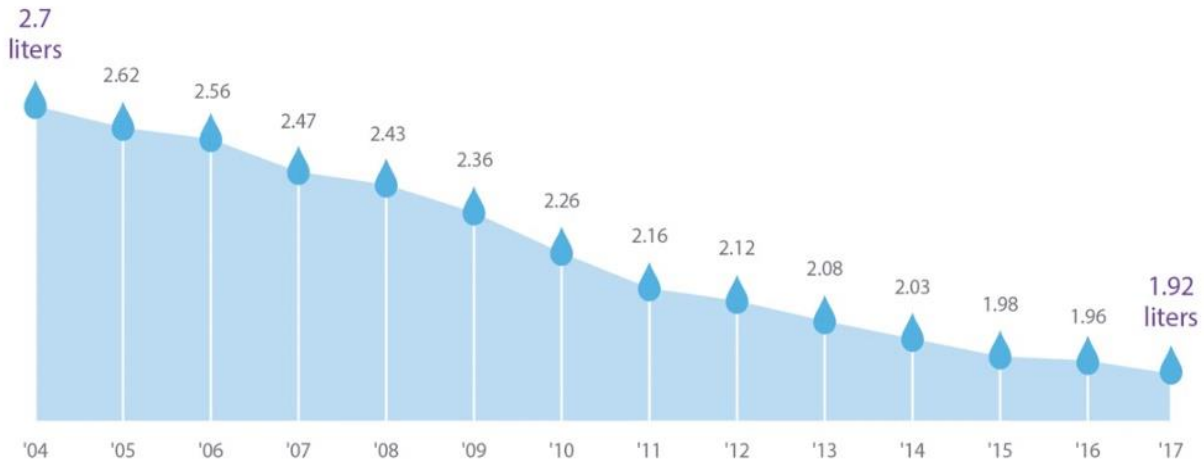

Figure A9: Water Footprint of The Coca Cola Company from 2004 to 2017

In particular, it can be seen from *Figure A9* that, in 2017, the company's water efficiency improved for the fifteenth consecutive year, with a 2.55% improvement over 2016, a 15% improvement over 2010. It also equates to a 29.3% improvement since 2004, when the company began reporting efficiency progress as a global system [The Coca Cola Company, 2018]. Today, The Coca Cola Company is focusing on reducing its water consumption by another 25%, and thus to achieve an amount of 1.7 litres of water for the production of 1 litre of drink [The Coca Cola Company, 2010]. As well as The Coca Cola Company, many other companies are taking action to try to minimise water consumption mainly because the scarcity of water as a drinking resource and its excessive waste are very current issues that companies have to face every day.

ANNEX VI: Stretch-blow moulding

The production cycle of a PET bottle consists of two phases: the first is the making of the preform and the second is where the preform takes its final shape inside a blowing machine. Firstly, virgin PET in granular form is used for the production of preforms. A preform is characterised by a tubular structure, which will be blown; and a neck finish, which will not be changed by the blowing process and which differs in diameter and in the type of thread, which is the set of reliefs that are present on it and which guarantee the possibility of screwing to a type of cap. The PET mixture used to produce the preforms can have colouring substances added to it, which then also give the blown bottle its colour. An important parameter to consider when designing a preform is the neck finish, of which there are several types suitable for carbonated drinks. The design of

closures for carbonated beverages is also fundamental, since they must be characterised by the presence of openings designed for the gradual release of the pressure caused by the carbonated beverage during unscrewing, thus avoiding a possible sudden release of the product [www.husky.co]. Secondly, the preforms are transported from the feed hopper to the orientator by means of a special conveyor belt. The orientator inserts the preforms into an inclined guide from which they gravitationally fall to the star-shaped spacer wheel located at the entrance to the heating module. Before entering the heating module, which is equipped with infrared rays, each individual preform is subjected to two types of checks: the first detects its appropriate size and vertical position; the second checks its permitted temperature. During heating, the preforms rotate constantly on themselves to ensure symmetrical heat distribution. The heating module is equipped with two different cooling systems: a liquid cooling system, which cools down the protective ring, so that the thread of the preforms does not deform during the heating process, and an air-cooling system, which keeps the internal temperature of the heating module sufficiently low, so that the external walls of the preforms are not exposed to too high temperatures. A special group of grippers picks up the preforms from the star wheel located at the exit of the heating module and places them inside the stretch-blow moulding stations. The preform, which has been previously heated to the optimum temperature, is brought to a length that allows a more optimal processing during the blowing phase. Pre-blowing takes place at the same time as the stretching of the preform and consists of the injection of compressed air at low pressure into the preform. These two simultaneous operations allow the PET preform to be pre-formed in such a way as to evenly distribute the material along the entire length of the container. A final blowing operation using high-pressure compressed air gives the containers their final shape. The finished bottles are taken from the stretch-blowing stations by a second set of grippers, placed on an air conveyor belt and finally conveyed to the filling plants [Ottmar B., 2016].

ANNEX VII: Rotameter

A rotameter is an instantaneous meter for small flow rates consisting of a cylindrical tube, inside of which is a movable float (*Figure A10*). Due to the effect of gravity, the float is positioned at the bottom of the tube when there is no flow. On the contrary, when carbon dioxide starts to flow through the tube, the float is pushed upwards. The float reaches an equilibrium position when the vertical forces are balanced [Palumbo M., 2018]. *Figure A11* shows how the rotameter works.

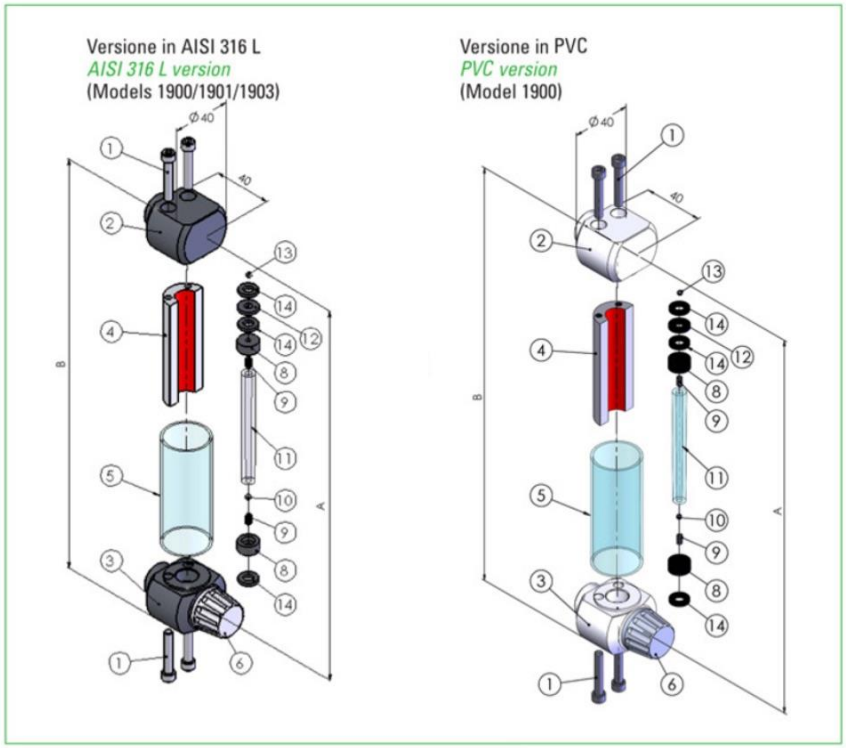

Model	A=mm	B=mm
1900	100	128
1901	170	198
1903	320	348

Figure A10: Rotameter

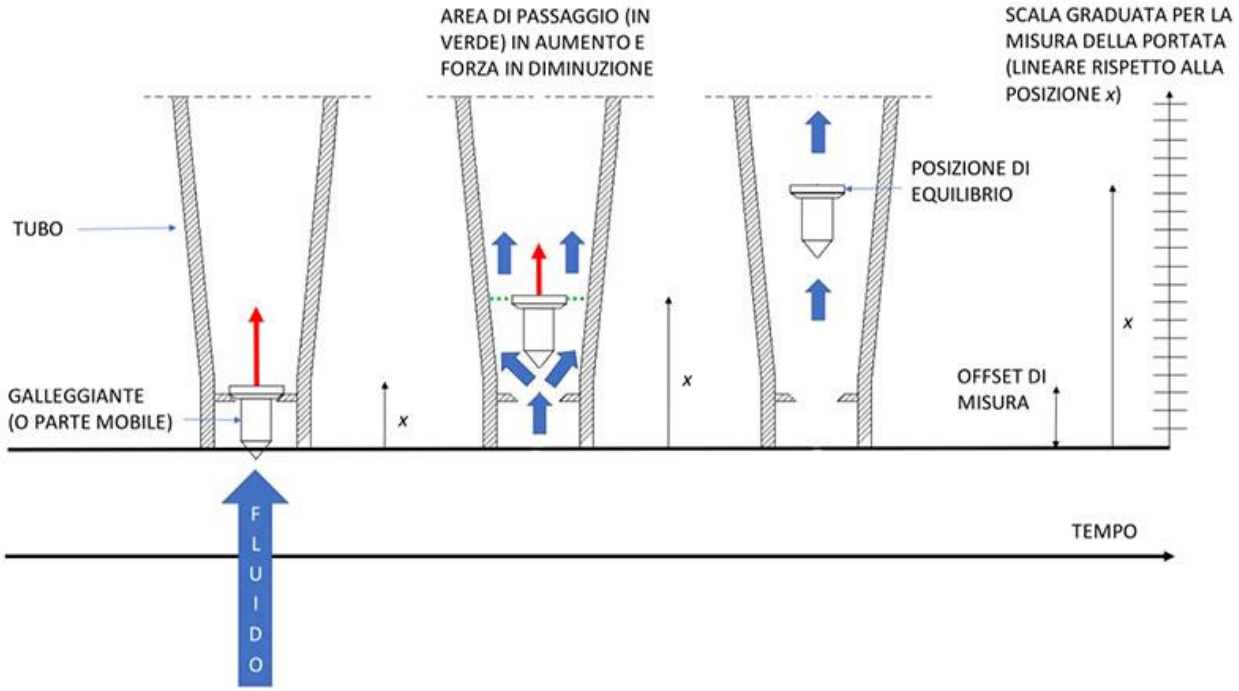

Figure A11: Working principle of a rotameter

As mentioned above, the flow of carbon dioxide is not fed into the reactor in precise quantities, as is the case with the other ingredients, but in variable quantities that can be detected by the rotameter. The rotameter has several notches which, as the flow rate of carbon dioxide entering the reactor increases, are reached by the float. Each notch of the rotameter corresponds to a maximum and minimum value of carbon dioxide leaving the gas cylinder and therefore to a certain range of values that can be identified by an average value. Precisely in order to associate each notch of the rotameter with a certain average value of the flow of carbon dioxide entering the reactor, a calibration of the rotameter itself was carried out before proceeding with the experiment. The initial calibration was carried out by placing only water in the reactor, to which an ever-increasing flow rate of carbon dioxide was added, and observing the gradual rise of the float inside the rotameter from notch to notch. At each notch of the rotameter, once the float had reached equilibrium inside the rotameter, a displacement of the bubbles formed inside the reactor of 10 cm3 was considered in order to assess the corresponding amount of carbon dioxide. For each equilibrium position of the float, the time t taken for the bubbles to travel uphill through a volume V equal to 10 cm3 was timed. This timing was carried out ten times for each equilibrium position of the float, after which the corresponding value of the flow rate Q of carbon dioxide was found for each measurement by means of *Equation A1*:

$$Q = \frac{V\,60}{t} \tag{A1}$$

Four rotameter values were taken as reference and therefore four equilibrium positions: 4, 8, 10 and 20. With regard to equilibrium position 4, *Table A1* shows the measurements of the bubble rise times and the corresponding values of the carbon dioxide flow rates from the gas cylinder, while *Figure A12* shows the rotameter float in position 4:

Table A1: Rising time of bubbles and volumetric flow rate of CO_2 related to a volume of 10 cm^3 (4)

Time [s]	Volumetric flow rate [cm^3/min]
8,78	68,33712984
8,63	69,52491309
8,86	67,72009029
8,88	67,56756757
8,79	68,25938567
9,12	65,78947368
9,03	66,44518272
9,05	66,29834254
9,16	65,50218341
9,13	65,71741512

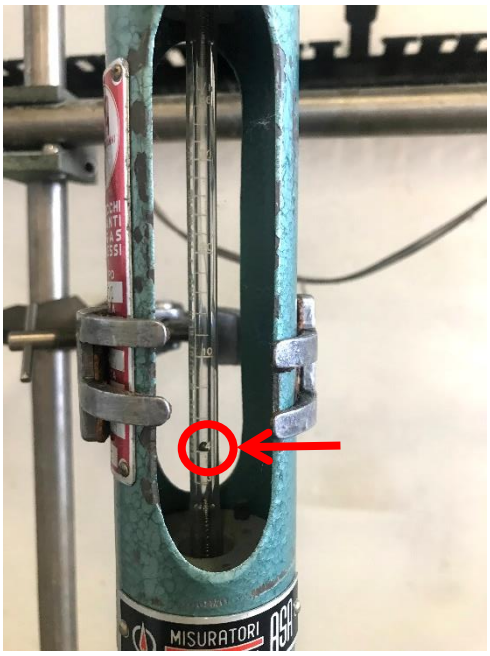

Figure A12: Rotameter value of 4

This rotameter value corresponds to a maximum and minimum volumetric flow rate of carbon dioxide of approximately 69 cm3 / min and 65 cm3 / min respectively and finally an average flow rate of approximately 67 cm3 / min. From *Table A1,* it can be seen that the longer the time taken by the bubbles to cross the reference volume, the lower the flow of carbon dioxide that comes out of the gas cylinder. This happens because a longer rise time corresponds to a lower speed of the gas flow exiting the valve. The opposite occurs for shorter ascent times. The trend of CO2 in relation to the rising time of the bubbles in the unit of volume of 10 cm3 is represented in the graph in *Figure A13:*

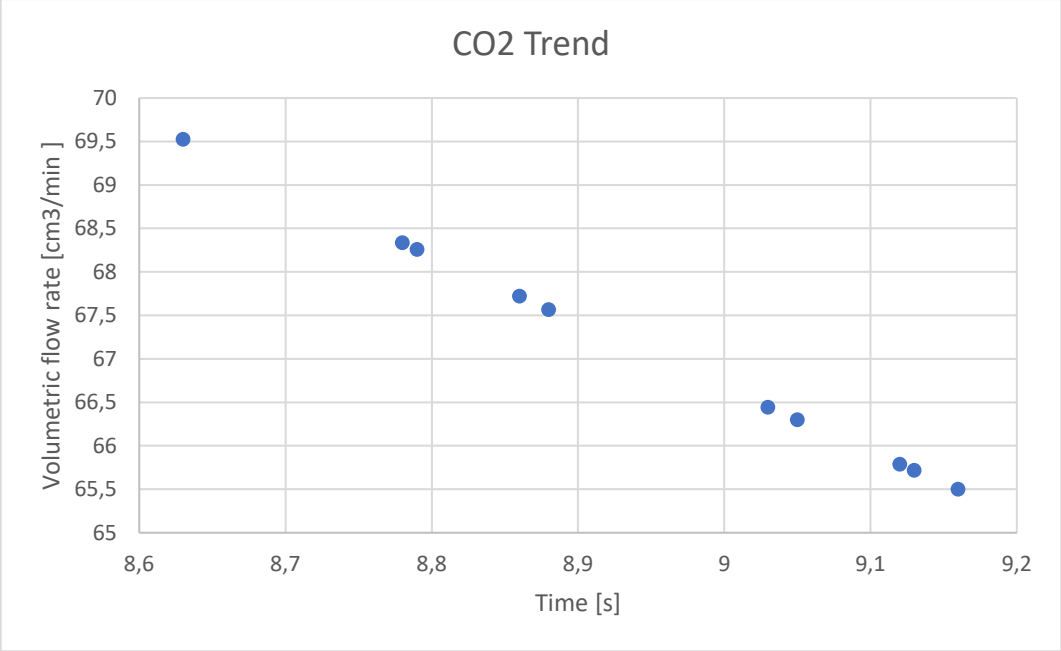

Figure A13: CO_2 trend over time for a rotameter value of 4

As regards the equilibrium position 8, *Table A2* shows the measurements of the rising times of the bubbles and the corresponding values of the carbon dioxide flow rates exiting the gas cylinder, while *Figure A14* shows the float of the rotameter in position 8:

Table A2: Rising time of bubbles and volumetric flow rate of CO_2 related to a volume of 10 cm^3 (8)

Time [s]	**Volumetric flow rate [cm^3/min]**
5,08	118,1102362
5,2	115,3846154
5,07	118,3431953
5,02	119,5219124
5,3	113,2075472
5,16	116,2790698
5,09	117,8781925
5,1	117,6470588
5,1	117,6470588
5,15	116,5048544

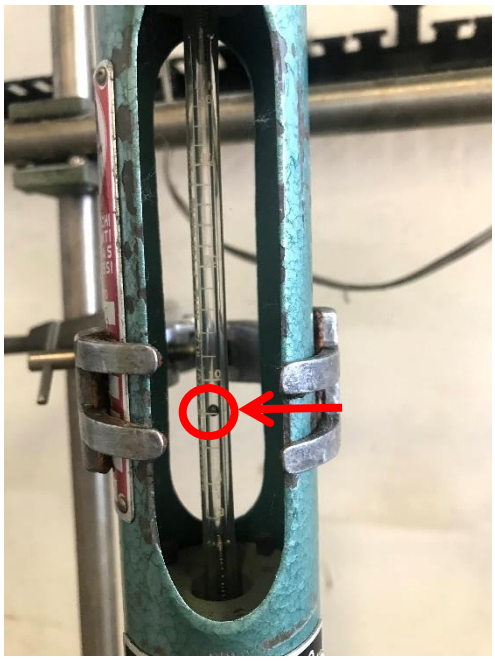

Figure A14: Rotameter value of 8

To this value of the rotameter correspond a maximum and minimum volumetric flow rate of carbon dioxide respectively of about 119 cm3 / min and 113 cm3 / min and finally an average flow rate of about 116 cm3 / min. From *Table A2,* it can be seen that the longer it takes for the bubbles to cross the reference volume, the lower the flow of carbon dioxide that comes out of the gas cylinder. This happens because a longer rise time corresponds to a lower speed of the gas flow exiting the valve. The opposite occurs for shorter ascent times. The trend of CO2 in relation to the rising time of the bubbles in the volume unit of 10 cm3 is represented in the graph in *Figure A15*:

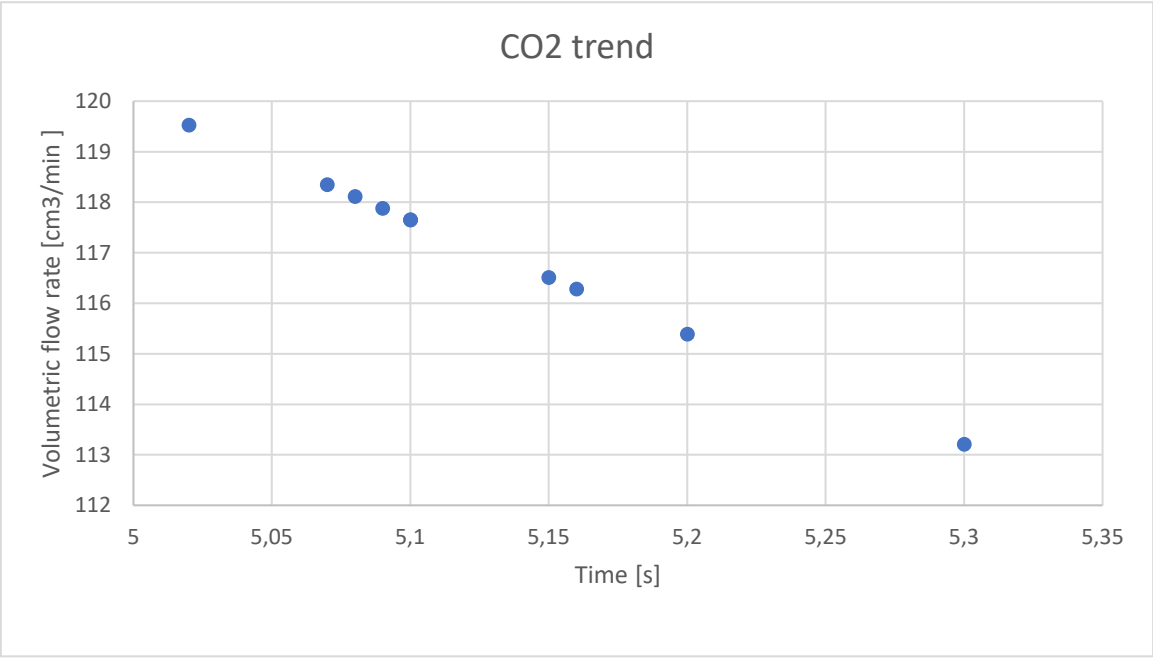

Figure A15: CO_2 trend over time for a rotameter value of 8

As regards the equilibrium position 10, *Table A3* shows the measurements of the rising times of the bubbles and the corresponding values of the carbon dioxide flow rates exiting the gas cylinder, while *Figure A16* shows the float of the rotameter in position 10:

Table A3: Rising time of bubbles and volumetric flow rate of CO_2 related to a volume of 10 cm^3 (10)

Time [s]	Volumetric flow rate [cm^3/min]
3,79	158,3113456
3,69	162,601626
4,08	147,0588235
4	150
4,02	149,2537313
4	150
4,02	149,2537313
4	150
3,83	156,6579634
3,82	157,0680628

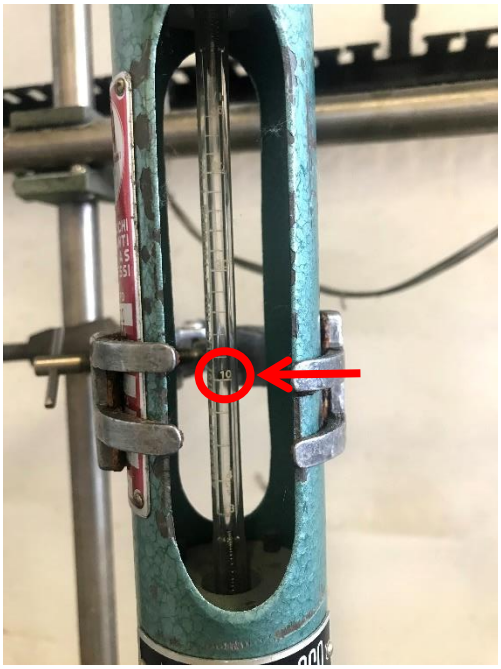

Figure A16: Rotameter value of 10

To this value of the rotameter correspond a maximum and minimum volumetric flow rate of carbon dioxide respectively of approximately 162 cm3 / min and 147 cm3 / min and finally an average flow rate of approximately 155 cm3 / min. From *Table A3*, it can be seen that the longer the time taken by the bubbles to cross the reference volume, the lower the flow of carbon dioxide exiting the gas cylinder. This happens because a longer rise time corresponds to a lower speed of the gas flow exiting the valve. The opposite occurs for shorter ascent times. The trend of CO2 in relation to the rising time of the bubbles in the volume unit of 10 cm3 is represented in the graph in *Figure A17:*

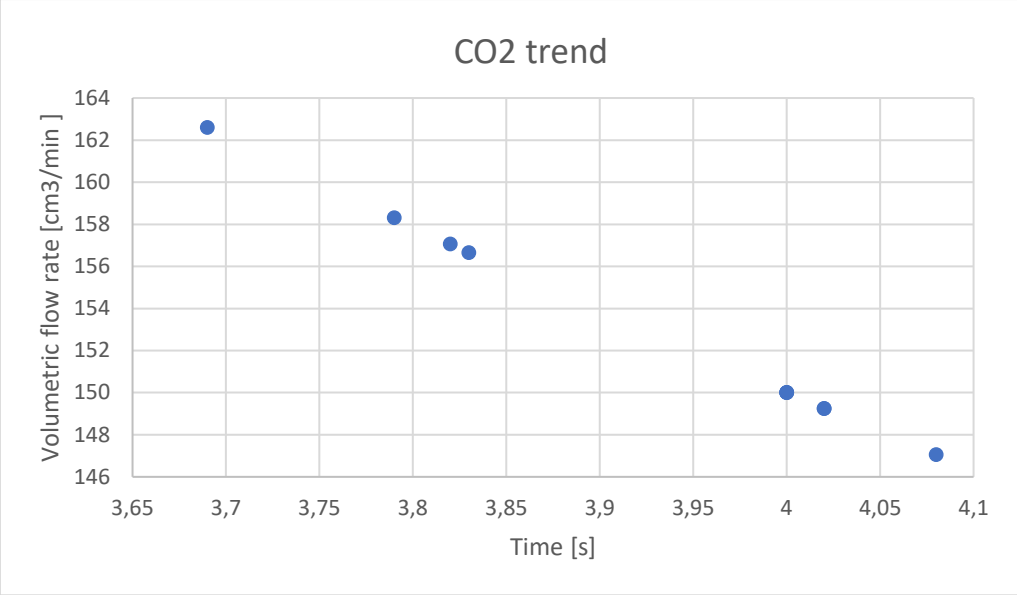

Figure A17: CO_2 trend over time for a rotameter value of 10

Finally, as regards the equilibrium position 20, Table A4 shows the measurements of the rising times of the bubbles and the corresponding values of the carbon dioxide flow rates exiting the gas cylinder, while *Figure A18* shows the float of the rotameter in position 20. To this value of the rotameter correspond a maximum and minimum volumetric flow rate of carbon dioxide respectively of about 315 cm3 / min and 288 cm3 / min and finally an average flow rate of about 302 cm3 / min.

Table A4: Rising time of bubbles and volumetric flow rate of CO_2 related to a volume of 10 cm^3 (20)

Time [s]	**Volumetric flow rate [cm^3/min]**
2,05	292,6829268
1,9	315,7894737
2,03	295,5665025
1,92	312,5
1,93	310,880829
2,06	291,2621359
1,99	301,5075377
1,97	304,5685279
2,08	288,4615385
1,9	315,7894737

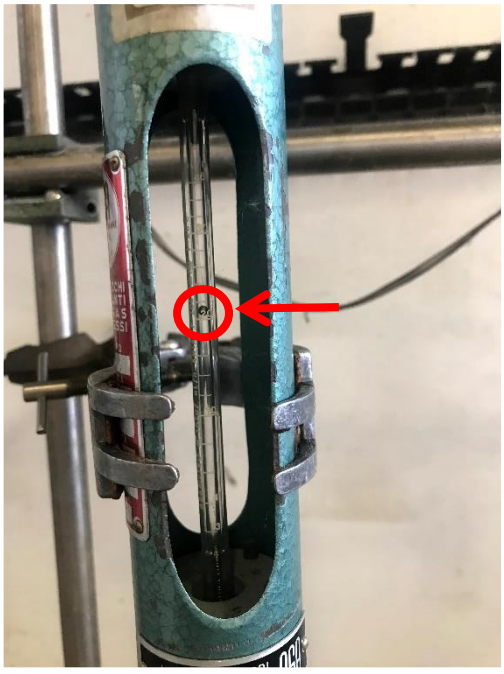

Figure A18: Rotameter value of 20

From *Table A4*, it can be seen that the longer the time taken by the bubbles to cross the reference volume, the lower the flow of carbon dioxide exiting the gas cylinder. This happens because a longer rise time corresponds to a lower speed of the gas flow exiting the valve. The opposite occurs for shorter ascent times. The trend of CO2 in relation to the rising time of the bubbles in the volume unit of 10 cm3 is represented in the graph in *Figure A19:*

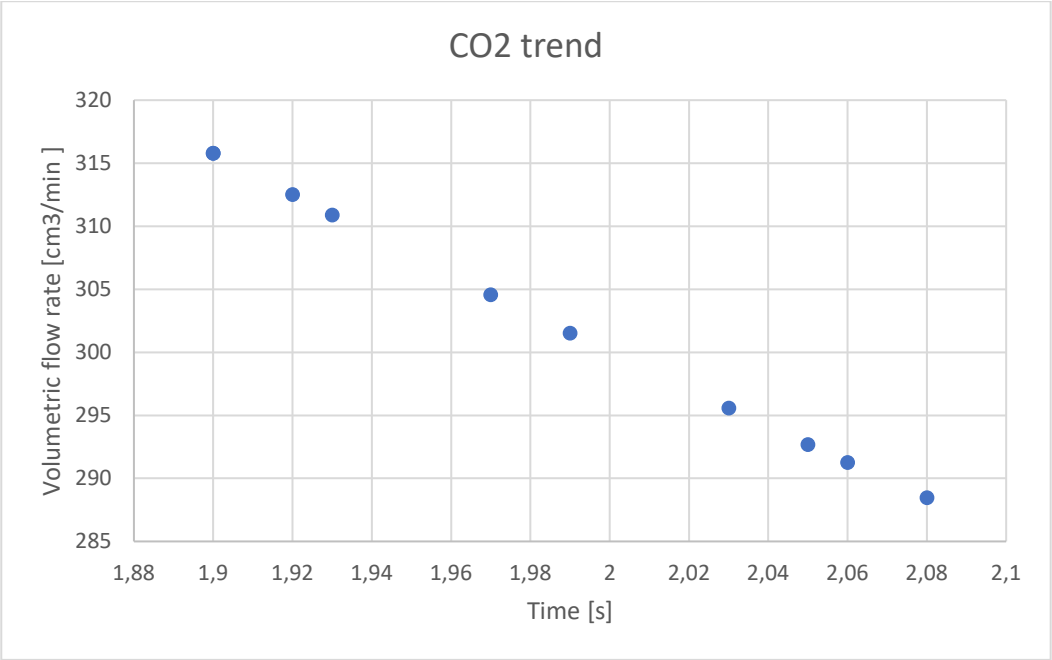

Figure A19: CO_2 trend over time for a rotameter value of 20

LIST OF FIGURES

Figure 1: Percentages of world beverage market shares ……7

Figure 2: Wet and dry foams ……11

Figure 3: Process flow diagram for the manufacture of carbonated soft drink ……14

Figure 4: Carbon Dioxide solubility in water ……16

Figure 5: Basic carbonation system ……17

Figure 6: Counter-pressure filler system ……19

Figure 7: Criterion for gas entrapment when a semi-infinite sheet of liquid advances over a conical groove with half-angle ……28

Figure 8: Development of an air crater under the liquid free surface of a deep-water pool caused by the impact of a jet disturbance ……29

Figure 9: Entrainment regimes produced by a cylindrical liquid jet impinging on a deep pool of the same liquid……30

Figure 10: Lifetime of the cloud of bubbles as a function of the initial dissolved CO_2 concentration for the three different cases of carbonated water……33

Figure 11: Series of snapshots during the pouring process ……34

Figure 12: Time sequence showing bubbles growing stuck on the bottom of the plastic goblet poured with the carbonated water sample……35

Figure 13: The diameter of the single bubble far from neighbouring bubbles (a), grows faster than the diameters of the three bubbles growing close to each other's (b) ……35

Figure 14: Bubble diameter vs. time, for single bubbles for the three various carbonated water samples ……36

Figure 15: Diffusion boundary layer and bubble interface ……37

Figure 16: Plateau borders ……40

Figure 17: Thinning of the liquid film between two adjacent bubbles due to drainage ……41

Figure 18: Coalescence mediated by a spherical hydrophobic particle bridging two bubbles ……42

Figure 19: Components of a high-speed carbonated soft drink flow rate filling system ……44

Figure 20: Filling process algorithm ……45

Figure 21: Filler bowl pressure control structure ……46

Figure 22: Tank containing carbon dioxide ……49

Figure 23: Cylindrical glass reactor ……49

Figure 24: Trend of foam at CO_2 variation (mixture 1) ……52

Figure 25: Screenshot of the variation of the foam formed on the free surface of the mixture 1 53

Figure 26: Trend of foam at CO_2 variation (mixture 2) 54

Figure 27: Screenshot of the variation of the foam formed on the free surface of the mixture 2 54

Figure 28: Trend of foam at CO_2 variation (mixture 3) 55

Figure 29: Screenshot of the variation of the foam formed on the free surface of the mixture 3 56

Figure 30: Comparison of foam growth in the three cases 57

Figure 31: Height of foam, height of liquid and total height vs time of bottling 67

Figure A1: Codd's bottle 71

Figure A2: The Crown Cork by William Painter 72

Figure A3: Type of profiles of bottles for carbonated soft drinks 76

Figure A4: The shoulder and the neck of bottles for carbonated soft drinks 76

Figure A5: Petaloid bottom of bottles for carbonated soft drinks 77

Figure A6: Champagne bottom of bottles for carbonated soft drinks 77

Figure A7: The handle of bottles for carbonated soft drinks 78

Figure A8: The ribs of bottles for carbonated soft drinks 79

Figure A9: Water Footprint of The Coca Cola Company from 2004 to 2017 80

Figure A10: Rotameter 82

Figure A11: Working principle of rotameter 82

Figure A12: Rotameter value of 4.....84

Figure A13: CO_2 trend over time for a rotameter value of 4 85

Figure A14: Rotameter value of 8 85

Figure A15: CO_2 trend over time for a rotameter value of 8 86

Figure A16: Rotameter value of 10 87

Figure A17: CO_2 trend over time for a rotameter value of 10 88

Figure A18: Rotameter value of 20 88

Figure A19: CO_2 trend over time for a rotameter value of 20 89

LIST OF TABLES

Table 1: Carbonated soft drink brands 7

Table 2: Standards of water used in Carbonated soft drinks 9

Table 3: Physicochemical pertinent properties of the three carbonated waters investigated 32

Table 4: Experimental bubble growth rates, and corresponding thickness of the diffusion boundary layer around the growing bubble, in relation with the difference in dissolved CO_2 38

Table 5: Three mixtures used in the experiment 47

Table 6: Ingredients of mixture 1 48

Table 7: Ingredients of mixture 2 48

Table 8: Ingredients of mixture 3 48

Table 9: Characteristic dimensions of the cylindrical reactor, nozzle and wire mesh 50

Table 10: Variation of foam as CO_2 flow rate changes (mixture 1) 52

Table 11: Variation of foam as CO_2 flow rate changes (mixture 2) 53

Table 12: Variation of foam as CO_2 flow rate changes (mixture 3) 55

Table 13: Properties of mixture 1 58

Table 14: Properties of mixture 2 58

Table 15: Properties of mixture 3 59

Table 16: Release times of mixture 1 61

Table 17: Release times of mixture 2 61

Table 18: Release times of mixture 3 61

Table 19: Surface tension values of mixture 1 63

Table 20: Surface tension values of mixture 2 63

Table 21: Surface tension values of mixture 3 63

Table 22: Experimental data useful for the filling model 64

Table 23: The foam height, the liquid height, the total height and the length of each step 66

Table A1: Rising time of bubbles and volumetric flow rate of CO_2 related to a volume of 10 cm^3 (4).....84

Table A2: Rising time of bubbles and volumetric flow rate of CO_2 related to a volume of 10 cm^3 (8) 85

Table A3: Rising time of bubbles and volumetric flow rate of CO_2 related to a volume of 10 cm^3 (10) 87

Table A4: Rising time of bubbles and volumetric flow rate of CO_2 related to a volume of 10 cm^3 (20) 88

7. REFERENCES

[Aldaya M. M., 2010]: Aldaya M. M., "Corporate Water Footprint Accounting and Impact Assessment: The Case of the Water Footprint of a Sugar-Containing Carbonated Beverage", *Springer*, 2010

[Alipour B., 2012]: Alipour B., "Effect of inulin and stevia on some physical properties of chocolate milk", *Health promot perspect,* 2012

[Anjali C., 2004]: Anjali C., "Static Foam Destruction: Role of Ultrasound." *Ultrasonics Sonochemistry* 11 (2): 67–75, 2004

[ASA Srl, 2021]: https://asaspa.com, 2021

[Assobibe, 2020]: http://www.assobibe.it, 2020

[Balaban M.O., 2012]: Balaban M. O., "Dense Phase Carbon Dioxide: Food and Pharmaceutical Applications", *Wiley Blackwell*, 2012

[Bamforth C. W., 2004]: Bamforth C. W., "The Relative Significance of Physics and Chemistry for Beer Foam Excellence: Theory and Practice", *Journal of the Institute of Brewing*, Volume 110, Issue 4, 2004

[Belair G., 2006]: Belair G., "Modeling the Kinetics of Bubble Nucleation in Champagne and Carbonated Beverages", *The Journal of Physical Chemistry*, Volume 110, 2006

[Belair G., 2015]: Belair G., "Bubble Dynamics in Various Commercial Sparkling Bottled Waters." *Journal of Food Engineering*, 2015

[Beverfood, 2019]: https://www.beverfood.com, 2019

[Bisperink C. G. J., 1994]: Bisperink C. G. J., "Bubble Growth in Carbonated Liquids." *Colloids and Surfaces A: Physicochemical and Engineering Aspects*, 1994

[Brennen C. E., 2013]: Brennen C. E., "Cavitation and bubble dynamics", *CambridgeUniversity Press*, 2013

[British Soft Drink Association, 2021]: https://www.britishsoftdrinks.com, 2021

[Bruno D., 2015]: Bruno D., "Una bottiglia con la biglia", 2015

[Cilindre C., 2010]: Cilindre C., "Foaming properties of various Champagne wines depending on several parameters: grape variety, aging, protein and CO2 content", *Elsevier*, 2010

[Coca-Cola Italia, 2021]: https://www.coca-colaitalia.it, 2021

[Coffey T. S., 2008]: Coffey T. S., "Diet Coke and Mentos: What is really behind this physical reaction?", *American Journal of Physics*, Volume 76, Issue 6, 2008

[Cyr D. R., 2001]: Cyr D. R., "Bubble growth behavior in supersaturated liquid solutions", *Digital Commons UMaine,* 2001

[Dow, 2009]: AA.VV., "DOW UF and RO Technology Used to Produce High Quality Water for the Beverage Industry in East Europe", 2009

[Drenckhan W., 2015]: W. Drenchan, "Structure and energy of liquid foams", *Advances in Colloid and Interface Science,* 1-16, 2015

[Duncan J. H., 2011]: "The Impact of a Translating Plunging Jet on a Pool of the Same Liquid." *Journal of Fluid Mechanics*, 2011

[Endan J., 2010]: Endan J., "A Survey on Rheological Properties of Fruit Jams", *International Journal of Chemical*

Engineering and Applications, 2010

[Enqvist K., 1992]: Enqvist K., "Nucleation and bubble growth in a first-order cosmological electroweak phase transition", *Physical Review*, 1992

[Enriquez O. R., 2013]: Enriquez O. R., "Growing Bubbles in a Slightly Supersaturated Liquid Solution." *Review of Scientific Instruments*, 2013

[Euromonitor International, 2015]: https://www.euromonitor.com, 2015

[EUWA, 2021]: https://www.euwa.com, 2021

[Focus, 2002]: https://www.focus.it, 2002

[Food Additives and Ingredients Association, 2021]: https://www.faia.org.uk, 2021

[Food Standards Agency, 2021]: https://www.food.gov.uk, 2021

[Frank X., 2021]: Frank X., "Bubble nucleation and growth in fluids", *Chemical Engineering Science, Elsevier*, 2021

[Gabas A. L., 2007]: Gabas A. L., "Viscosity of aqueous carbohydrate solutions at different temperatures and concentrations", *International Journal of Food Properties,* 2007

[GDO, 2021]: https://www.gdonews.it, 2021

[Gerbens P. W., 2003]: Gerbens P. W., "Design and development of a measuring method for environmental sustainability in food production systems", *Elsevier,* 2003

[Gerth W. A., 2014]: Gerth W. A., "Gas Supersaturation Thresholds for Spontaneous Cavitation in Water with Gas Equilibration Pressures up to 570 atm", *Journal Zeitschrift für Naturforschung A*, 2014

[Giornale della Birra, 2014]: Editorial board of Giornale della Birra, "La rivoluzione della corona", *Giornale della Birra,* 2014

[Gros L., 2006]: Gros L., "Chemistry changes everything", *Chemistry and Industry for Teachers in European Schools,* 2006

[Gruppo San Pellegrino, 2021]: https://bibite.sanpellegrino.it, 2021

[Guzzonato C., 2021]: Guzzonato C., "Meno zucchero in cibi e bevande: primi passi negli USA", *Focus,* 2021

[Hepworth N. J., 2004]: Hepworth N. J., "Novel application of computer vision to determine bubble size distributions in beer", *Journal of Food Engineering*, 2004

[Hiemenz P. C., 1997]: Hiemenz P. C., "Principles of colloid and surface chemistry", Third edition, Marcel Dekker Inc., 1997

[Horeca, 2020]: https://www.horeca.it, 2020

[Hu H., 1998]: Hu H., "Numerical and Experimental Study of a Hydrodynamic Cavitation Tube." *Metallurgical and Materials Transactions B: Process Metallurgy and Materials Processing Science*, 1998

[Hung S., 2011]: Hung S., "The Enhancement of Foam Generated by Low Power Ultrasound and Its Application to Foam Fractionation." *Colloids and Surfaces A: Physicochemical and Engineering Aspects* 380 (1–3): 35–40, 2011

[Inter Upgrade, 2021]: https://interupgrade.com, 2021

[International Sweeteners Association, 2021]: https://www.sweeteners.org, 2021

[Jana A., 2021]: Jana A., “Food Technologies: Carbonated Beverages”, 2021

[Jones S. F., 1999]: Jones S. F., “Bubble nucleation from gas cavities — a review”, *Advances in Colloid and Interface Science*, 1999

[Karakashev S., 2012]: “Foams and Antifoams.”, *Advances in Colloid and Interface Science* 176–177: 1–17, 2012

[Karthika S., 2016]: Karthika S., “A Review of Classical and Nonclassical Nucleation Theories”, *American Chemical Society Publications*, 2016

[Khezzar L., 2011]: Khezzar L., “Characterization of plunging liquid jets: A combined experimental and numerical investigation”, *International Journal of Multiphase Flow*, 2011

[Lee W. T., 2011]: Lee W. T., “Mathematical Modelling of Bubble Nucleation in Stout Beers and Experimental Verification”, *Proceedings of the World Congress on Engineering*, 2011

[Leong T., 2011]: Leong T., “The Fundamentals of Power Ultrasound - A Review.” *Acoustics Australia* 39 (2): 54–63, 2011

[Lockwood G., 2002]: Lockwood G., “Expansion of air bubbles in aqueous solutions of nitrous oxide or xenon”, *British Journal of Anaesthesia*, 2002

[Long T., 2009]: Long T., “1693: Dom Pérignon ‘Drinks the stars’”, *Wired,* 2009

[Lubetkin S. D., 1989]: Lubetkin S. D., “The Nucleation and Detachment of Bubbles”, *Journal of the Chemical Society, Faraday Transaction 1*, 1989

[Mahnazmezen, 2021]: https://it.mahnazmezon.com, 2021

[Mente A., 2018]: Mente A., “Coca-Cola pianifica il lancio di energy drink: scatta la competizione con Monster Beverage”, *Beverfood,* 2018

[Min O., 2019]: Min O., “Development of High-Efficiency, High-Speed and High-Pressure Ambient Temperature Filling System Using Pulse Volume Measurement.” *Applied Sciences (Switzerland)* 9 (12), 2019

[Morey M., 1999]: Morey M., “Foam Destabilization by Mechanical and Ultrasonic Vibrations.” *Journal of Colloid and Interface Science* 219 (1): 90–98, 1999

[Napolitano G., 2019]: Napolitano G., “Sugar Tax, la tassa sulle bevande zuccherate”, *Starting Finance,* 2019

[Natural Food Colours Association, 2021]: https://natcol.org, 2021

[Ottmar B., 2016]: Ottmar B., “Stretch Blow Molding”, *Elsevier Science,* Chapter 7, 2016

[Palumbo M., 2018]: Palumbo M., “La misura di portata dei fluidi con il flussimetro”, *ASV Stubbe Italia Srl*, 2018

[Pepsico, 2021]: http://www.pepsico.co.it, 2021

[Perry R. H., 2007]: Perry R. H., “Perry's Chemical Engineers' Handbook”, Eight edition, Mc Graw Hill, 2007

[Petkova B., 2020]: Petkova B., “Foamability of aqueous solutions: Role of surfactant type and concentration”, *Colloids and Interface,* 2020

[Pollution Research Group, 2015]: Pollution Research Group, “Water and Wastewater Management in the Soft Drink Industry”, Second Edition, 2015

[Porges R., 1961]: Porges R., “Wastes from the Soft Drink Bottling Industry”, *Journal of Water Pollution Control Federation, 1961*

[Prosperetti A., 2000]: “On the Mechanism of Air Entrainment by Liquid Jets at a Free Surface.” *Journal of Fluid Mechanics*, 2000

[Pugh R. J., 1996]: Pugh R. J., “Foaming, Foam Films, Antifoaming and Defoaming.” *Advances in Colloid and Interface Science*, 1996

[Qu X., 2013]: “Experimental Characterization of Air-Entrainment in a Plunging Jet.” *Experimental Thermal and Fluid Science*, 2013

[Ronteltap A. D., 1989]: Ronteltap A. D., “Beer foam physics”, *Wageningen University and Research*, 1989

[Salerno E., 2014]: Salerno E., “Bottled fluid dynamics: foam formation during the bottling process of carbonated beverages”, 2014

[Shokribousjein Z., 2011]: Shokribousjein Z., “Hydrophobins, Beer Foaming and Gushing.”, *Cerevisia*, 2011

[Starov V., 2021]: Starov V., “Foam Quality of Foams Formed on Capillaries and Porous Media Systems”, *Advances in Colloid and Interface Science*, 2021

[Statista, 2019]: https://www.statista.com, 2019

[Steen D. P., 2006]: Steen D. P., “Carbonated Soft Drinks: Formulation and Manufacture”, *Blackweel Publishing*, 2006

[The Coca Cola Company, 2010]: The Coca Cola Company, “Product water footprint assessments: practical application in corporate water stewardship”, 2010

[The Coca Cola Company, 2018]: The Coca Cola Company, “Improving our water efficiency: meeting goals and moving goalposts”, 2018

[Treccani, 2021]: https://www.treccani.it, 2021

[Winterburn J., 2007]: Winterburn J., “Sound Methods of Breaking Foam,” 65, 2007

[Wu J., 2008]: Wu J., “Ultrasound, cavitation bubbles and their interaction with cells”, *Elsevier*, 2008

[Zhou Z. A., 1998]: “Effect of Surface Properties of Fine Particles on Dynamic Bubble Formation in Gas-Supersaturated Systems.” *Industrial and Engineering Chemistry Research*, 1998

[Zugno S., 2017]: Zugno S., “Analisi delle potenzialità del PET nel mondo del packaging design”, 2017